UNIVERSITAT POLITÈCNICA DE VALÈNCIA

ETS INGENIERÍA DE CAMINOS, CANALES Y PUERTOS

TRABAJO DE FIN DE MASTER

" Structural robustness assessment of the Pirelli Tower in Milan (Italy).
Consequences of local failures in lateral walls. "

Presentado por

Francesco Da Rif

Para la obtención del

Master Universitario en Ingeniería de Caminos, Canales y Puertos

Curso: *2019/2020*

Fecha: *Diciembre 2020*

Tutor: *Adam Martínez, José Miguel*

Tutor: *Ballerini Marco*

Contents

Chapter 1

Introduction

Traditionally, structural engineers have always focused on cost optimization and on respecting the requirements of the regulations. Nonetheless, during the useful life, the facilities could be exposed to unpredictable exceptional events such as impacts, explosions or fires. These extraordinary circumstances are becoming more and more frequent due to: climatic changes (floods, landslides, hurricanes), terroristic threats (blast loading, vehicle impact) and ageing (lack of maintenance, corrosion). These special events typically cause local damage to the constructions that can degenerate causing the collapse of a significant part or even of the whole building. The following are three important examples of these types of partial or total collapses:

- **Ronan Point Tower**, London, 16 May 1968:

  The Ronan Point Apartment building, completed in London in March 1968, was 64 meters high and had 23 storeys. The structural system consisted of precast concrete walls and floors both fitted by slots and bolted together with dry-packed mortar connections. Therefore, this structure was characterised by minimal ability to redistribute loads and was predisposed to progressive collapse in case of local damage. On May 16, 1968, an exterior panel of the 18th floor was blown out due to an internal gas explosion of a leaking gas stove. The loss of the panel caused the progressive collapse of the underneath floors down to the ground level (Fig. 1.1).

Figure 1.1: Collapse of the south-east corner Ronan Point Tower. From [1].

- **Murrah Federal Building**, Oklahoma, April 19 1995:

  The Alfred P. Murrah Federal Building was an office facility of the U.S. government built between 1970 and 1976. It was a nine-storey, reinforced concrete structure, 61 meters long and 21,4 meters wide. The structural system involved columns, beams and slabs. The frame was quite regular, but on the north elevation the span between columns was doubled, and these columns supported deep transfer girders. On April 19, 1995, the Alfred P. Murrah Federal Building was hit by a terrorist attack. The terrorists used an explosive truck, situated four meters from one of the columns, loaded with 1800 kilograms of TNT equivalent. The direct explosion shot down the nearest column, while the shock wave destroyed floors and beams, which in turn was the cause for buckling the other columns due to lack of lateral supports. The progressive collapse generated can be seen in Fig. 1.2.

Figure 1.2: Collapse of the Murrah Federal Building. From [2].

This event was so significant that many studies were carried out, attempting to understand what went wrong. The results of these investigations allowed to identify four essentials principles that should be respected in order to prevent progressive collapses. Kokot, in his paper [3], has summarized them:

- Avoiding important irregularities in the structure scheme and, to ensure the presence of alternative load paths, the use of transfer girders should be taken into account;
- Slabs and walls should be able to fail without destroying the frame;
- The frame, thanks to his robustness and ductility, should be able to sustain large deformations;
- The vertical load-bearing elements, like walls and columns, at the base of the structure, should be designed to withstand explosion as much as possible.

- **World Trade Center**, New York City, September 11 2001:

  The structure of the Twin Towers consisted of a tubular system with perimetral columns spaced one meter and an internal core of reinforced concrete. The square plan had sides of about 63 meters and truss girders supported the steel decks. The impact of the aircraft caused considerable damage to the towers and triggered a series of intense fires in the nearest storeys. As the fires spread, the temperatures reached in some points the 1000 Celsius degrees, weakening the truss girders and the steel columns consequently. In particular, the collapse of the truss girders, due to the loss of resistance produced from excessive warming, triggered the progressive collapse, pulling the columns of the perimeter inwards, until both towers suffered a complete collapse. The losses in terms of human lives, damages and social impact were tremendous, more than 2700 people, including civilians, firefighters and law officers as well as the passengers and crew of the aeroplanes, died. Bazant [4] has called the collapse of the world trade centre *the most infamous paradigm* of progressive collapse.

Figure 1.3: Collapse of the World Trade Center. From [5].

The previous examples prove how these exceptional events are often catastrophic in terms of human casualties and economic, environmental and social losses. Thus, the ability of a structure to avoid, or at least substantially limit, this type of collapse, is called structural robustness and today represents a further requirement to consider within the framework of the fundamental characteristics of a structure. This property becomes particularly essential in the case of critical or strategic structures in civil protection. Indeed, in recent years, Structural Civil Engineers have shown more and more interest in structural robustness, developing many experimental and numerical studies that have lead to the delineation of technical criteria, however, without indicating real quantitative analytical assessments.

The aim of this thesis consists of the assessment of the structural robustness of an iconic building located in Milan: the Pirelli Tower. This objective will be pursued, creating a finite element model in SAP2000 and realizing various analyses idealizing an extraordinary event like the loss of several parts belonging to vertical load-bearing elements. Since the building was designed in the fifties, the structural robustness assessment will be accomplished considering exceptional scenarios that were not contemplated during the design of the structure.

Hence, the contents of this thesis have been structured as follow:

- **Chapter 2** contains a review of the more significant structural typologies of high-rise buildings and explains the main characteristics of each one of these categories;
- **Chapter 3** illustrates the general theory of robustness, first describing the concept and definitions existing in the literature and secondly, explaining the meaning of accidental actions, risk and consequences of disproportionate collapse. Furthermore, possible measuring indices of robustness and design strategies will be explained;
- **Chapter 4** summarizes the most significant prescriptions stated by the Eurocodes;
- **Chapter 5** describes the fundamental aspects of the Pirelli Tower and the most relevant structural characteristics;
- **Chapter 6** explains the characteristics of the finite element model realized in SAP2000 and the type of finite elements used;
- **Chapter 7** eventually outlines the most notable results of the dynamic linear modal analyses carried out considering the removal of some parts of the vertical load-bearing elements in agreement with the standards and the “threat independent approach”.

Chapter 2

High-rise buildings

The design of a high-rise building is a very complex activity that involves engineers and architects in a heterogeneous mix of competences. These skills are needed to satisfy all the requirements of these type of structures. Indeed, the challenging problem to solve consists of identifying a reliable structure system that allows the skyscraper to withstand horizontal and vertical actions and, at the same time, that fulfil the space requirements needed for the destination use of the edifice. Another peculiar aspect of a high-rise building that must be considered in the design is the living comfort. Indeed, the design of tall and slender buildings must not only meet the strength and deformability requirements imposed by the regulations but also consider the effects of motion, such as state of concern, anxiety, fear, sense of dizziness, nausea and migraine that could occur on people who work and live in the structure. Eventually, a current requirement, which becomes day by day more crucial, concerns the structural robustness, in other words, the ability of the structure to oppose to the progressive collapse that could be originating from a local failure. In the next sections, a review of the most crucial aspect of a high-rise building as much as a recap of the most used static schemes will be exposed.

2.1 Actions acting against the buildings

Gravitational actions produce a growing effect with the height caused by their accumulation along with the structure elevation and lead to a significant increase in the size of the structural elements. Though, the effect of the various vertical loads is not predominant as horizontal actions, as well as extreme events, are much more significant than vertical ones for what concern high-rise buildings. Therefore, the most critical efforts that must be taken into account are:

- Wind;
- Earthquakes;
- Extreme events such as hurricanes, tornados, blast loads, explosions, collisions, fire, landslides and floods.

Since the next chapters will extensively treat themes related to exceptional events, such as structural robustness, and progressive collapse, this section is entirely focused on the main horizontal actions. Hence, wind and earthquake have some aspects in common; they have a dynamic nature as well as marked random behaviour. However, there are also a few dissimilarities. For instance,

an earthquake is a ground movement whose effects on the structure depends on the ground acceleration, the characteristics of the resistant structure, from his mass, stiffness and damping. In contrast, the wind is a pressure that acts perpendicularly to the exposed areas of the building and depends mostly on the wind speed for a determined period of return.

2.2 Deformations and accelerations

With horizontal loads, attention should be paid to lateral deformation and horizontal accelerations.

2.2.1 Lateral deformations

The most crucial requirements that must be verified are related to:

Total displacement Local displacement

Typical limit values of these two maximum displacements, reported in the building codes, are correlated to the total height of the building and the storey height:

- Total displacement<1/500 maximum height;
- Local displacement<1/250 inter-storey height.

Controlling lateral deformations is crucial. Very often, during an earthquake, people are severely injured by structural elements or objects whose movement is caused by the excessive lateral deformation of the building.

2.2.2 Horizontal accelerations

The horizontal acceleration of the building is strictly related to living comfort, and in very high buildings, oscillations can also cause the breaking of coatings, partitions and windows. More in detail, the dynamic nature of the wind is the primary cause of the discomfort of the building occupants and the functionality problems of the structure. The movement of a building is perceived by people when the acceleration exceeds a particular value called “Threshold of perception”. This value has been investigated through many studies on existing buildings. However, quantifying the accelerations threshold for comfort is complicated since each person has a different feeling. Nevertheless, some classifications have been made. The first proposal identifies four comfort classes, depending on the acceleration [6]:

- Acceleration no perceptible $a_{hg} < 0,004\,g$;
- Acceleration rarely perceptible $0,004\,g < a_{hg} < 0,0075\,g$;
- Acceleration perceptible $0,0075\,g < a_{hg} < 0,02\,g$;
- Disturbing acceleration $a_{hg} > 0,02\,g$.

Another proposal is represented from the graph in Fig. 2.1:

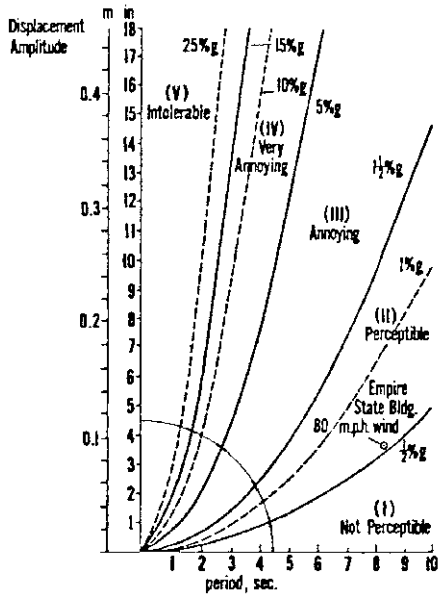

Figure 2.1: Comfort limits correlated to vibrations period and amplitude. From [6].

2.3 Structural schemes of high-rise buildings

The structure of a high-rise building can be considered as a large vertical Vierendeel beam, firmly attached at the base, subjected to horizontal and vertical loads that principally produce internal bending moment and shear forces in the element. During the years, many structural systems have been proposed and used in the design of the high-rise buildings. In the next sections, a review of the most important is presented.

2.3.1 Frame system

This type of structural system is suitable for buildings with less than 20 floors. It is constituted by vertical columns embedded in the concrete slabs floors of the building. Its configuration is mainly determined by vertical loads and does not interfere with the functional system of the building. The operation key of this particular system lies in the joints nodes connecting beams and columns. Notably, it must have sufficient rigidity to maintain unchanged the angle between the structural elements that are connected through it. This type of systems have a behaviour, under a horizontal load, that is very similar to a Vierendeel beam. The monolithic behaviour and relative stiffness of the joints, which characterize these structural solutions, make this system particularly suitable for reinforced concrete constructions. It is crucial to keep in mind that strength and stiffness are proportional to the dimensions of beams and columns, and inversely proportional to the distance between them. Therefore in order to obtain an efficient action of the frame, it is necessary to provide suitable dimensions and spacing of the elements. For buildings higher than 20 floors, it is necessary to consider other structural solutions.

2.3.2 Frame system with concrete diaphragm wall

For buildings higher than 20 floors, a frame system alone is not adequate. In this case, a wall or a bracing system is required in order to provide rigidity and improve the functionality of the frame against the main horizontal actions. Therefore, these combined systems are more rigid and cost-effective. The diaphragm walls can have various forms: circular, oval, rectangular, triangular or straight but must be well-positioned in the plan of the structure minimizing the distance between the mass-centre and the stiffness-centre, thus avoiding in this way, critical torsional effects.

An important aspect that must be considered is that, while the frame acts as a Vierendeel beam, the structural behaviour of the walls is cantilever beam type. Therefore, complex interaction phenomena must be considered: the diaphragm walls will withstand more efforts than the frame at the base of the structure and less on top. Two examples of this structural typology are shown in Fig. 2.2. Both are located in Europe, the Pirelli Tower in Milano (all the structural aspects of this building will be described in chapter 5) and the Commerzbank Tower in Frankfurt.

Figure 2.2: The Pirelli Tower (left) and the Commerzbank (right). From [7] and [8].

2.3.3 Core resistant system

This solution represents a particular case of structures designed with diaphragms, and wherein the walls are connected between each other, forming a robust core with a great torsional and flexural stiffness. Moreover, since usually the core is positioned within the building perimeter, it is possible to achieve a significant weight reduction of the structural elements of the facade. Usually, these structures have excellent symmetry and great behaviour against lateral loads.

A variant of this typology is represented by the combination of two tubes, one internal and one external: these two structural elements, designed coaxially, share the overall effort and increase the degree of collaboration of each component allowing better use of materials, and an increase in the maximum height of the construction. This system can be used for buildings with more than

100 storeys and is particularly useful when the lateral displacement is a critical and conditioning element in the design. The Colon Towers (Madrid) represents an example of a core system building (Fig. 2.3).

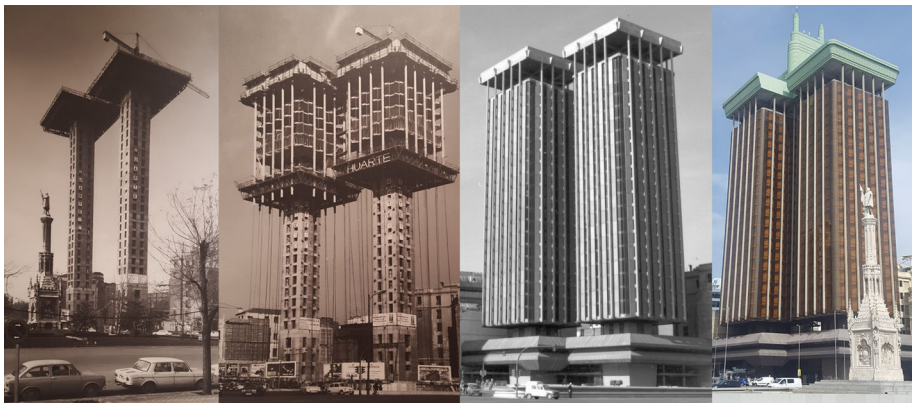

Figure 2.3: The Colon Towers during various construction steps. From [9].

2.3.4 Outrigger system

The idea behind this system consists of increasing the stiffness of the structure against horizontal actions with the use of outrigger systems. Therefore, this method is a modification of the bracing or diaphragm walls types. It includes a central core and horizontal beams, simple or reticular (Outrigger) connecting the core to the peripheral columns. In case the building is subject to horizontal actions, the constraint outrigger blocks the rotation of the core stressing the lateral supports. These structures can be used for buildings with more than 100 floors and have a better lateral resistance if the thickness of the outrigger system includes more than one storey. Various theoretical studies demonstrate that the efficiency of this system is maximum if the outrigger is positioned between 3/5 and 2/3 of the total height of the structure. The differences in the bending moment in a building without and with an outrigger system are shown in Fig. 2.4.

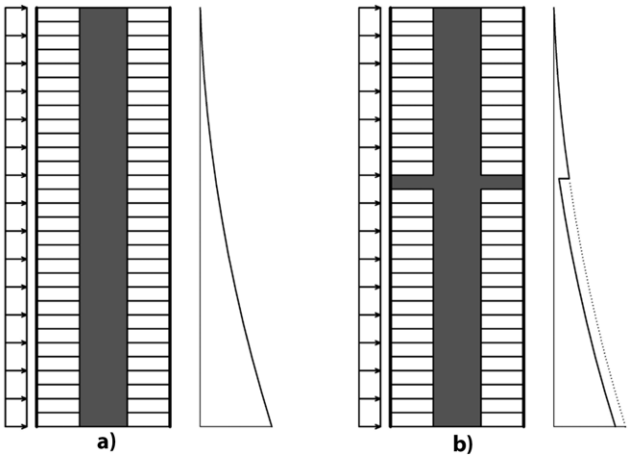

Figure 2.4: Bending moment in a building without outrigger system (a) and with (b). From [10].

An example of a structure built with this system is the Trump International Tower (Fig. 2.5). The outrigger layers are visible in correspondence of every narrowing of the building.

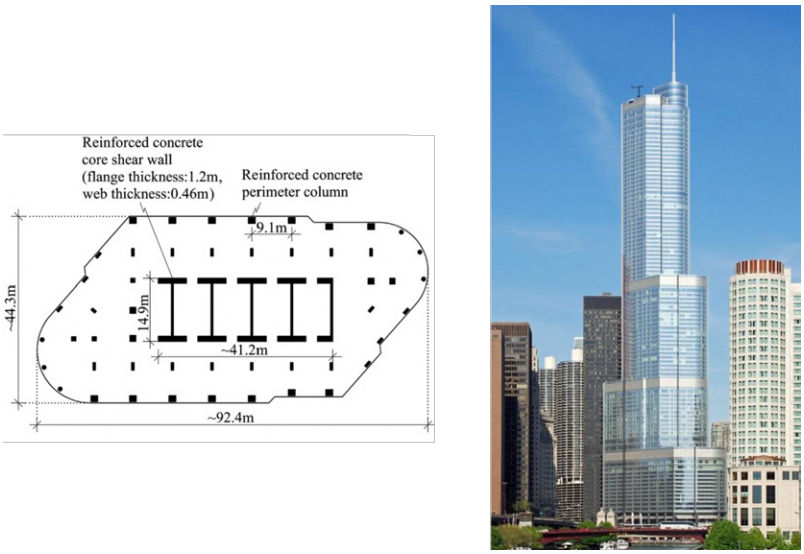

Figure 2.5: The Trump International Tower. From [10].

2.3.5 Tubular system

This system, which was introduced by the famous engineer Fazlur Khan, is characterized for the presence of very close columns in the perimeter, allowing the building to work as a single massive cantilevered beam. This arrangement ensures resistance to lateral actions thanks to the high number of rigid unions along the perimeter that recreate a large tube. Thus, the overall stiffness is concentrated in the facade incrementing the inertia of the building. The positive and negative aspects of this solution can be resumed as follows:
- Positive aspects:

- Considerable space is gained inside of the building;
- Incremented structural inertia.

- Negative aspects:

- The space for entrances at the base of the building is limited;
- The distortion of the vertical stress distribution along the perimeter of the building (shear lag phenomenon) is very significant. In fact, under a lateral load (for instance the wind) the vertical actions, along the cross-section of the building, should be distributed as in a true cantilever beam (Fig.2.6A). Nevertheless, due to the flexibility of beams and columns, the real distribution that occurs is represented in Fig.2.6B, and is characterized by a nonlinear hyperbolic behaviour that produces an increment in corners columns stresses.
- Windows are tiny, so only a little amount of light can enter in the internals spaces.

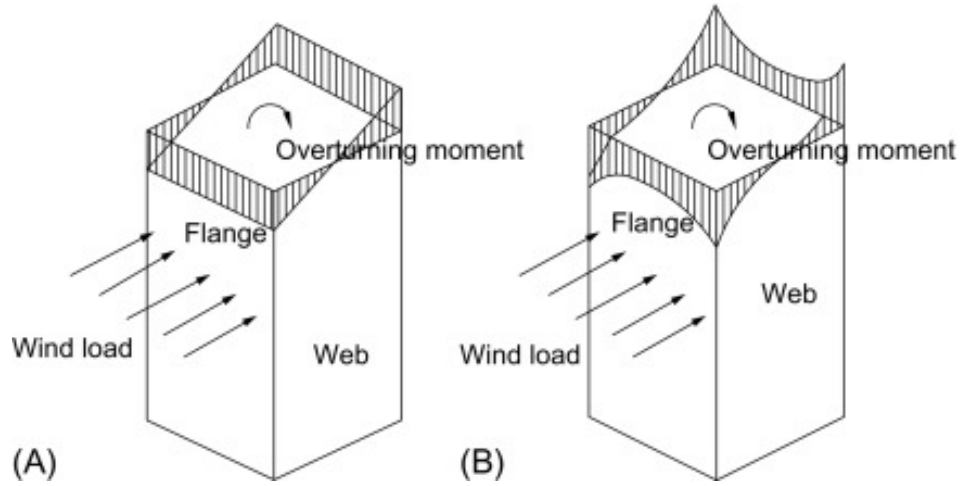

Figure 2.6: Linear vertical load distribution (A) and in the presence of the shear lag (B). From [11].

In order to achieve more space for the accesses at the base, three solutions have been identified:

1) Transition of the columns at the base of the building with structural arches (Fig. 2.7a). This solution was used in the "Torre Picasso"in Madrid;

2) Transition of the columns in the building with bridges-beams (Fig. 2.7b). This structural choice was applied in the "One Shell Plaza"in Houston;

3) Union of some columns at the base of the building (Fig. 2.7c). This methodology was used in the World Trade Center in New York.

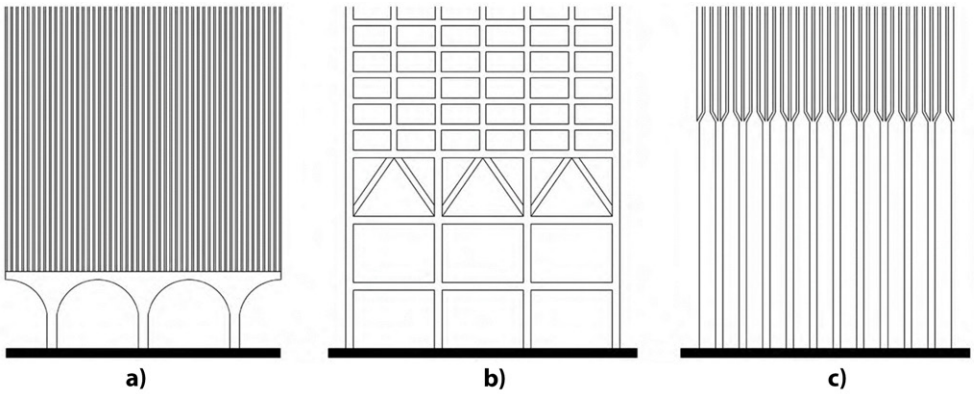

Figure 2.7: Columns transitions strategies at the base of a tube building. From [10].

Two examples of famous buildings with a tube structure system are the World Trade Center and the Picasso Tower. These buildings can be seen in Fig. 2.8.

Figure 2.8: The Picasso Tower (left) and the World Trade Center (right). From [8].

2.3.5.1 Braced tubular systems

This typology represents a further improvement compared to the typical tubular system. It was used for the first time in the construction of the John Hancock Center (Chicago, USA) by Fazlur Kahn (see Fig. 2.9). With this variant, several improvements were introduced, such as the substantial reduction of the shear lag, the increased space between peripheral columns and better use of materials. Therefore, the structure presents a more rigid behaves allowing buildings to be higher and to reduce the lateral displacements. However, the presence of the diagonals beams in the facade produce some difficulties, such as the technical complexity of the nodes and the negative interaction with windows. Some examples of this typology of buildings are shown in Fig. 2.9.

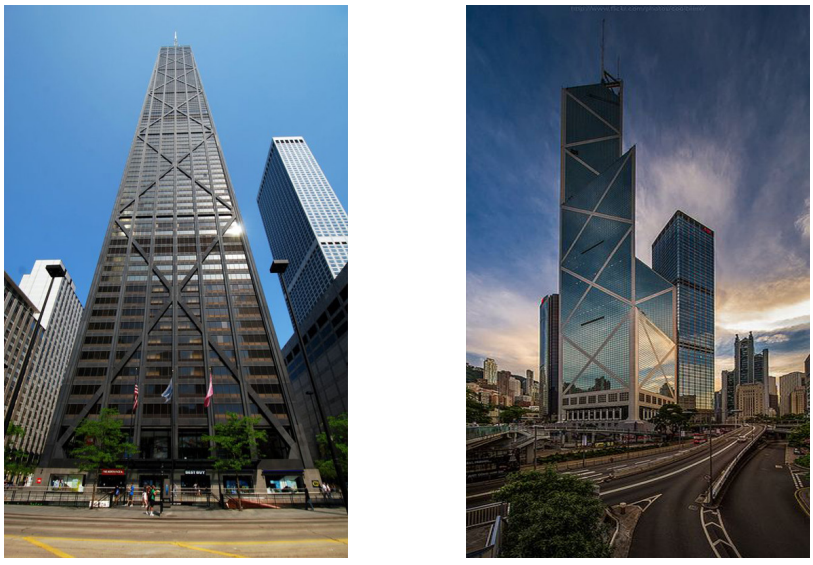

Figure 2.9: The John Hancock Center (left) and the Bank of China (right). From [8].

2.3.5.2 Multiple tube system

Since the tubular system was less effective with the increase of the height and the complexity of the building, Fazlur Kahn thought to use a group of independent tubes, connected for the slab floors and one or more walls, in order to realize a system that works in a monolithic way. The main advantages of this solution are the elasticity in planning the interior space and, overall, the mitigation of the shear lag problem that is hugely reduced, allowing a saving of material and a reduced shear deformation. The benefits deriving by the adoption of this structural system can be well understood considering the case of the Willis Tower (Fig 2.10) where thanks to the adoption of this method and the subsequent reduction of the shear lag effect, a substantial amount of steel have been saved while still providing an excellent structural behaviour.

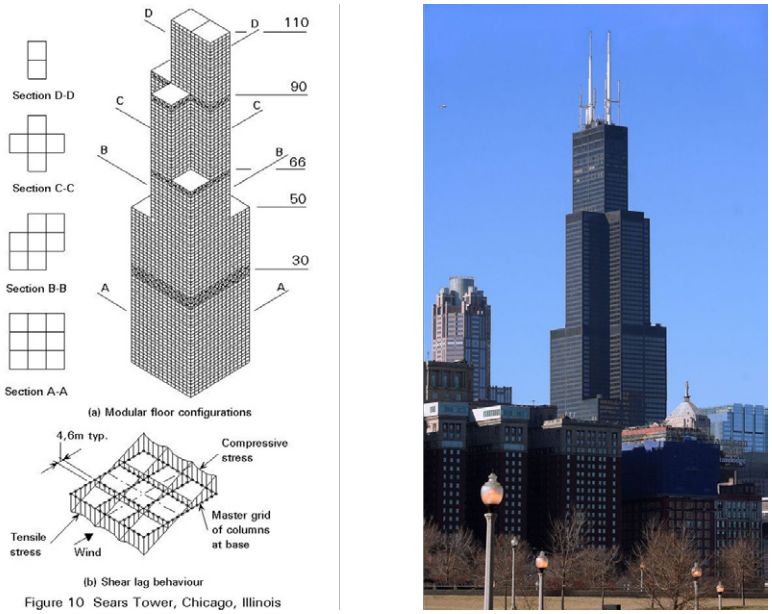

Figure 2.10: The willis Tower structural system. From [8].

Chapter 3

Structural robustness in literature

3.1 Conceptual definitions from the literature

"Structural robustness"is a term that encloses multiple aspects related to the civil engineering world. For long times an unambiguous definition of disproportionate collapse, progressive collapse and structural robustness have been sought by the researchers. Therefore, after several years of investigation and applications, various proposals have been introduced in the literature. Nevertheless, unique definitions, terminology and precise procedures are still lacking, hindering the work of the principal figures involved in the structural design and construction activities such as professional engineers and stakeholders like building officials, owners, lenders, insurers, government agencies and emergency planners [12].

3.1.1 Alternative load paths

In whatever structure, the loss of one or more vertical load-bearing, such as columns or walls, represents the worst local failure scenario. Indeed, this type of damage can lead very often to a progressive collapse originated by a chain of subsequent failures. To avoid these series of failures, that might cause the collapse of the entire building or a considerable part of it, alternative load paths must be able to develop, ensuring the distribution of loads in the structural elements surrounding the damaged part of the building. Otherwise, in the absence of other design measures, for instance, key elements or segmentation, the progressive collapse is inevitable. More precisely, considering a framed building, five resisting mechanisms have been individuated by the researchers. Adam et al., in his paper [12], gives the following descriptions for each one of the possible alternative load paths:

a) The first mechanism is generated by the bending of the beams situated near to the failed columns. Commonly, it is not very considered as it leads to over-dimensioned beams.

b) The Vierendeel behaviour of the frame over the failed column is an important mechanism in order to prevent progressive collapse. (Fig. 3.1a);

c) Another mechanism is the arch effect of the beams where the column has failed. However, this mechanism is ineffective when the lateral displacement of the nearest columns is large;

d) The large rotations and displacements of the beams and slabs surrounding the damaged columns generate the catenary/membrane behaviour (Fig. 3.1b);

e) The last contribution derives to non-structural elements, overall from external walls and partitions (Fig. 3.1c).

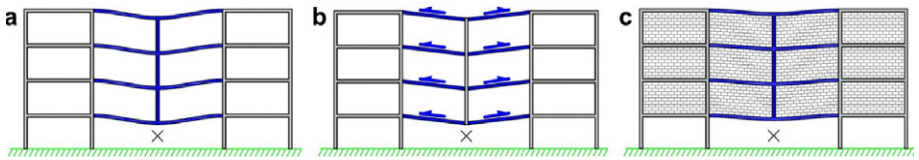

Figure 3.1: Alternative load paths: (a) Vierendeel action; (b) catenary action; and (c) contribution of non-structural elements. From [12].

3.1.2 Differences between progressive and disproportionate collapse

The earliest studies on this topic date back to the forties, during the Second World War, and concerned the behaviour of bomb-damaged buildings with regards to the progressive collapse. Later, some significant collapses such as the previously described Ronan Point apartment, A.P. Murrah Federal Building and the World Trade Center (New York, 2001), stimulated considerable attention in the public opinion as well as in scientific community leading to an increasing number of studies. Thus, a growing number of criteria and recommendations were developed over the years and subsequently introduced in the various standards all over the world.

Progressive collapse can be defined as the result of a chain of subsequent failures that begin with local damage, concerning one or more structural elements, and ends with the destruction of the entire building or a large part of it. Starossek, in his paper [13], presents six types of progressive collapse mechanism:

1- *Pancake-collapse* is identified by the following characteristics:

- Failure of one or more vertical load-bearing element;
- Partial or total disconnection followed by vertical fall of elements in a rigid body motion;
- Consequent transformation of potential energy into kinetic energy;
- Collision between the falling structural components against the residual structure;
- Collapse of the vertical load-bearing component due to the impact;
- Progression of the collapses chain in the direction.

2- *Zipper-collapse* is identified by the following characteristics:

- Initial failure of one or a few structural elements;
- Redistribution of forces in the residual structure;
- The suddenness of the initial failure cause an impulsive loading in the structure;
- The residual structure withstand the impulsive loading with a dynamic response;

- A load concentration is generated by the combined static and dynamic effects, in the proximity of the initially failed elements;
- The load concentration generate a collapse progression in a transverse direction to the principal forces in the failing components.

3- *Domino-collapse* is identified by the following characteristics:

- Initial failure of one or a few structural elements;
- The element fall in an angular rigid-body motion around a bottom edge;
- Consequent transformation of potential energy into kinetic energy;
- A horizontal force is generated by the sudden deceleration of the element's motion due to the impact against other structural parts. Since the force origins from the tilting and the motion of the first element, it has a static and dynamic origin;
- The horizontal force caused by the deceleration of the first element induce the overturning of other elements;
- The collapse progresses in the horizontal direction.

4- *Section-collapse* is very often classified as "fast fracture"but can be still included in the progressive collapse typology due to its similarities and analogies. Therefore, it can be more efficiently explained, considering the case of a beam subjected to an axial load or bent. When a section of the beam fails, the internal forces must be redistributed to the other remaining cross-sections. In the same way, act a structure subjected to this particular collapse, when a local failure appear.

5- *Instability-collapse* is identified by the following characteristics:

- Initial failure of one or a few components that support the vertical load-bearing members subjected to a compression load;
- Subsequent instability of the vertical load-bearing members if the compression load is sufficient;
- Sudden failure of the vertical load-bearing elements due to small perturbations;
- Failure progresses in the adjacent areas of the structure.

6- *Mixed-type collapses* are different varieties of progressive collapse mechanisms that can be a combination of the types mentioned above. Fall into this class also the collapses that can not be recognised and described. Starossek, in his paper [13], gives, as an example of this particular collapse class: the partial destruction of the Alfred P. Murrah Federal Building presented in chapter 1.

Moreover, These six collapse classes, described above, may be further categorised considering their main peculiarities:

- *Redistribution class*: In this class can be grouped the collapses in which the surviving structure must redistribute the forces of the failed elements (Zipper-type and Section-type collapses).

- *Impact class*: In this class can be grouped the collapses in which the majority of the potential energy is transformed into kinetic energy (Pancake-type and Domino-type collapses).
- Since Instability-type and Mixed-type do not share distinct aspects, form their own classes.

However, when a massive difference (disproportion) in size, between the local damage and the final collapse, is detected, we speak of **Disproportionate collapse**.

Therefore, considering the two definitions of progressive and disproportionate collapse explained above, it can be inferred that the former is linked to the failure propagation in the structure and then with the system response against the local failure. Instead, the latter is closely related to the relationship between the initial damage and the final structural losses suffered by the system. Thus, no descriptions of the structural behaviour are needed from the definition of disproportionate collapse. Furthermore, differently from the progressive collapse that can be described and identified, disproportionate collapse needs to be quantified via a precise measure. Besides, it should be noticed that a progressive collapse might be proportionate in size (for instance if the structure has been designed considering the presence of some elements that might stop the chain of failures) and contrarily, a collapse might be disproportionate in size even if the propagation of failures does not happen. Eventually, Table 3.1 resumes some definitions of progressive and disproportionate collapse, according to Adam et al. [12].

A reduction of the progressive collapse risk may be reached by donating adequate structural robustness to the structure. In section 3.1.3, the notion of structural robustness will be extensively explained.

3.1.2.1 Progressive collapse risk

In their papers, Ellingwood and Dusenberry [14] and Ellingwood [15], proposed a method to evaluate the probability of progressive collapse. The procedure was based on the following equation:

$$P(C) = P(C|DH) \cdot P(D|H) \cdot P(H) \tag{3.1}$$

where:

- $P(C)$ is the progressive collapse probability;
- $P(H)$ is the hazard occurrence probability H;
- $P(D|H)$ is the probability of local damage D as a result of the hazard H;
- $P(C|DH)$ is the probability of progressive collapse C of the structure as a result of local damage D caused by the hazard H.

Looking at Eq. 3.1, it should be noticed that three ways can be followed to reduce the probability of progressive collapse: controlling accidental events, controlling the behaviour of the local elements and controlling the behaviour of the global system. Obviously, it is almost impossible controlling accidental events for a structural engineer. Therefore, designers should focus on controlling the local and global system behaviour, namely $P(D|H)$ and $P(C|DH)$.

Table 3.1: Selected definitions of progressive and disproportionate collapse from [12].

Source	***Definition***
Allen and Schriever	*Progressive collapse [...] can be defined as the phenomenon in which local failure is followed by collapse of adjoining members which in turn is followed by further collapse and so on, so that widespread collapse occurs as a result of local failure.*
Gross and McGuire	*A progressive collapse is characterized by the loss of load-carrying capacity of a relatively small portion of a structure due to an abnormal load which, in turn, triggers a cascade of failure affecting a major portion of the structure.*
GSA guidelines	*Progressive collapse is a situation where local failure of a primary structural component leads to the collapse of adjoining members which, in turn, leads to additional collapse. Hence, the total damage is disproportionate to the original cause.*
ASCE 7-05	*Progressive collapse is defined as the spread of an initial local failure from element to element resulting, eventually, in the collapse of an entire structure or a disproportionately large part of it.*
Ellingwood	*A progressive collapse initiates as a result of local structural damage and develops, in a chain reaction mechanism, into a failure that is disproportionate to the initiating local damage.*
Canisius et al.	*Progressive collapse, where the initial failure of one or more components results in a series of subsequent failures of components not directlyaffected by the original action is a mode of failure that can give rise to disproportionate failure.*
NISTIR 7396	*Progressive collapse — The spread of local damage, from an initiating event, from element to element resulting, eventually, in the collapse of anentire structure or a disproportionately large part of it; also known as disproportionate collapse.*
Agarwal and England	*Disproportionate collapse results from small damage or a minor action leading to the collapse of a relatively large part of the structure. [...]Progressive collapse is the spread of damage through a chain reaction, for example through neighbouring members or storey by storey. [...]Often progressive collapse is disproportionate but the converse may not be true.*
Krauthammer	*Progressive collapse is a failure sequence that relates local damage to large scale collapse in a structure.*
Starossek and Haberland	*Disproportionate collapse. A collapse that is characterized by a pronounced disproportion between a relatively minor event and the ensuing collapse of a major part or the whole of a structure.Progressive collapse. A collapse that commences with the failure of one or a few structural components and then progresses over successively affected other components.*
Kokot and Solomos	*Progressive collapse of a building can be regarded as the situation where local failure of a primary structural component leads to the collapse of adjoining members and to an overall damage which is disproportionate to the initial cause.*
Parisi and Augenti	*Progressive collapse [...] is a chain reaction mechanism resulting in a pronounced disproportion in size between a relatively minor triggering event and resulting collapse, that is, between the initial amount of directly damaged elements and the final amount of failed elements.*

3.1.2.2 Inadequacy of current design methods for progressive collapse resistance

According to Starossek [16], the current design methods are not suitable to design a structural system with the proper progressive collapse resistance. Kokot [3], summarize in detail the reasons for this inadequacy:

- Actual design standards are focused on local failure and do not consider enough global failure. Indeed, global structural safety is a function that depends on the safety of all the

elements against local failure. Moreover, different types of structures can react differently to local damage. Therefore, considering Eq. 3.1, actual codes do not consider the term $P(C|DH)$.

- Another aspect that is not enough treated by actual codes refers to the low-probability events. Indeed, events E for which $P(E)$ is minimal are not considered by standards. The problem derives from the fact that if we consider an initial local failure for a high-rise building, which consists of loosing many vertical load-bearing elements in a storey, the probability of collapse becomes the sum of the failure probability of each element. This means that for buildings with a high number of floors, a low likelihood of local failure becomes a high probability of global failure that should be considered.

- The last inadequacy of current design procedures regards the fact that the probabilistic approach needs a specification of acceptable failure probability. Until now, the target failure probabilities have been derived from early deterministic design codes and considering the massive losses that could derive from a progressive collapse it would be tough to reach agreement from the society on acceptable value for the probability of progressive failure.

3.1.2.3 Different strategies of progressive collapse design

Kokot, in his paper [3], summarizes the most relevant aspects of the two general strategies that can be followed in the structural design against progressive collapse, the "Specific Local Resistance Method"and the "Alternative Load Path Method". Especially describing the research work done by Starossek and Wolff [17], he explains the differences between the two design strategies applying them to a simplified scheme of the Alfred P. Murrah Federal Building (Fig. 3.2). In the **Specific Local Resistance Method**, local damage is not permitted. Therefore, the most critical load-bearing elements must be designed to withstand a high level of loading. A graphic representation of this can be seen in Fig. 3.3, where the columns at the base of the building are designed to withstand intense accidental action such as explosions and car collisions. Another viable option consists of using particular barriers to shield the columns from impact, creating a protecting perimeter around the vertical elements (Fig. 3.4).

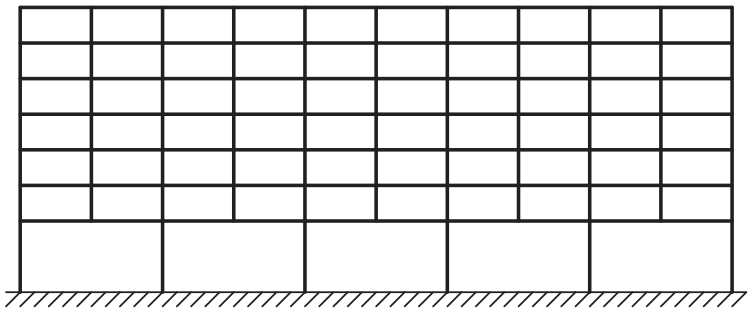

Figure 3.2: Base structure. From Kokot [3].

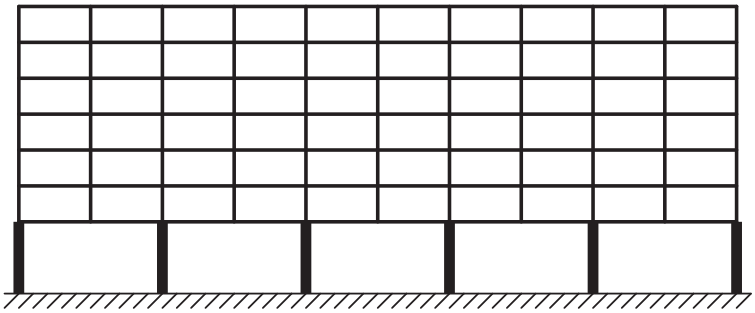

Figure 3.3: Specific Local Resistance Method. From Kokot [3].

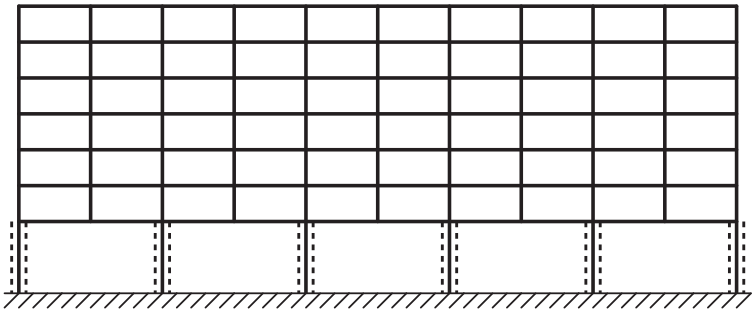

Figure 3.4: Protective barriers. From Kokot [3].

The other possible strategy is represented by the **Alternate Load Path Method**. In this approach, some local damage is allowed, but the structure must be designed guaranteeing the development of alternative load paths that ensure the redistribution of loads after the loss of the vertical load-bearing elements (Fig. 3.5). This behaviour of the structure can be achieved in various forms such as, designing more load-bearing elements (Fig. 3.6) or strengthening the transfer slabs, as shown in Fig. 3.7. Speaking on high-rise buildings, due to the complication caused by this type of structures and the high losses that could derive from a collapse, the design becomes more challenging. Indeed, Starossek, in a different paper [18], analyses the progressive collapse strategies that might be applied. These include nonstructural protective measures, use of the specific local resistance method and alternative paths method, isolation of collapsing sections and application of prescriptive design rules.

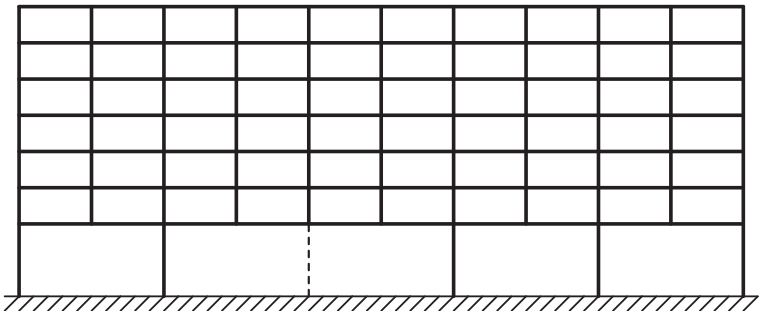

Figure 3.5: Vertical load-bearing element failure. From Kokot [3].

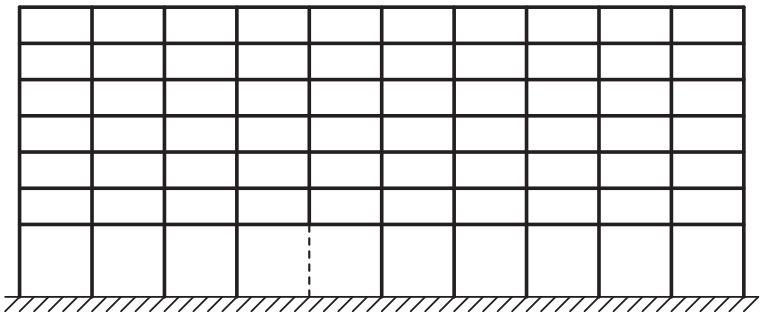

Figure 3.6: Introduction of more columns. From Kokot [3].

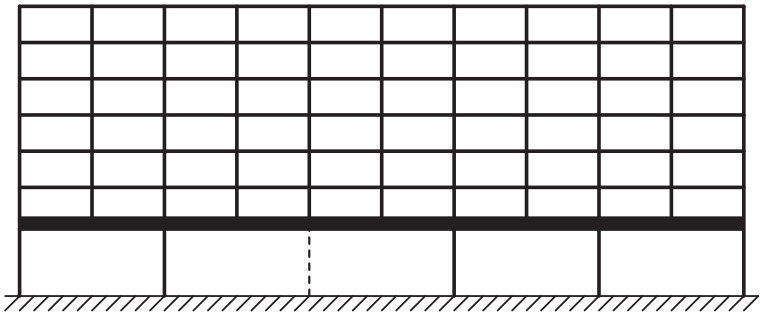

Figure 3.7: Reinforcing of transfer girders. From Kokot [3].

Always considering the case of a high-rise building, applying the specific local resistance approach, Starossek proposes that a primary load transfer system could take the form of a massive tube, as shown in Fig. 3.8. As the core is a key element, the tubular system should be realized, for example, with high-resistance reinforced concrete walls with a thickness of at least one meter. Moreover, since any openings in the core could decrease the resistance of the structure, the core should not be placed in the external perimeter (see Fig. 3.8). Furthermore, a secondary load transfer system should be used, for instance, in the form of cantilever floors fixed to the primary system (the core). These cantilever floors should be designed in accordance with the alternate load path method, guaranteeing that any local damage does not lead to a partial or total collapse. Admissible damages that could happen to the secondary load transfer system are resumed in Fig. 3.9. As can be seen from Figure 3.9, an adequate rotational capacity of the plastic hinges, as well as a sufficient ductility, must be ensured. However, Starossek precise, in his paper, that these requirements are not so easy to be reached in reinforced concrete elements and therefore haunched steel girders should be used. A different solution to limit the consequences of local damage is represented by the segmentation of the second load transfer system using particular joints, as shown in Fig. 3.10. Nevertheless, considering some examples such as the collapse of the World Trade Center in 2001, Starrosek concludes that the alternate load paths method, for the primary structural level, is almost impossible to be achieved for modern high-rise buildings. Therefore, the segmentation approach could be more effective in limiting the chain of collapses originated by a local failure, in Fig. 3.11, a representation of this methodology applied to a tall building is explained. More in detail, assuming that in case of failure of one or more storeys, the failure front progresses verti-

cally and, simultaneously, the upper part of the building moves down as a rigid body, the height of each segment should not be higher than one-tenth of the total height of the building.

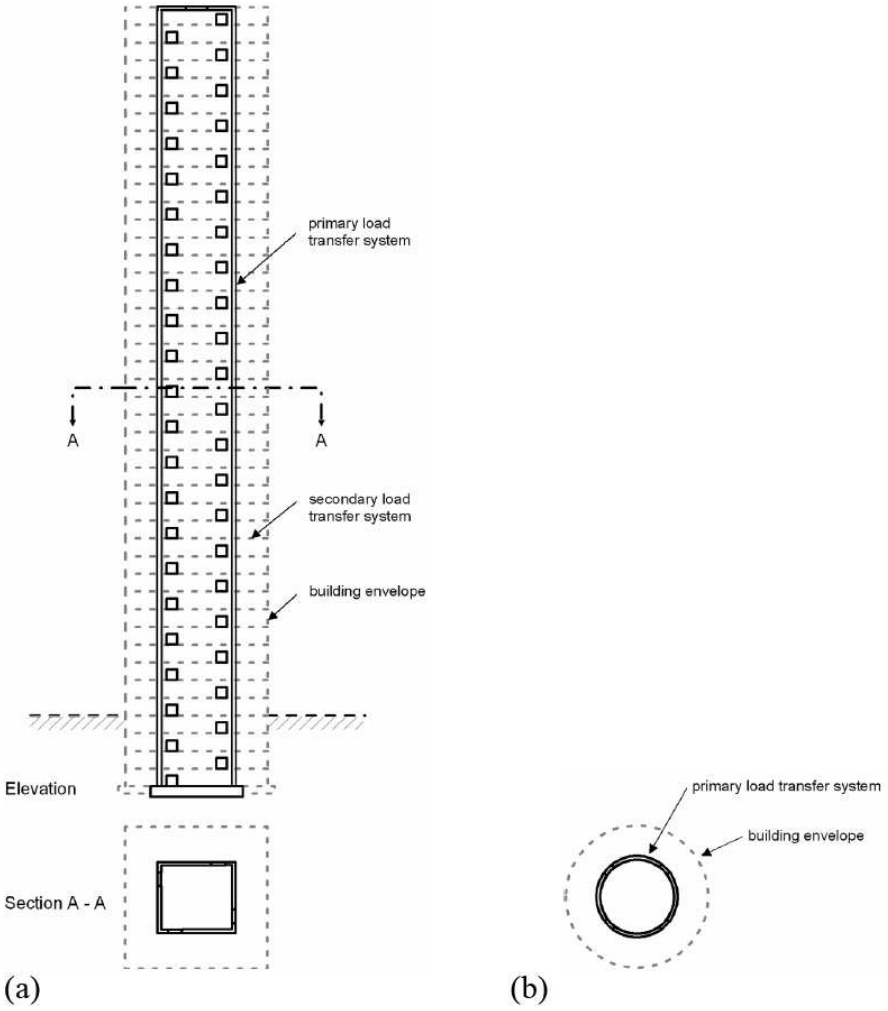

Figure 3.8: Primary load transfer system: a) Elevation and rectangular cross-section, b) Circular cross section. From Starossek [18].

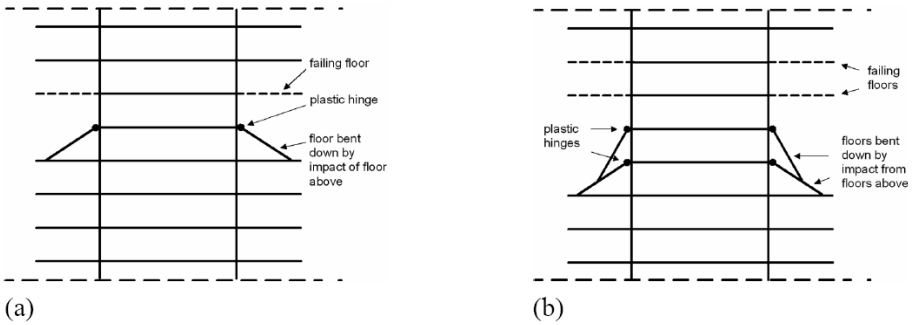

Figure 3.9: Assumed damage and admissible deformation in secondary load transfer system: a) Considering the impact of one floor on another below, b) Considering the impact of two floors on another two below. From Starossek [18].

The most massive forces originated during the impact, occurs when the upper part of the building, together with the debris, collide against the lower section of the structure. During this type of failure, there are several options to prevent progressive collapse. A thick prestressed concrete slab could be designed to withstand the impact. One other option consists of designing two slabs which contain shock-absorbing devices between them (Fig. 3.11). These shock-absorbing devices could be designed as telescoping steel tubes of large diameter filled with a material that enables high compressive strain such as scrap metal or porous tuff gravel (Fig. 3.11c).

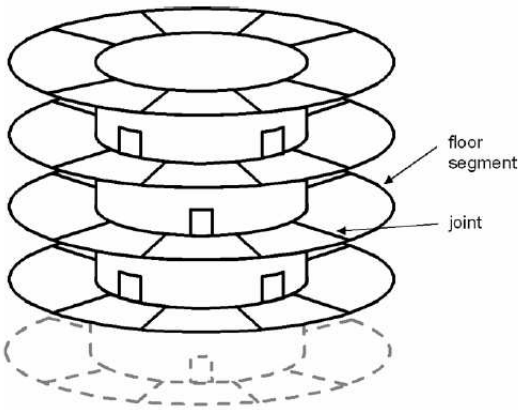

Figure 3.10: Segmentation of secondary load transfer system. From Starossek [18].

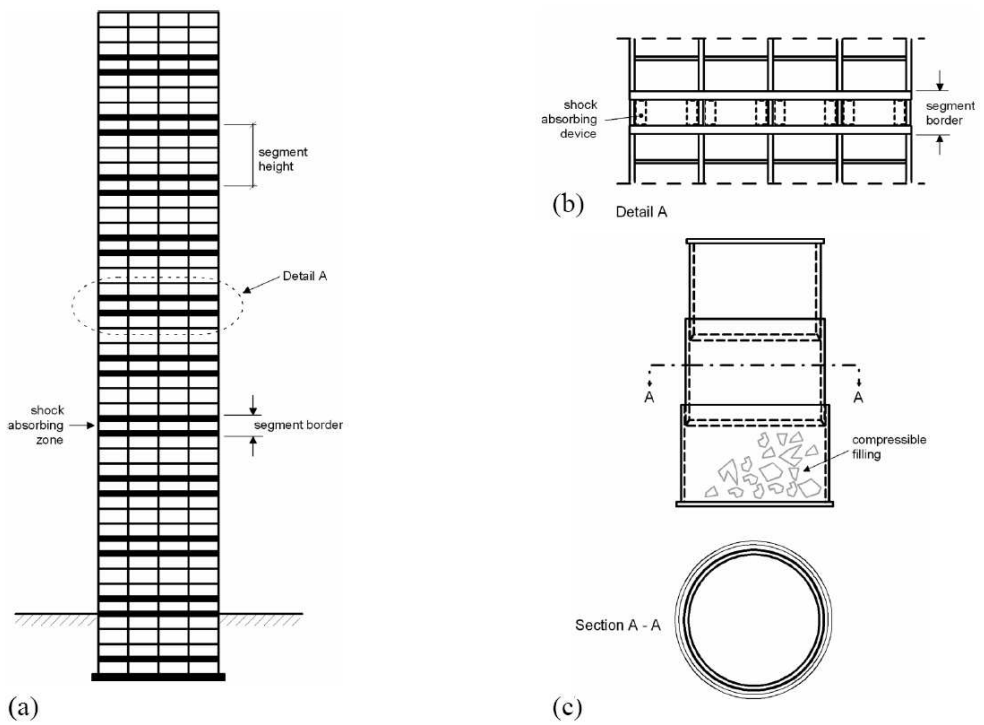

Figure 3.11: Segmentation approaches: (a) Overall view of a building with vertical segmentation, (b) Detail of the shock-absorbing section, (c) Shock-absorbing apparatus: telescoping steel tubes with compressible filling. From Starossek [18].

3.1.3 Structural robustness definitions

As said in the previous sections, a reasonable approach to mitigate the consequences that could derive from a progressive collapse is based on risk reduction through structural robustness. The structural robustness of a building is a threat-dependent characteristic of the whole structural system as it depends on various factors. Indeed, some system's features such as strength, ductility, redundancy, continuity but also the attributes of the accidental loading, that could be single or multiple, dynamic or impulsive, monotonic or cyclic, are very relevant in defining the structural robustness of the system. The next table provides some definitions of structural robustness from the literature resumed by Adam et al. in his paper [12].

Table 3.2: Selected definitions of progressive and disproportionate collapse from Adam et al. [12].

Source	***Definition***
GSA guidelines	*Robustness – Ability of a structure or structural components to resist damage without premature and/or brittle failure due to events like explosions, impacts, fire or consequences of human error, due to its vigorous strength and toughness.*
EC1 – Part 1–7	*Robustness: The ability of a structure to withstand events like fire, explosions, impact or the consequences of human error, without being damaged to an extent disproportionate to the original cause.*
Bontempi et al.	*The robustness of a structure, intended as its ability not to suffer disproportionate damages as a result of limited initial failure, is an intrinsic requirement, inherent to the structural system organization.*
Agarwal and England	*Robustness is [...] the ability of a structure to avoid disproportionate consequences in relation to the initial damage.*
Biondini et al.	*Structural robustness can be viewed as the ability of the system to suffer an amount of damage not disproportionate with respect to the causes of the damage itself.*
Vrouwenvelder	*The notion of robustness is that a structure should not be too sensitive to local damage, whatever the source of damage.*
JCSS	*The robustness of a system is defined as the ratio between the direct risks and the total risks (total risks is equal to the sum of direct and indirect risks), for a specified time frame and considering all relevant exposure events and all relevant damage states for the constituents of the system.*
Starossek and Haberland	*Robustness. Insensitivity of a structure to initial damage. A structure is robust if an initial damage does not lead to disproportionate collapse.*
Fib Model Code 2010	*Robustness is a specific aspect of structural safety that refers to the ability of a system subject to accidental or exceptional loadings (such as fire, explosions, impact or consequences of human errors) to sustain local damage to some structural components without experiencing a disproportionate degree of overall distress or collapse.*
Brett and Lu	*[...] ability of a structure in withstanding an abnormal event involving a localized failure with limited levels of consequences, or simply structural damages.*

3.1.4 Abnormal loads definition

In general, actions can be defined as forces, acting statically or dynamically. The entity of an effort depends on the probability of occurrence considered or through the definition of particular exceptional events or scenario such as a terrorist's attack which by their nature cannot be dealt with on a probabilistic basis with classical methods.

By definition, an exceptional load is an action, usually of short duration but of a significant entity, with a very low probability of occurrence during the useful design life of the structure itself. Therefore accidental actions are related to low-probability/high-consequence (LPHC) events that have a low probability of occurrence, but they are expected to induce considerable losses in terms of victims, restoration costs, and downtime. The following is a list of possible LPHC events:

- Extreme natural events, such as large landslides, flash floods, windstorms, strong earthquakes;
- Explosions, impacts, and fire;
- Malicious actions;
- Human errors in design, construction, usage or maintenance;
- Deterioration phenomena.

For generic accidental situations, if the threat can be probabilistically modelled and determined, are possible two design typology, a “Threat Dependant Approach”and a “Threat Independent Approach”. Differently, if the evaluation is carried out concerning events that are even not imaginable, due to a knowledge gap, only a “Threat Independent Approach”is allowed for the design or assessment, considering initial damage to the building or notional actions.

3.2 Measures of structural robustness and vulnerability

To assess the safety against progressive collapse, a measure of structural robustness is needed. Moreover, robustness measures are also used to estimate losses, and to decide when a level of robustness is acceptable or not. However, it is essential to remark that any qualitative definition of structural robustness does not allow to estimate the consequences of a possible future accidental event. Adam et al., in his paper [12], indicates the general requirements that a robustness measure should have:

- *Expressiveness* ensures a correct evaluation of the structural robustness without influence by other aspects. A measure with this attribute allows distinguishing robust structure from a non-robust structure;
- *Objectivity* ensures that the measure is not sensitive to user decisions;
- *Simplicity* is a characteristics of the measure’s description;
- *Calculability* guarantees the evaluation of the measure with low computational costs;
- *Generality* ensure that the measure is suitable for all the possible types of structures.

Therefore, a measure of structural robustness which respects these five attributes allows evaluating different structural types with high reliability and low costs. The different measures of robustness, present in the literature, which have been summarized by Kokot [3], can be divided into two types, those based on structural behaviour and those based on structural attributes.

3.2.1 Measures based on structural behaviour

3.2.1.1 Proposals by Starossek and Haberland

Starossek and Haberland [19] [20] introduced two measures of robustness based on structural behaviour and another one based on structural attributes. Thus, the first measure introduced by the authors is based on structural damage and defined as follow:

$$R_d = 1 - \frac{p}{p_{lim}} \tag{3.2}$$

Where:

- R_d: is the robustness measure based on structural damage;
- p: is the maximum damage progression caused by the assumed initial damage i_{lim};
- p_{lim}: is the maximum accetable extent of damage.

A different variant of this measure of robustness can be written as:

$$R_{d,\,int} = 1 - 2\int_0^1 [d(i) - i]di \tag{3.3}$$

Where:

- $R_{d,\,int}$: is the integral robustness measure based on damage;
- $d(i)$: is the maximum amount of total damage caused by including the initial damage i. It is based on the value for an intact building;
- i: is the extent of initial damage based on the intact building.

Kokot, in his paper [3], provides an effective graphic representation of this robustness measure. The illustration in Fig. 3.12 represents the damage progression. More in detail, curve A represents a non-robust structure where even modest initial damage can lead to considerable global damage $d(i)$. Differently, curve B represents a robust structure where only extended initial damages can lead to significant structural deterioration.

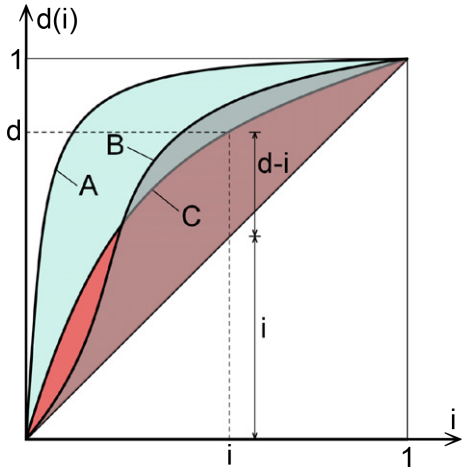

Figure 3.12: Damage evolution graph. From Kokot [3].

The second measure of robustness, proposed by Starossek and Haberland [19] [20], is based on energy and can be written as:

$$R_e = 1 - \max_j \frac{E_{r,j}}{E_{s,k}} \tag{3.4}$$

Where:

- R_e: is the robustness measure based on energy;
- $E_{r,j}$: is the amount of energy released by the initial failure of the structural element j and available for damaging the next structural element k;
- $E_{s,k}$: is the energy required for the failure of the next structural element k.

3.2.1.2 Proposal by Lind

Lind [21] [22] proposed a probabilistic representation of vulnerability, robustness and their related measures. The presented definitions are aimed to apply to all kinds of engineering systems. Lind, to defines the vulnerability, expresses $P(r, S)$ as the probability of failure of the system in a state r for loading S and r_0 as an initial system state. Eventually, indicates r_d as a particular damaged status. Then the vulnerability is defined as:

$$V = V(r_d, S) = \frac{P(r_d, S)}{P(r_0, S)} \tag{3.5}$$

It should be noticed that the vulnerability presented in Eq. 3.5 reach the unit value if the probability of failure in the damaged configuration is the same as the one in the undamaged arrangement. Furthermore, the measure of the structural robustness is defined as the reciprocal of the vulnerability:

$$T = \frac{P(r_0, S)}{P(r_d, S)} \tag{3.6}$$

It is crucial to assign realistic distributions of probability to obtain realistic measures of robustness and vulnerability.

3.2.1.3 Proposal by Baker et al.

Baker et al. [23] proposed a procedure to evaluate the structural robustness for systems subjected to structural damage. The idea consists of creating an event tree, as explained below. The first step is assuming that the structure is affected by a specific abnormal load situation. Subsequently, the structure system could be damaged or not. In case of no damage, no additional analyses are needed, but instead, if the damage happens, different scenarios can appear. For each possible damage states, a probability of failure and its potential direct and indirect consequences must be assigned. More in detail, consequences take multiple forms such as inconvenience to system users, injuries, victims and costs. Moreover, direct consequences are connected to initial damage, and the indirect ones are related to subsequent system failure.

When each value is defined, Lind proposed the evaluation of an index of robustness I_R, that measures the fraction of the total system risk resulting from direct consequences. This Index can

be defined as follow:

$$I_R = \frac{R_{Dir}}{R_{Dir} + R_{Ind}} \tag{3.7}$$

Where R_{Dir} and R_{Ind} represents direct and indirect risks. These direct and indirect risks are estimated by multiplying the consequences of each possible event scenario by its probability of occurrence and then integrating over all the random variables in the event tree.

3.2.1.4 Proposal by Wisniewski et al.

Wisniewski et al., in his paper [24], describe the load-capacity evaluation of existing railway bridges carried out with robustness quantification. The notion of structural robustness applied to a bridge is correlated to the capacity of the structure to carry loads after the failure of one or more structural elements. The authors of the paper, to calculate the robustness of a railway bridge, define a redundancy factor based on redundancy ratios that compare the load-carrying capacity in the ultimate limit states with the design value. The critical value for the redundancy factor is one. Bridges with a smaller value should be considered not safe while bridges with grater values should be considered as safe structures.

3.2.1.5 Proposals by Maes et al.

Maes et al. [25] introduced three measures of structural robustness. The first measure is based on the assumption that the system's resistance, after the loss of an element i, can be maintained to a sufficient level. This measure of robustness can be calculated as follow:

$$R_1 = \min_i \frac{RSR_i}{RSR_0} \tag{3.8}$$

Where RSR_i is the reserve strength ratio when a structural element i is compromised, and RSR_0 is the reserve strength ratio when no structural component is compromised.

The second measure proposed by Maes el al. can be described in terms of system reliability as:

$$R_2 = \min_i \frac{P_{s0}}{P_{si}} \tag{3.9}$$

where P_{s0} is the probability of failure of the undamaged system subjected to a design load and P_{si} is the probability of failure of the system when an element i is compromise.

The last measure introduced by Maes et al. is based on sample functions of failure consequences versus hazard intensity and the conditional probability of exceedance versus failure consequences. Calculating the inverse of the tail heaviness H of the conditional probability of exceedance versus failure consequences the measure of robustness R_3 can be obtained. Maes et al. [25], states that the tail of any given probability distribution can be simply calculated and if the value H is inferior to one, it means that the robustness of a structure is very high. Otherwise, if H is one or larger than one the structural robustness of the structure low and very low respectively.

3.2.1.6 Proposal by Smith

Smith [26] suggested a measure of structural robustness based on the theory of fast fracture in fracture mechanics. The theory states as follow:

> *If the energy released by loss of a damaged member is greater than the energy absorbed by the totally damaged member and other partially damaged members, then the progressive collapse will occur.*

This method consists of realizing finite element analysis applied to the structure and using graph theory finding the sequence of damage events that requires the smallest amount of energy. Therefore, the minimum damage energy needed is the measure of the robustness of the structure considered.

3.2.1.7 Proposal by Menchel

Menchel [27] proposed a measure of the structural robustness considering the removal of a column. He defines an indicator as to the maximum multiplying load factor that can be applied to the vertical loads (dead and live) when applied statically on the structure that has lost a vertical load-bearing element. The indicator of robustness can be determined following the order below:

1) Removal of a vertical load-bearing element from the model;
2) Apply the loads statically and multiplying them for an increasing factor;
3) When the structure is not able to redistribute the loads anymore, the factor that is applied to the vertical loads is the indicator of robustness.

Therefore, the indicator of robustness is a measure of the reserve resistance of a structure with reference to the vertical loads applied to it and considering the removal of a specific vertical load-bearing element.

3.2.2 Measures based on structural attributes

3.2.2.1 Proposal by Starossek and Haberland

As mentioned before the third measure of robustness defined by Starossek and Haberland [20], falls into the category of measures based on structural attributes. In this particular case, the measure utilizes structural stiffness and can be expressed as:

$$R_s = \min_j \frac{det\ \mathbf{K}_j}{det\ \mathbf{K}_0} \tag{3.10}$$

where R_s is the robustness measure based on the structural stiffness, $\mathbf{K}_0$ and $\mathbf{K}_j$ are the global stiffness matrix of the undamaged structure and the one of the structure after the vertical load-bearing element j removal. It should be noticed that this approach can be suitable for Zipper-type collapse and worthless for Pancake-type or Domino-type collapses as defined in section 3.1.2. Moreover, this formulation is relatively simple and easy to be calculated.

3.2.2.2 Proposal by Agarwal et al.

Agarwal et al.[28] proposed a topological measure of vulnerability. The focus of this methodology investigates the potential hazards existing in the structural form, which could be activated by unexpected events or abnormal loads situations. The methodology presents three steps that should be followed: the first consists of identifying structural rings and rounds. In the second, a hierarchical description of the structure should be realized. Eventually, in the last step, it is necessary looking for vulnerable scenarios hidden in the hierarchical description. This methodology can be applied to 2D and 3D frames.

3.3 Numerical modelling

The progressive collapse of a structure is a complex event for many reasons. Indeed, it includes nonlinear materials behaviour, impacts and collisions, large deformation and dynamics. However, thanks to the improvements reached in the modelling programs, today, it is possible to treat and analyze these complex problems through numerical models obtaining accurate results, how have been demonstrated by comparing them to experimental results. Furthermore, numerical simulation has numerous advantages. For instance, it is an inexpensive method as it does not need experimental tests and the destruction of real structures. Adam et al., in his paper [12], summarized the most relevant typology of numerical modelling actually used:

- **Finite Element Method (FEM)**:

  Actually, it is the most used methodology of numerical modelling. It is employed on different levels and degree of approximation. Moreover, this technique allows the creation of macro-models, micro-models, macro-models of joints-connections and also hybrid models.

- **Discrete Element Method (DEM)**:

  The DEM models have not been used frequently so far by the researchers to analyze progressive collapse problems. However, this technique has various advantages, such as the capability to combine DEM and FEM models and obtain very accurate results.

- **Applied Element Method (AEM)**:

  The AEM models have been used very often during the past years for simulation of entire buildings but also sub-assemblages. One of the main reasons for its success between the researchers is that it has demonstrated to be very effective, giving accurate results.

- **Cohesive Element Method (CEM)**:

  This particular method is more often used in the fracture mechanics field but can also be employed to simulate the progressive collapse of structures. The results obtained using this method have demonstrated that CEM is as precise as conventional nonlinear analysis and sometimes even more accurate.

Due to its simplicity and reliability, in this Thesis work, the *Finite Element Method (FEM)*, will be used to create a 3D model of the Pirelli Tower and assess its structural robustness. Therefore, the next section deepens the characteristics of this methodology.

3.3.1 Finite Element Method

As said before, the Finite Element Method is the most extensively used approach in the numerical simulation of progressive collapse of structures. The simulation of progressive collapse using a FEM model can be realized at different levels of approximation and complexity. For instance:

a) Using micro or macro-models;

b) Using linear or non-linear analysis;

c) Considering static or dynamic behaviour;

d) Realizing 2D or 3D models;

e) Implicit or explicit calculation.

The differences between a macro and a micro-model are mostly related to the precision that can be achieved. Usually, for an entire structure, a macro-model is preferable, otherwise, for small elements, a micro-model is more suitable. More in detail, macro-models simulate the structure with beam and shell elements and are mostly used to analyze progressive collapse from a threat-dependent viewpoint. However, special attention should be paid to beam-column and slab-beam joints. These parts are the more complex zones of the buildings because they are characterized by large rotations, deformations and catenary-membranes actions. Therefore, in order to better capture the structural behaviour under large deformations, different types of elements are sometimes combined. These models that are recognized as multi-scale or hybrid models have one critical aspect that consists of the interaction between the different types of elements. This aspect should be very well considered to ensure deformation compatibility and reasonable constraint conditions.

With regards to linear or non-linear analysis, actual standards allow both types but the latter option lead to models that are capable of obtaining more accurate results as it is possible to follow the structure iteratively until its failure. The same happens considering static or dynamic analyses, the latter is way more precise. However, it should be noticed that with the precision also the computational costs groove with non-linear or dynamic analyses. Indeed, although, modern computers can handle cumbersome calculations, a simulation considering non-linear dynamic analysis could take considerable time to be processed. Moreover, implicit calculation very often has convergence problems in non-linear dynamic simulations, while explicit calculation leads to more accurate results.

Eventually, it should be kept in mind that some regulations do not allow the use of 2D simulation to verify the behaviour of a structure against the progressive collapse.

3.4 Thoughts on the state of research

The purpose of this chapter was to summarize the most relevant results of the research in the progressive collapse field. As said before, this research area is very recent and involves very complex aspects, needing much time and resources. For these reasons, the progressive collapse studies, developed until now, were mostly focused on restricted structural classes:

- Substructures;
- Frame buildings;
- Low-rise building.

The focus of the speech is that many aspects concerning the structural robustness and progressive collapse still need to be investigated. For instance, very few studies involving high-rise buildings and how these can develop alternative load paths in case of local failures, have been realized so far. This lack of studies is precisely the reason why the assessment of the structural robustness of an iconic Italian skyscraper was chosen as the argument of this Thesis.

Chapter 4

Structural robustness in Eurocodes

4.1 EN 1990 - Eurocode 0: Basis of structural design

The Eurocodes are the European standards of the structural design. Ten different parts cover the various construction disciplines and the *Eurocode 0: Basis of structural design* [29] summarizes the philosophy of these structural norms. Therefore, it establishes the principles and requirements for safety, serviceability and durability of structures. Lastly, it describes the basis for design and verification. More in detail, the § 2.1 (4)P of the EN 1990 [29] has particular relevance to structural robustness; it states that:

> *A structure shall be designed and executed in such a way that it will not be damaged by events such as: explosion, impact and the consequences of human errors, to an extent disproportionate to the original cause.*

In § 2.1 (5)P of the EN 1990 [29], there is another important statement that has particular relevance in the structural robustness field:

> *Potential damage shall be avoided or limited by appropriate choice of one or more of the following*:
>
> - *Avoiding, eliminating or reducing the hazards to which the structure can be subjected;*
> - *Selecting a structural form which has low sensitivity to the hazards considered;*
> - *Selecting a structural form and design that can survive adequately the accidental removal of an individual member or a limited par t of the structure, or the occurrence of acceptable localised damage;*
> - *Avoiding as far as possible structural systems that can collapse without warning;*
> - *Tying the structural members together.*

As said before, the EN 1990 [29] contains structural philosophies rather than precise design directives. For detailed guidelines and accurate definitions, it is necessary referring to the EN 1991 [30].

4.1.1 Load combinations for accidental design situations

Agreed with the indications provided in EN 1990 [29] at § 6.4.3, accidental actions should be applied simultaneously and in combination with permanent and variable loads:

$$\sum_{j\geq 1} G_{k,j} + P + A_d + (\Psi_{1,1} \text{ or } \Psi_{2,1})Q_{k,1} + \sum_{i>1} \Psi_{2,i}Q_{k,i} \tag{4.1}$$

Where:

- G: Permanent load;
- P: Prestressing action;
- A_d: Design accidental action;
- Q: Variable load;
- Ψ_1: Factor for frequent value of a variable action;
- Ψ_2: Factor for quasi-permanent value of a variable action.

In agreement with the prescriptions of the norm, the value of the accidental action A_d should include an explicit accidental action for fire and impact. In case of a reference to the particular situation after an accidental event, A_d should be taken equal to zero. Recommended values for Ψ_1 and Ψ_2, depending on the building categories, can be found in Table A1.1 of Annex A of EN 1990 [29] and the choice between the two coefficients is related to the relevant accidental design situation (impact, fire or survival after an accidental situation). With regards to the value of A_d, the EN 1990 [29] says that should be specified for individual projects based on EN 1991 [30].

With regards to the dynamic actions, at § 5.1.3(3) in EN 1990 [29], is indicated that, when a structure is analyzed in a quasi-static way, the dynamic effects should be included by applying an equivalent dynamic amplification factor to the static actions. However, the Eurocode does not specify the value for the dynamic amplification factor.

4.2 EN 1991 - Eurocode 1: Actions on structures

The precise directives to design and realize buildings that are capable of preventing progressive and disproportionate collapses under abnormal loads, or in other words that possess the necessary robustness, are established from the Eurocode EN 1991 [30]. Indeed, in *Part 1-7: general actions-accidental actions* [31] structural robustness has a specific definition:

> *Robustness is the ability of a structure to withstand events like fire, explosions, impact or the consequences of human error, without being damaged to an extent disproportionate to the original cause.*

As said before, this definition points out how structures designed following the indications of these standards, will have the necessary robustness not to suffer disproportionate and progressive collapse.
The same Eurocode also defines what an accidental design situation is:

> *Accidental design situations are design situations involving exceptional conditions of the structure or its exposure, including fire, explosion, impact or local failure.*

The fundamental aim of these standards is to ensure that structures do not suffer a disproportionate collapse under an abnormal load situation. For this purpose, the code provides procedures and rules for safeguarding civil structures against accidental actions. Furthermore, the Eurocode states that localised failure due to accidental actions can be acceptable, given that:

- The local damage must not compromise the stability of the structure;
- The overall load-bearing resistance of the structure must be saved;
- The local damage must not endanger the emergency measures.

Another important aspect handled by the Eurocodes regarding the minimum period that buildings need to survive following an accident. This time should have at least the duration required to facilitate the safe evacuation and rescue of people present inside of the structure and possibly, its surroundings. Clearly, a more considerable amount of time might be necessary for facilities where hazardous materials are used or for strategical systems for national security reasons.

Furthermore, at § 3.2 of the EN 1991 [31], is stated that:

> *The exceptional actions that should be considered depend on:*
>
> - *The measures and actions that have been taken to prevent or reduce the severity of an accidental action;*
> - *The probability of occurrence of the accidental action considered;*
> - *The consequences that a possible failure of the structure could lead;*
> - *The public perception of the risk;*
> - *The considered level of acceptable risk.*

Therefore, local damage due to an accidental action could be acceptable, but it must be granted that this local failure does not threaten the stability and safety of the building. Moreover, one of the following measures should be considered to reduce the risk of accidental actions:

- Preventing the action from occurring;
- Protecting the structure against the effects of an accidental action by reducing its effects on the construction;
- Ensuring that the structure has sufficient robustness.

4.2.1 Design strategies from EN 1991-1-7

Two possible approaches for designing structures against accidental actions are given in this code:

a) Strategies based on identified accidental actions;

b) Strategies based on unidentified accidental actions.

These strategies are also represented in Figure 4.1. About that, the EN 1991-1-7 [31] specifies that:

> *Strategies based on unidentified accidental actions cover a wide range of possible events and are related to strategies based on limiting the extent of localised failure. The adoption of strategies for limiting the extent of localised failure might provide adequate robustness against those accidental actions not specifically covered by this code such as external explosions and terrorist activities, or any other action resulting from an unspecified cause.*

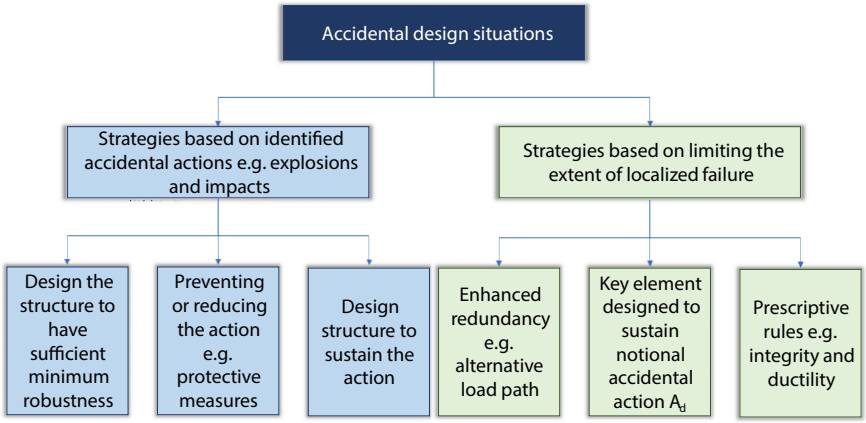

Figure 4.1: Strategies for accidental design situations.

4.2.1.1 Strategies based on identified accidental actions

The EN 1991-1-7 [31] at § 3.2 states:

> *A localised failure due to accidental actions may be acceptable, provided it will not endanger the stability of the whole structure and that the overall load-bearing capacity of the structure is maintained and allows the necessary emergency measures to be taken.*
>
> *Measures should be taken to mitigate the risk of accidental actions and these measures should include, as appropriate, one or more of the following strategies:*
>
> - *Preventing the action from occurring;*
> - *Protecting the structure against the effects of the accidental action;*
> - *Ensuring that the structure has sufficient robustness, by adopting one or more of the following approaches:*

- *By designing certain components of the structure upon which stability depends as key elements;*
- *Designing structural members, and selecting materials, to have sufficient ductility, capable of absorbing significant strain energy without rupture;*
- *Incorporating sufficient redundancy in the structure to facilitate the transfer of actions to alternative load paths following an accidental event.*

4.2.1.2 Strategies based on unidentified accidental actions

For unidentified accidental actions, strategies for limiting the localised failure could be applied. At this purpose, the standard states:

> *In the design, the potential failure of the structure arising from an unspecified cause shall be mitigated.*
> *The mitigation should be reached by adopting one or more of the following approaches:*
>
> - *Designing key elements, on which the stability of the structure depends, to sustain the effects of a model of accidental action A_d;*
> - *Designing the structure so that in the event of a localised failure (e.g. failure of a single member) the stability of the whole structure or of a significant part of it would not be endangered;*
> - *Applying prescriptive design/detailing rules that provide acceptable robustness for the structure (e.g. three dimensional tying for additional integrity, or a minimum level of ductility of structural members subject to impact).*

4.2.1.3 Consequences classes:

The Eurocode allows choosing the strategies for accidental design situations according to consequences classes. The Code's indications are resumed in Table 4.1.

Table 4.1: Consequences class design strategies. From [31].

Consequences class	***Consideration for accidental design situation***
CC1*: low consequences failure*	*No specific consideration is necessary for accidental actions except to ensure that the robustness and stability rules given in EN 1990 to EN 1999, as applicable, are met.*
CC2*: medium consequences failure*	*Depending upon the specific circumstances of the structure, a simplified analysis by static equivalent action models may be adopted or prescriptive design/detailing rules may be applied.*
CC3*: high consequences failure*	*An examination of the specific case should be carried out to determine the level of reliability and the depth of structural analyses required. This might require a risk analysis to be carried out and the use of refined methods such as dynamic analyses, non-linear models and interaction between the load and the structure.*

In the same way, as shown in table 4.2, the Annex A of the EN 1991-1-7 [31] provides a categorisation of building kinds in consequences classes:

Table 4.2: Categorisation of consequences classes. From [31].

Consequences class	*Example of categorisation of building type and occupancy*
CC1	*Single occupancy houses not exceeding 4 storeys. Agricultural buildings. Buildings into which people rarely go, provided no part of the building is closer to another building, or area where people do go, than a distance of 3/2 times the building height.*
CC2a *- Lower Risk Group*	*5 storey single occupancy houses. Hotels not exceeding 4 storeys. Flats, apartments and other residential buildings not exceeding 4 storeys. Offices not exceeding 4 storeys. Industrial buildings not exceeding 3 storeys. Retailing premises not exceeding 3 storeys of less than 1000 m^2 floor area in each storey. Single storey educational buildings All buildings not exceeding two storeys to which the public are admitted and which contain floor areas not exceeding 2000 m^2 at each storey.*
CC2b *- Higher Risk Group*	*Hotels, flats, apartments and other residential buildings greater than 4 storeys but not exceeding 15 storeys. Educational buildings greater than single storey but not exceeding 15 storeys. Retailing premises greater than 3 storeys but not exceeding 15 storeys. Hospitals not exceeding 3 storeys. Offices greater than 4 storeys but not exceeding 15 storeys. All buildings to which the public are admitted and which contain floor areas exceeding 2000 m^2 but not exceeding 5000 m^2 at each storey. Car parking not exceeding 6 storey.*
CC3	*All buildings defined above as Class 2 Lower and Upper Consequences Class that exceed the limits on area and number of storeys. All buildings to which members of the public are admitted in significant numbers. Stadiums accommodating more than 5000 spectators. Buildings containing hazardous substances and lor processes.*

The recommended methods, based on the categorisation described in Table 4.2, are summarised in the following figure:

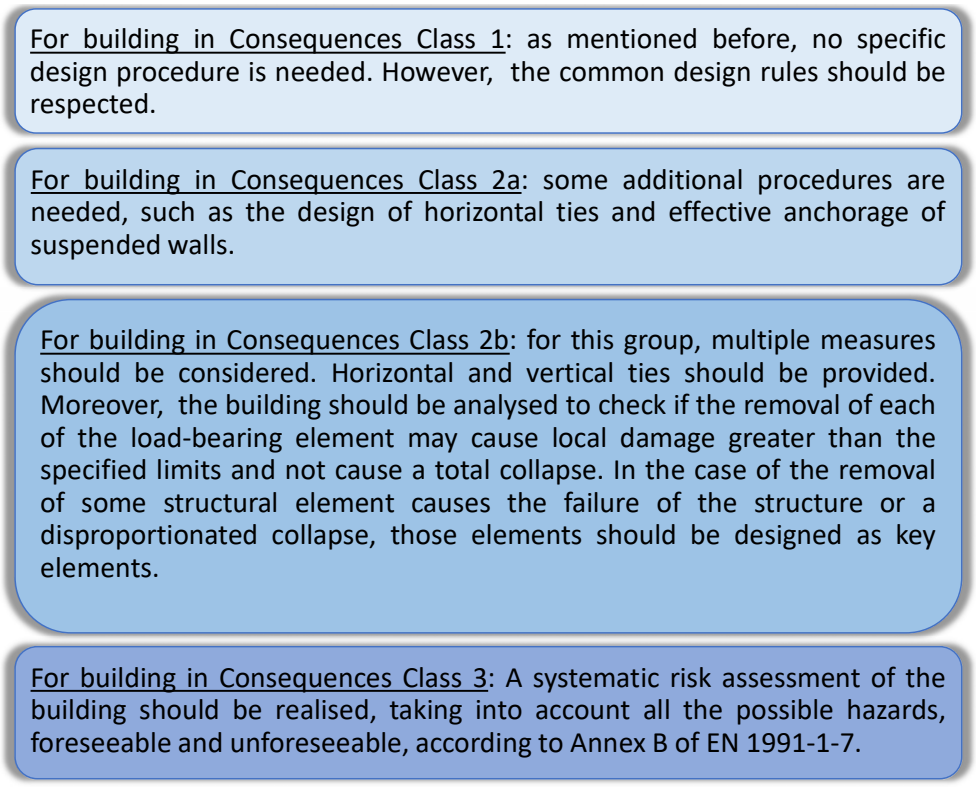

Figure 4.2: Recommended methods for each building category described in Table 4.2.

4.2.1.4 Horizontal ties

Horizontal tying is important for a structure subjected to accidental actions for two main reasons:

- It enables Catenary action to develop (see section 3.1.1 and Fig. 3.1b);
- It helps in holding the columns in place.

For framed structures, the internal ties (and their connections), should be designed to withstand the following tensile load:

$$T_i = 0,8(g_k + \Psi \cdot q_k)sL \quad \text{or} \quad 75\,KN \quad \text{whichever is greater} \tag{4.2}$$

Furthermore, for peripheral ties, the design tensile force is:

$$T_p = 0,4(g_k + \Psi \cdot q_k)sL \quad \text{or} \quad 75\,KN \quad \text{whichever is greater} \tag{4.3}$$

Where:
- s: the spacing of ties;
- L: the ties span;
- Ψ: the same combination factor as in Eq. 4.1.

For load-bearing walls systems, the ties should be incorporated into the building depending on the consequence class. For CC2a buildings, adequate robustness is provided by adopting a cellular form of construction. In this way, the interaction of all components is guaranteed. For CC2b buildings, internal continuous and horizontal ties should be provided on floors and should be distributed throughout the floors in both orthogonal directions. Moreover, peripheral ties extending around the perimeter of the floor slabs within 1,2 meters width of the slab should be designed.

The design tensile forces, for internal and peripheral ties, can be calculated as follows:

- For internal ties:

$$T_i = \frac{F_t(g_k + \Psi \cdot q_k)}{7,5} \cdot \frac{z}{2}\ [KN/m] \quad \text{or} \quad T_i = F_t\ [KN/m] \quad \text{whichever is greater} \tag{4.4}$$

- For peripheral ties:

$$T_p = F_t \tag{4.5}$$

Where:
- F_t: 60 kN/m or $20 + 4n_s$ $[kN/m]$, whichever is less;
- n_s: number of storeys;
- z: smaller value of: $5 \cdot H$ or the greatest distance, in meters, in the direction of the tie, between the centers of the columns or other vertical load-bearing members whether the distance is spanned by a single slab or by a system of beams and slabs;
- H: clear storey height.

4.2.1.5 Vertical ties

Vertical tying is crucial in a structure subjected to abnormal loads as it allows the redistribution of loads through the system, activating alternative load paths that carry the load away from the damaged area (see section 3.1.1).

The Eurocodes specify how all vertical ties, both for frame and wall structures, should be continuous from the foundations to the roof level. Furthermore, in frame structures, vertical ties should be capable of resisting a tensile force equal to the largest design vertical permanent and variable reaction applied to the column of any one storey. This exceptional design load should not be considered acting simultaneously to the permanent and variable loads that can act against the structure.
In the end, at § A.6.(3), the EN 1991-1-7 [31] states that:

> *For wall structures, vertical ties may be deemed effective if:*
>
> a) *The thickness of the masonry walls is at least 150 mm and if they have a minimum compressive strength of 5 N/mm^2;*
>
> b) *The clear height of the wall, measured in meters between faces of floors or roof does not exceed 20 t, where t is the thickness of the wall in meters;*
>
> c) *If vertical ties are designed for the following force:*
>
> $$T = \frac{34 \cdot A}{8000} \cdot \left(\frac{H}{t}\right)^2 \quad \textit{or} \quad 100\,KN/m \quad \textit{of wall, whichever is greater} \tag{4.6}$$
>
> *where A – the cross-sectional area in mm^2 of the wall measured on plan, excluding the non load bearing leaf of a cavity wall;*
>
> d) *The vertical ties are grouped at 5 meters maximum centres along the wall and occur no greater than 2,5 meters from an unrestrained end of the wall.*

4.2.1.6 Notional removal of vertical load bearings elements

The annex A of the EN 1990-1-7, as said before, provides methods to design a building guaranteeing that it can withstand localised failure due to an unknown cause without suffering disproportionate or progressive collapse. In other words, this annex gives some indications to design the building properly against progressive collapse, applying the "Threat Independent Approach".
One of the more essential parts of the annex regards the extent of damage that should be considered in a structure. Indeed, at §A.4.1(c), for building at least in class 2b, states:

> *...The building should be checked to ensure that upon the notional removal of each supporting column and each beam supporting a column, or any nominal section of load-bearing wall as defined in §A.7 (one at a time in each storey of the building) the building remains stable and that any local damage does not exceed a certain limit.*

In the end, in §A.7 the standard provides some practical prescriptions:

The nominal length of load-bearing wall construction referred to in §A.4.1(c) should be taken as follows:

- *for a reinforced concrete wall, a length not exceeding 2,25 H;*
- *for an external masonry, or timber or steel stud wall, the length measured between lateral supports provided by other vertical building components (e.g. columns or transverse partition walls);*
- *for an internal masonry, or timber or steel stud wall, a length not exceeding 2,25 H.*

where:

H is the storey height in metres.

Therefore, the Eurocode provides only the value of maximum damage that should be considered in a structure and does not give the minimum.

4.2.1.7 Key elements

About the key elements, the EN 1991-1-7 [31] states:

A key element is a structural element on which integrity depends the stability of the remaining part of the structure. It should resist an accidental design action of A_d applied in horizontal and vertical directions (one direction at a time). Such accidental design loading should be applied in accordance with Eq. 4.1 and may be concentrated or distributed load. The recommended value of A_d for building structures is 34 kN/m^2.

4.2.1.8 Risk assessment

With regards to risk analysis, at § B.9.2.(1) the EN 1991-1-7 [31] recommends:

The analysis of structures subjected to abnormal loads should follow the following steps:

1 - *Assessment of the probability of occurrence of different hazards with their intensities;*

2 - *Assessment of the probability of different states of damage and corresponding consequences for given hazards;*

3 - *Assessment of the probability of inadequate performance of the damaged structure together with corresponding consequences.*

For category CC3 of buildings, Eurocode EN 1991-1-7 [31] requires a systematic risk assessment for the structure. Risk is defined as a measure of the combination of various aspects, such as the probability of occurrence of a hazard and the magnitude of the consequences. It is expressed as follows:

$$R = \sum_{i=1}^{N_H} p(H_i) \sum_{j}^{N_D} \sum_{k=1}^{N_s} p(D_j|H_i) \cdot p(S_k|D_j) \cdot C(S_k) \tag{4.7}$$

Where:

- N_H: number of different hazards;
- N_D: number of ways the hazards may damage the structure;
- N_S: number of adverse states into which the damage structure can be discretised;
- S_k: adverse states;
- $C(S_k)$: consequences of an adverse state;
- $p(H_i)$: probability of occurrence (within a reference time interval) of the i-th hazard;
- $p(D_j|H_i)$: the conditional probability of the j-th damage state of the structure given the i-th hazard;
- $p(S_k|D_j)$: the conditional probability of the k-th adverse overall structural performance S given j-th damage state.

As can be noticed looking at Eq. (4.7), there are three possible approaches to manage the risk. These are summarized in Fig. 4.3:

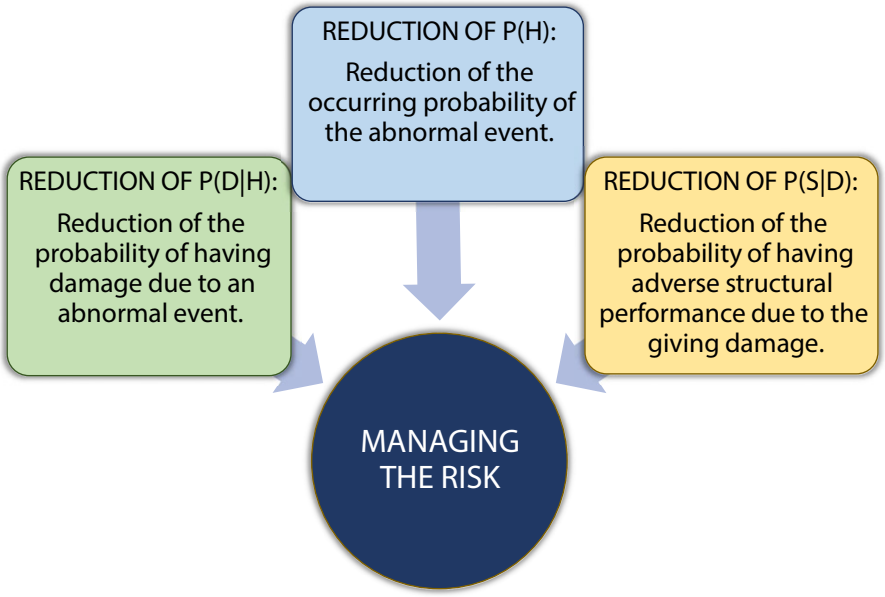

Figure 4.3: Possible approaches to manage the risk.

Chapter 5

The Pirelli Tower

5.1 History of the building

The Pirelli Tower (Fig. 5.1 and subsequent), also called the "Pirellone", was built in front of Milan's Central railway and, with it's 127 meters, was for 35 years, the tallest building in Italy. Moreover, for 50 years it was the highest structure in Milan exceeded only by the Lombardy Building (167 meters height) in 2010. The Pirelli Tower has 31 storeys out of the ground plus two of them underground and used for parking. After its construction, it became one of the best known Milan's symbols and, more generally, the representation of one of the best moment of economic growth in Italy. Even today, this building remains one of the most iconic buildings in Italy, and it is a real symbol of the city of Milan.

The history of this building is fascinating for many reasons. Indeed, the project was really ambitious, especially for the tremendous impact that would have taken on the city of Milan, but also on the architectural history of Italy. Furthermore, in the history of this building, there was a controversial accident: in 2002, an aeroplane crashed into the building, causing three victims [32].

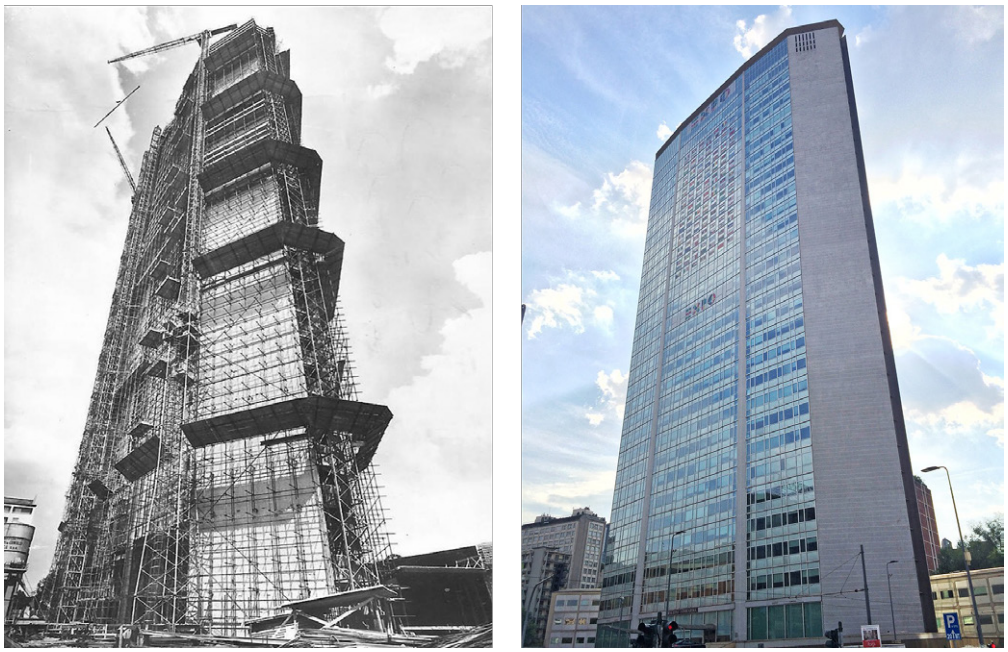

Figure 5.1: Main facade of the Tower during construction (from [33]) and finished (from [7]).

Figure 5.2: Different views of the rear facade. From [34] and [35].

Figure 5.3: Different lateral views of the Pirelli Tower. From [34] and [36].

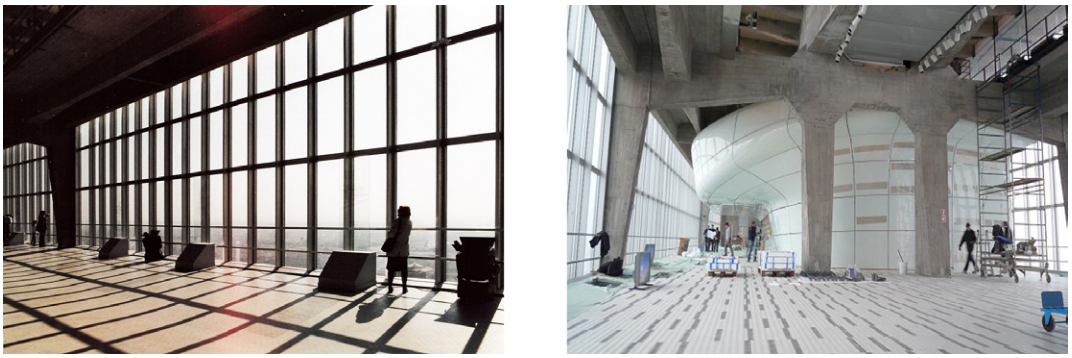

Figure 5.4: Interior views of the "Belvedere"on the 31st floor. From [37].

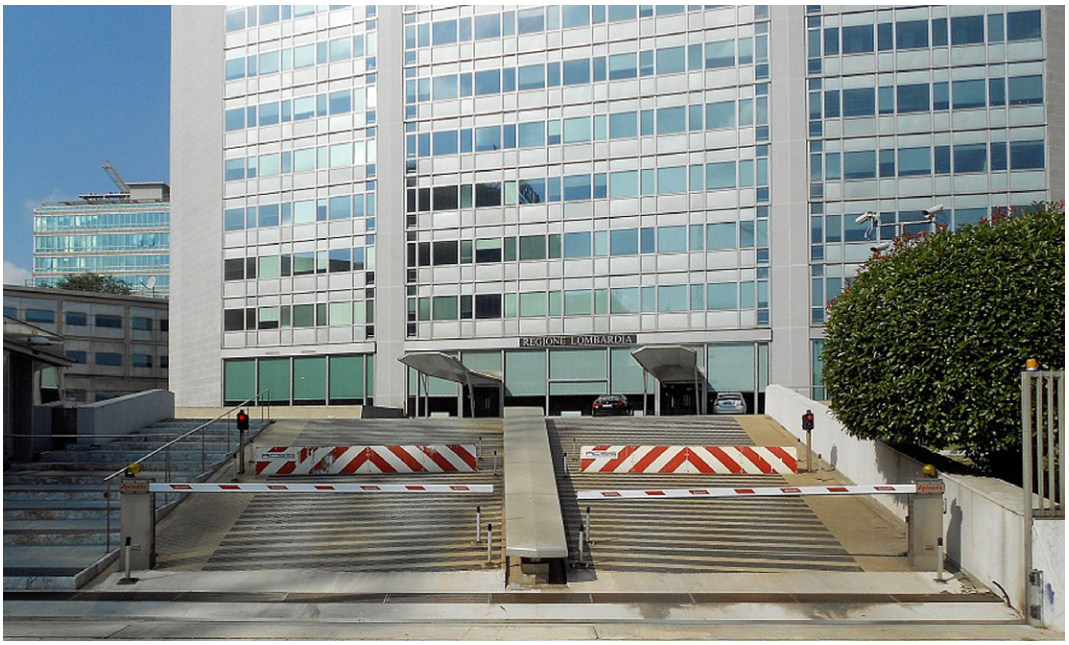

Figure 5.5: Main entrance from Milan's Central railway. From [37].

Figure 5.6: Memorial (26th floor) and generic views of interior spaces. From [38].

5.1.1 The Project

Piero and Alberto Pirelli, owners of the "Pirelli Group", thinking it was time to create a new headquarters in the centre of Milan, ordered the construction of this new important building. The design of the structure began in 1950 and was carried out by Pier Luigi Nervi, Gio Ponti, Giuseppe Valtolina, Antonio Fornaroli, Alberto Rosselli, Giuseppe Rinardi and Egidio Dell' Orto. More in detail, Gio Ponti followed the architectural part while the renowned engineer Pier Luigi Nervi with Giuseppe Valtolina, Arturo Danusso, Piero Locatelli, Guglielmo Meardi focused on the structural aspects. The ambition of the project justified the high number of engineers and architects involved in the design. Indeed, the structure was revolutionary for that time: despite the reduced height-width ratio, the building had to withstand the intense action of the wind. Moreover, it was the first building with a 24 meters span slab floor. In order to achieve this purpose, the team of engineers opted for the use of reinforced concrete and chose to use a structural scheme based on four massive central columns and four triangular diaphragms walls placed on the extreme sides. It was already clear from the early stages of the design that the building would have been higher than the Milan's Madonnina (located above the Duomo of Milan at 108,5 meters a.s.l.). In order not to violate the tradition of Milan that does not allow to have buildings higher than the Milan's Madonnina, the future Pope Paul VI, Giovanni Battista Montini, decided to place a copy of the Madonnina on top of the structure. The imitation was clearly smaller than the original one (four meters in height) and reached only 85 centimetres height. This bizarre tradition further continued with others Milan's tallest structures, like the Lombardy building and the Unicredit Tower, also covered with a copy of the Madonnina.

5.1.1.1 The ISMES models

Nervi, in line with the ideas of other distinguished European structural designers, as Eduardo Torroja, was convinced of the inadequacy, or at least the limits, of the theory of the time in the design of advanced structures such as the Pirelli Tower. For this reason, together with his team of designers, decided in 1954 to build in the new headquarters of the ISMES (Experimental Institute Models and Structures), some scale models of the Pirelli Tower to verify his design intuitions. In particular, the most complex aspects of the structure, that needed to be confirmed, were the verification of the static behaviour of the structural scheme identified and the dynamic response of the same in relation to dynamic stresses such as that of the wind. In particular, the structural element that most needed to be tested was the long central floor. Indeed, since during the design phase, other vertical bearing elements in addition to the four triangular diaphragm walls and the four pillars have been excluded, the central floor reached 24 meters of length. Nervi and Danusso thought of using a cement slab with thicker beams near the supports but, despite this, the elastic calculations returned significant central lowering in the floor slab, too high to be considered acceptable. For this reason, among the team of designers, the hypothesis of introducing pre-compression elements in the floor was examined, even if this choice would have significantly complicated the execution phases. Then, to ascertain these unknowns, two models were made at the ISMES institute:

- Structural concrete model of the entire building in scale 1:15 (Fig. 5.7);
- Concrete model of the slab floor working as a continuous hyperstatic beam in scale 1:5 (Fig. 5.8).

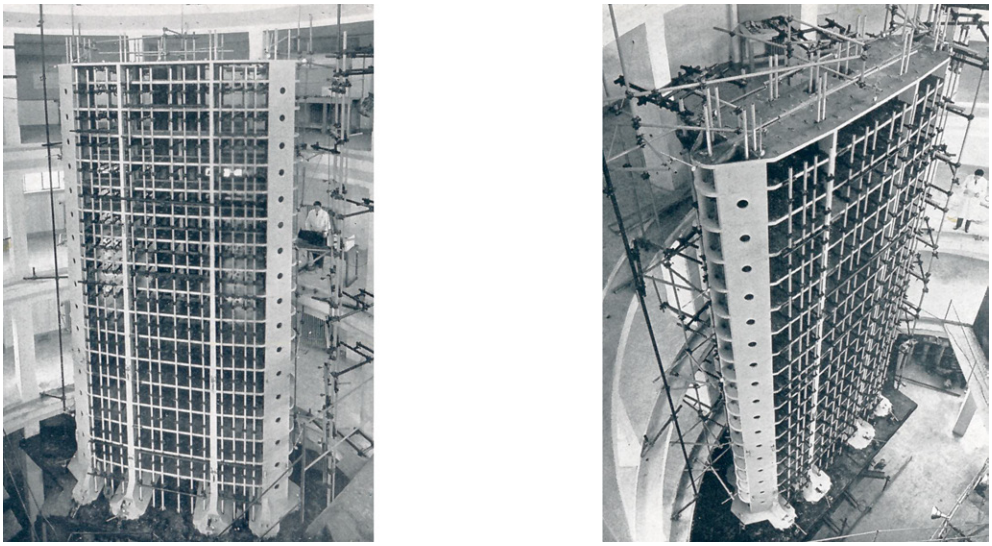

Figure 5.7: Structural model of the entire building (scale 1:15). From [39].

The model of the entire tower was previously loaded with settling loads, and subsequently, two distinct loading phases were carried out in which the main structural elements (columns and triangular diaphragm walls) were tested, and static and dynamic load tests were made for wind action. Finally, after carrying out all the tests in the elastic field, the model was brought to failure with a proportional increase of the main loads, that are the weight of the structure and the wind action. Instead, for the slab floor, the tests were divided into three phases:

- In the first step, the not prestressed slab was tested and subjected to the provisional loading of the upper storeys;
- In the second one, the pre-compressed slab was tested without additional loads;
- In the third one, the pre-compressed slab was tested with design loads.

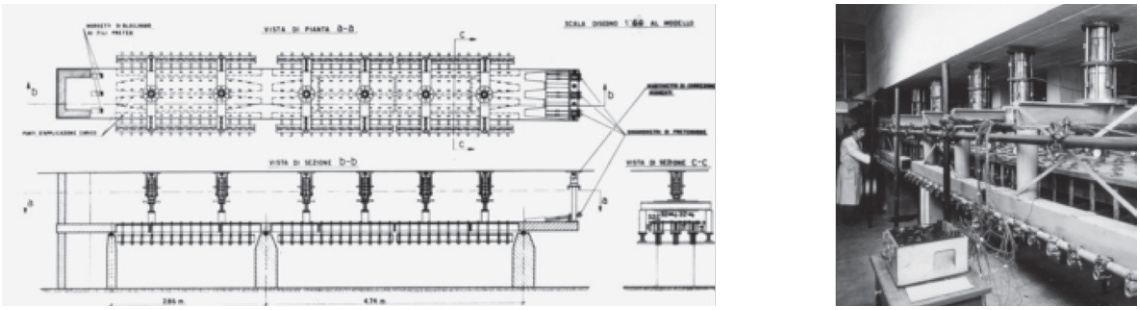

Figure 5.8: Structural model of slab floor (scale 1:5). From [40].

The results of the tests on the experimental models confirmed the quality of the design work carried out and led only to the adoption of some minor measures such as the insertion of architraves to connect the columns, even in the highest portions of the building, and allowed to improve the torsional behaviour generated by the eccentric position of the lift tower. Concerning the issue of pre-compression on the slab floors, the evidence showed that the elastic calculations, not taking into account the plastic reserves of the materials, were excessively on the safe side. Indeed, the behaviour of the not prestressed floors was satisfactory and allowed to discard the hypothesis of introducing the pre-compression that would have significantly complicated the executive phases of the work.

This example demonstrates the great importance that models have played in an era where numerical modelling did not exist, and the theories of elastic field design were often too limited.

5.1.2 The construction

The design stage ended in 1955. So, the construction was assigned to the Bonomi's firm, which also cooperated with the Comolli and Silce's firms. The construction, which required 20 thousand cubic metres of concrete and 4000 tonnes of steel, began in 1956 and ended in 1960 when the building was eventually inaugurated. The facade was built using glass and enamelled sheet metal. In the end, the concrete structure was coated with ceramic tiles.

5.1.3 The airplane crash

On April 19, 2002, a small private aeroplane crashed against the 26th floor. The collision caused three victims, the pilot and two Lombardy Region employees that were working. The Pirelli Tower after the aeroplane crash can be seen in Fig. 5.9.

5.1.4 Restorations of the building

5.1.4.1 1978 restoration

In 1978, when the management costs of the tower overwhelmed the Pirelli Company, the building was sold to the Lombardy Region which, after various restoration works carried out by the architect Bod Noorda, utilised the structure as its Regional Council headquarters. To adapt the building to the needs of the new function, several renovations were carried out such as the transformation of the computer centre in the new council hall and the restoration of the representative entrance, the presidency and the vice presidency halls [41].

5.1.4.2 2002 restoration

After the explosions and consequent fire caused by the 2002 aeroplane crash, the 26th floor flooded with water arriving from the fire-fighting systems. The weight of the water lowered by about 40 centimetres the slab floor. The lower floors also suffered considerable damage, but the "Nervian"conception of the building guaranteed the overall strength of the supporting structure. For the restoration work, a working group was composed, made up of engineers, architects and

Figure 5.9: The Pirelli Tower after the airplane crash. From [42].

historians to decide the intervention criteria to be adopted: a conservative restoration was opted for, taking up the theories of Giò Ponti to restore the skyscraper to the original aspirations. The restoration began in the spring of 2003. The restructuring phases required were the following [41]:

1) The disassembly and re-anodizing of all enamelled sheet metal windows;
2) The replacement of the entire complex of ceramic tiles consists of $250\,000$ $2 \cdot 2$ cm elements;
3) The reintegration of linoleum floors according to the original design by Gio Ponti.

The most significant spaces created with the restoration works were [41]:

- **The Memorial:**

  The 26th floor was left empty in the central part dedicated to the memory of the two victims of the severe accident;

- **Giorgio Gaber Auditorium:**

  Completely renovated, the underground auditorium, left in disuse for more than twenty years, consisting of a large room with a capacity of about 350 seats, has been reopened. Complete with the necessary technological and logistical equipment, it was then suitable for congresses, musical performances, shows and film screenings. It is now used for institutional events, but can also be rented to external parties;

- **Belvedere:**

  The top floor of the skyscraper, the 31st one, is known as “Belvedere”for the particular and evocative 360-degree panoramic view. The storey is open to the public only on the occasion of some particular events, temporary exhibitions and other special initiatives.

5.2 Structural characteristics from original documentation

The fourth of September 2020, to obtain essential information about the “Pirellone”structure, a research trip to the headquarters of the “Cittadella degli archivi di Milano”has been realised. Indeed, this important organisation, which among other things takes care of preserving and enhancing the municipal archival heritage, has allowed us to examine documents of excellent engineering and historical value: the original hand made structural plans of the Pirelli Tower [43] and [44]. These phenomenal documents, which included more than 150 hands made drawing, were drawn on the original paper of the time in format A0, A1, A2 and A3. Furthermore, they were embellished by the original signatures of exceptional engineers of international fame, who contributed to the realisation of incredible engineer structures of their time, like Giuseppe Valtolina and above all the signature of the legendary engineer Pier Luigi Nervi. Moreover, the documentation comprised another fascinating piece of the design of the Pirelli Tower: the *Testing Report* signed by the engineer and then professor of the Polytechnic of Turin Guido Oberti. This report has allowed to improve the comprehension of the building and understand how in a time when computers and numerical models did not exists, it was, however, possible to assess the behaviour of complex structural elements by hand made calculations. Indeed, among other information, the report exhaustively describes the calculation of the lowering of one beam of the slab floor. Eventually, after inspecting the documentation very carefully, the “Cittadella degli archivi di Milano”permitted us to scan the most relevant papers for this Thesis work. Moreover, the same day, a visit to the building was planned. Unfortunately, due to the situation created by the COVID-19, it was not possible to go inside the tower, but the building was inspected from the outside, and several photos, like the one that can be seen in Fig. 5.10, were taken. Eventually, several original structural plans are shown as images in Figures 5.11, 5.12, 5.13, 5.14, 5.15, 5.16 and 5.17, while the entire collection of schemes is gathered in an external folder, called “Original Structural Schemes Pirelli Tower”, delivered with this document.

Figure 5.10: Photo of the Pirelli Tower taken on the 4th of September 2020 in Milan.

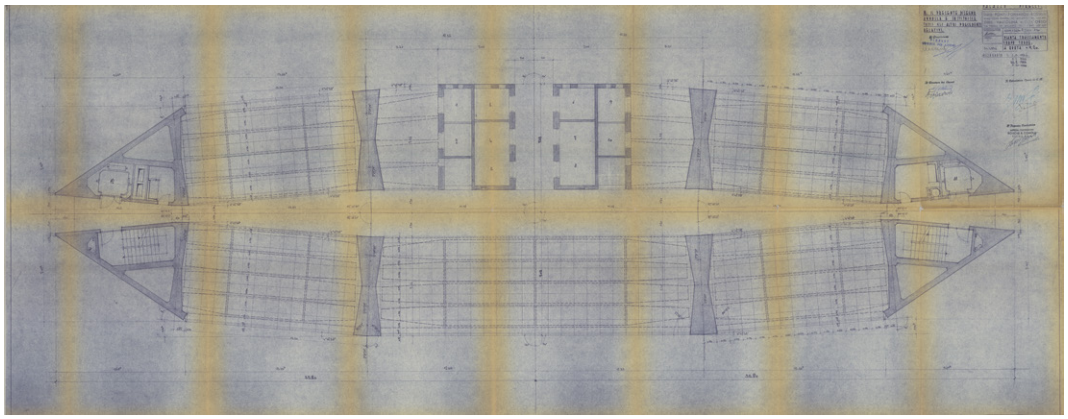

Figure 5.11: "Body tracing plan"of the Tower at $Q = 9,20\,m$.

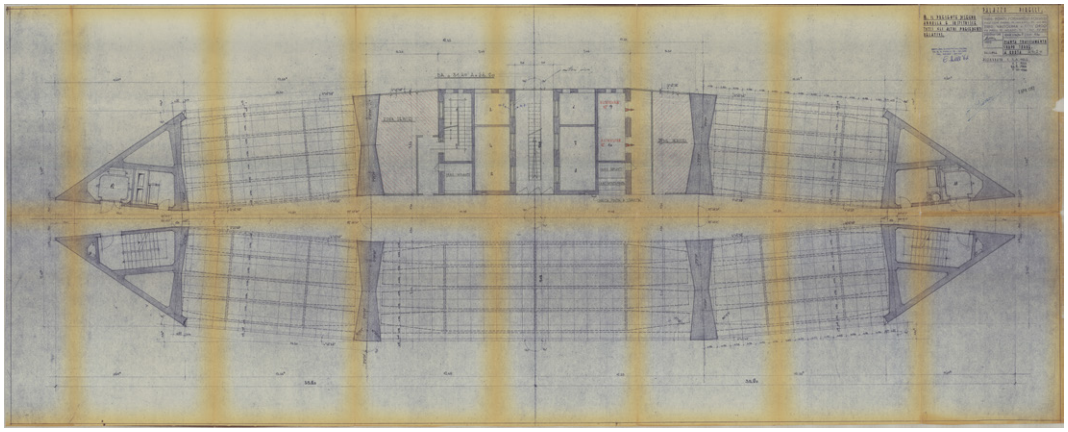

Figure 5.12: "Body tracing plan"of the Tower at $Q = 46,20\,m$.

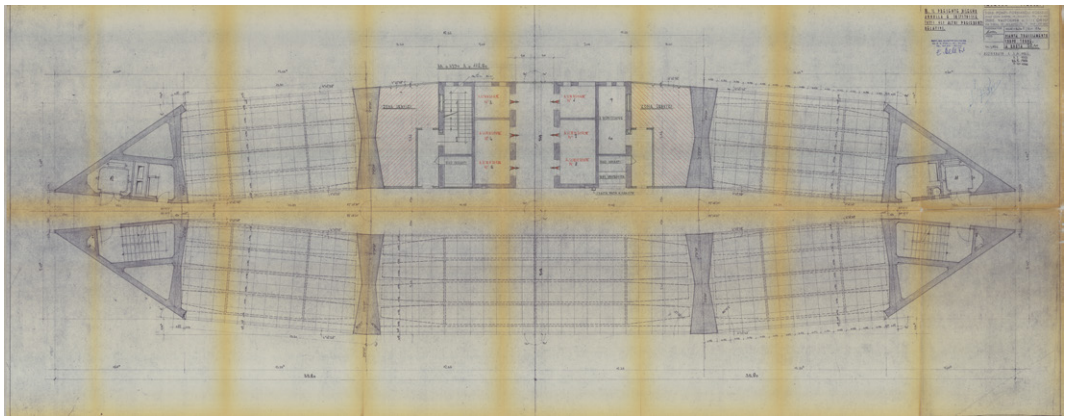

Figure 5.13: "Body tracing plan"of the Tower at $Q = 79,10\,m$.

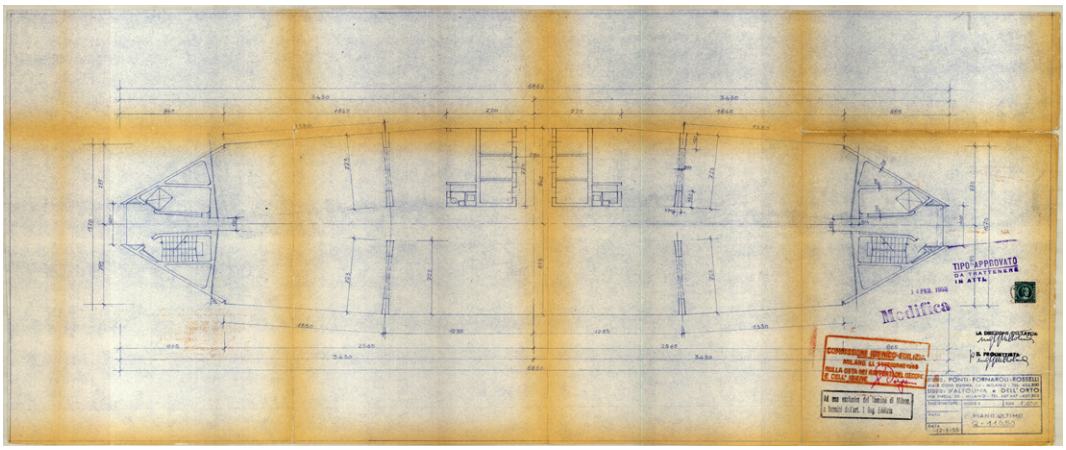

Figure 5.14: Technical scheme of the Tower at $Q = 116,50\,m$.

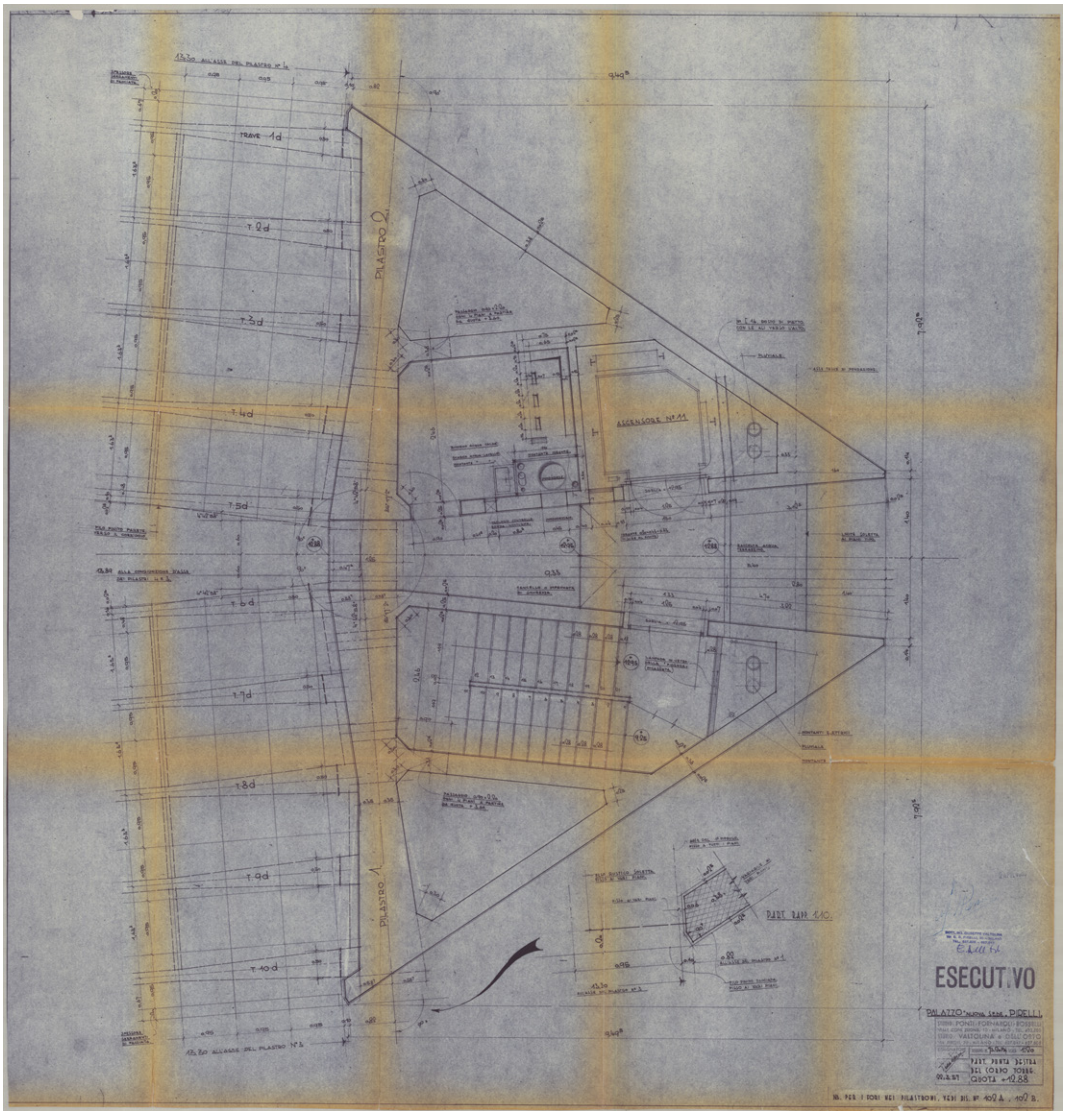

Figure 5.15: Particular of the right triangular element at $Q = 12,88\,m$.

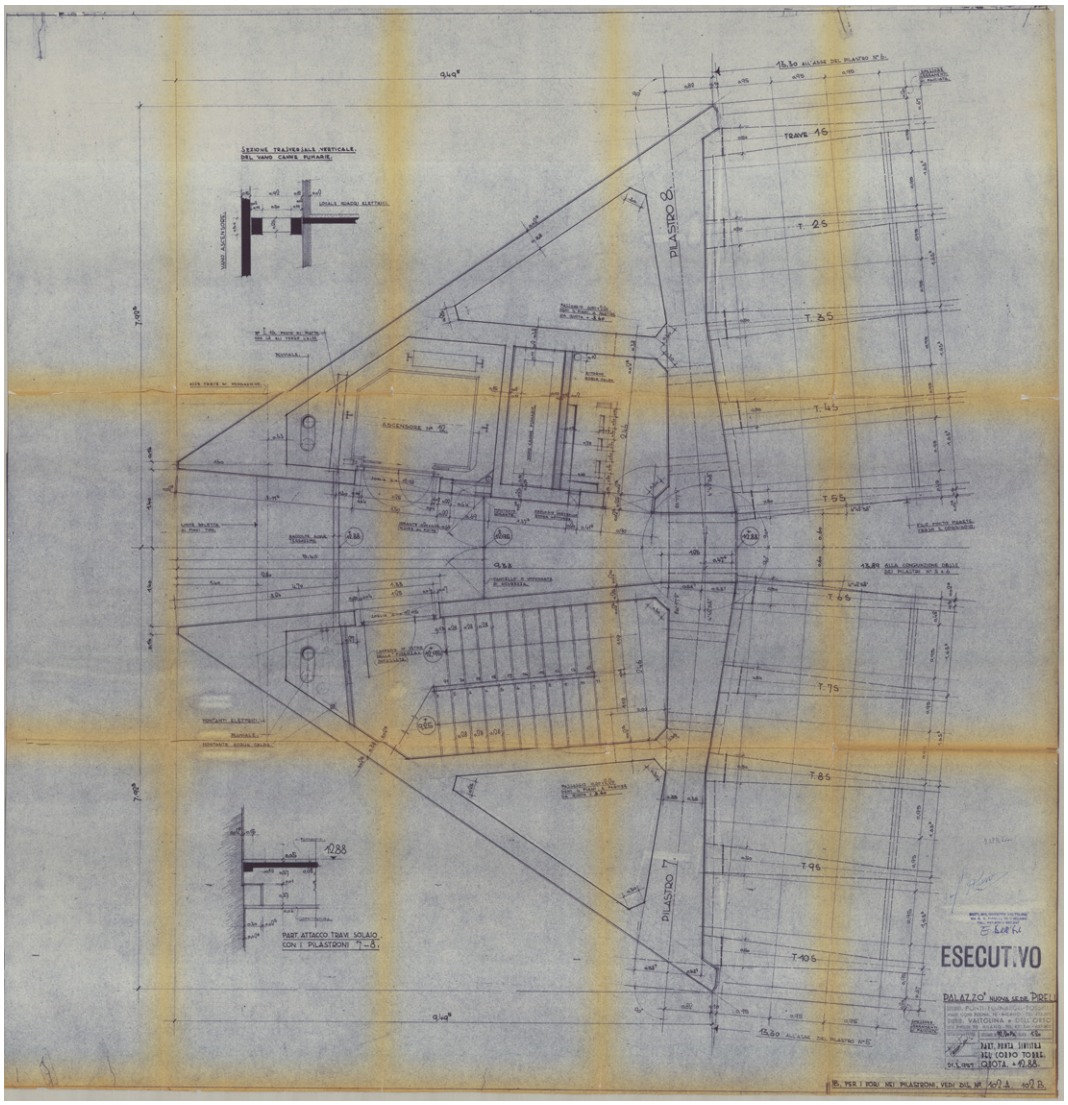

Figure 5.16: Particular of the left triangular element at $Q = 12,88\,m$.

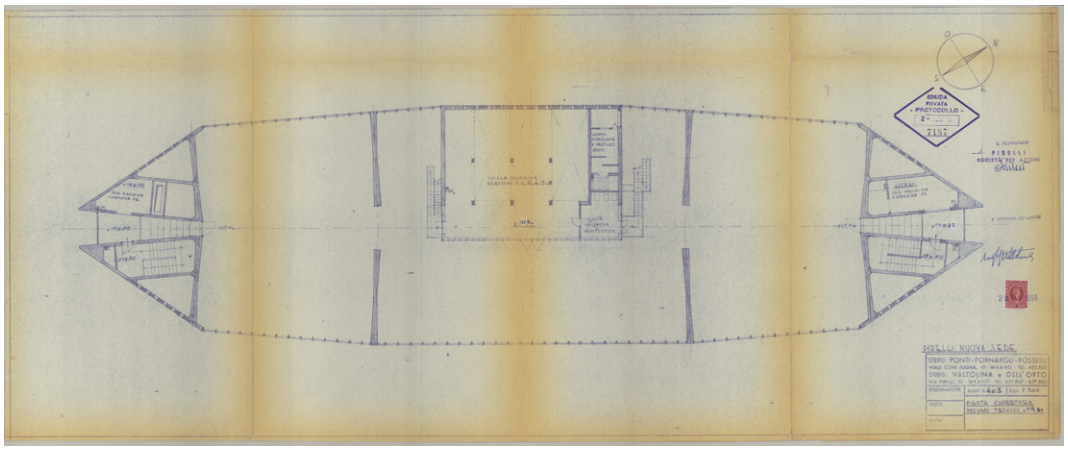

Figure 5.17: Technical scheme on top of the Tower, at $Q = 119,80\,m$.

5.2.1 Materials

The employed materials have been found in the original *Testing report* [43]. The reinforced concrete mixes used for the structure have been realized with 300 Kg/m^3 of cement type 680 for the foundations and 400 Kg/m^3 of the same cement for the columns, diaphragm walls and slab floors. Moreover, the slab floors have been reinforced with semi-hard iron "RUMI LU3"bars with a square shape with hollow sides (see Fig. 5.18) while columns and diaphragm walls have been reinforced with smooth circular bars of steel "Aq50". The resistant characteristics of the materials are summarized in Table 5.1.

Table 5.1: Resistant characteristics of the materials.

Concrete used for columns, diaphragm walls and slab floors Cement type 680 with 400 kg/m^3		
$R_{c,m}$ $[MPa]$	Standard deviation $[MPa]$	$f_{c,m} = 0,83 \cdot R_{cm}$ $[MPa]$
26,9	5,1	22,3
Concrete used for the foundations Cement type 500 with 300 kg/m^3		
$R_{c,m}$ $[MPa]$	Standard deviation $[MPa]$	$f_{c,m} = 0,83 \cdot R_{cm}$ $[MPa]$
38,1	4,6	31,6
Steel used in the reinforced bars of the concrete beams in the slab floors RUMI LU 3 steel 4400		
$f_{y,k}$ $[MPa]$	$f_{u,k}$ $[MPa]$	% Elongation
440	600	12
Steel used in the smooth reinforced bars of columns and diaphragm walls Smooth bars steel Aq50 (value from traction tests on sample)		
$f_{y,k}$ $[MPa]$	$f_{u,k}$ $[MPa]$	% Elongation
270	500	16

The resistant characteristics of the two types of concrete derive from the laboratory tests carried out on samples taken from the construction of the building between 1956 and 1958.

Figure 5.18: RUMI LU3 bars used in the slab floor beams of the Pirelli Tower. From [45].

5.2.1.1 Design parameters of the concrete

Following the methodology described in the Eurocode [46], it is possible to calculate the value of $f_{c,m}(t)$ with t equal to the age in day of the concrete:

$$f_{c,k}(t) = f_{c,m}(t) - 8 = [\beta_{cc}(t) \cdot f_{c,m}] - 8 = \left[exp\left(s \left[1 - \left(\frac{28}{t} \right)^{0,5} \right] \right) \cdot f_{c,m} \right] - 8 \quad (5.1)$$

Considering the following values of s, t:

- s=0,38
- t= 22174 days

we obtain the following results for the concrete used in columns, diaphragm walls and slab floors:

$$f_{c,k}(t) = \left[exp\left(0,38 \left[1 - \left(\frac{28}{22174} \right)^{0,5} \right] \right) \cdot 22,32 \right] - 8 = 32,20 - 8 = 24,2\, MPa \quad (5.2)$$

and for the foundation:

$$f_{c,k}(t) = \left[exp\left(0,38 \left[1 - \left(\frac{28}{22174} \right)^{0,5} \right] \right) \cdot 31,61 \right] - 8 = 45,62 - 8 = 37,6\, MPa \quad (5.3)$$

Furthermore, the design values of the concrete strength are:

$$f_{c,d}^{columns,\, walls,\, slab\, floors}(t) = \alpha_{cc} \cdot \frac{f_{c,k}}{\gamma_c} = 0,85 \cdot \frac{24,20}{1,5} = 13,7\, MPa \quad (5.4)$$

$$f_{c,d}^{foundations}(t) = \alpha_{cc} \cdot \frac{f_{c,k}}{\gamma_c} = 0,85 \cdot \frac{37,62}{1,5} = 21,3\, MPa \quad (5.5)$$

In the end, it is possible to evaluate the value of $E_{c,m}$ for both type of concrete:

$$E_{c,m}^{columns,\, walls,\, slab\, floors}(t) = 22000 \cdot \left(\frac{f_{c,m}(t)}{10} \right)^{0,3} = 31244\, MPa \quad (5.6)$$

$$E_{c,m}^{foundation}(t) = 22000 \cdot \left(\frac{f_{c,m}(t)}{10} \right)^{0,3} = 34687\, MPa \quad (5.7)$$

5.2.1.2 Design parameters of the steel

In analogy with what described for in the previous section, it is possible to calculate the design parameters of the two steel rebar used:

$$f_{y,d}^{RUMI\, LU3} = \frac{f_{y,k}}{\gamma_s} = \frac{440}{1,15} = 382,6\, MPa \quad (5.8)$$

$$f_{y,d}^{Aq\,50} = \frac{f_{y,k}}{\gamma_s} = \frac{270}{1,15} = 234,8\, MPa \quad (5.9)$$

and for the ultimate strength and Young modulus:

$$f_{u,d}^{RUMI\,LU3} = \frac{f_{u,k}}{\gamma_s} = \frac{600}{1,15} = 521,7\,MPa \qquad E_s = 200000\,MPa \tag{5.10}$$

$$f_{u,d}^{Aq\,50} = \frac{f_{u,k}}{\gamma_s} = \frac{500}{1,15} = 434,8\,MPa \qquad E_s = 200000\,MPa \tag{5.11}$$

5.2.2 Structural system

The building reaches 138 meters of height from the foundation base located at -11,30 meters and comprises 31 stories out of the ground and two subterranean levels. All the exceptional information obtained by the "Cittadella degli archivi di Milano"([43] [44]) has been studied to produce new original structural schemes with the help of drawing software. Thus, the new digital technical plans, created from scratch in AutoCAD, consist of the eight drawings collected in the Appendix A at the end of this document. The structural system, which can be seen in Drawing 1 and Fig.5.19, includes two triangular elements positioned on lateral sides, four massive columns between these two components and two rectangular cores set only in the rear portion of the building.

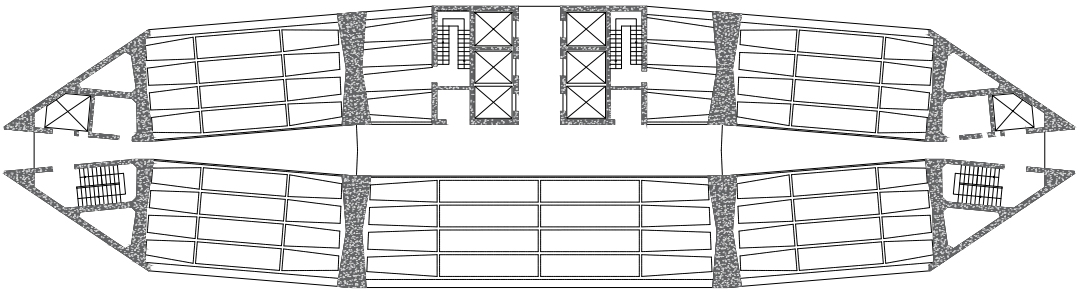

Figure 5.19: Plan view of a generic storey. From Drawing 1.

5.2.2.1 Slab floors

The slab floors can be considered to be divided into three parts with different spans: 24 meters for the central section and 12 meters for the lateral segments. The concrete slab has a variable thickness between 8 and 12 centimetres in the front portion of the building and reaches the thickness of 22 centimetres in the rear part of the edifice (see Drawing 1). The beams of the slab floor have a distance between centres of 1,63 meters and a height of 75 centimetres (see Drawing 1). Moreover, the supporting beams have a variable thickness and "RUMI LU3"reinforcing bars, as shown in Drawing 2 and Fig. 5.20. Furthermore, an important aspect regards the constraints between the slab floors and the vertical elements. Indeed, to manage the tremendous thermal variations on the floors, that could have occurred in the executive phase, the designers used the "ISMES"models to evaluate until which height, walls and columns, would have enough deformability to allow horizontal displacements equivalent to the thermal deformation of the floors. Thus, they decided to use a simply supported beam scheme till the fourth floor and rigid fixing constraints for the upper storeys.

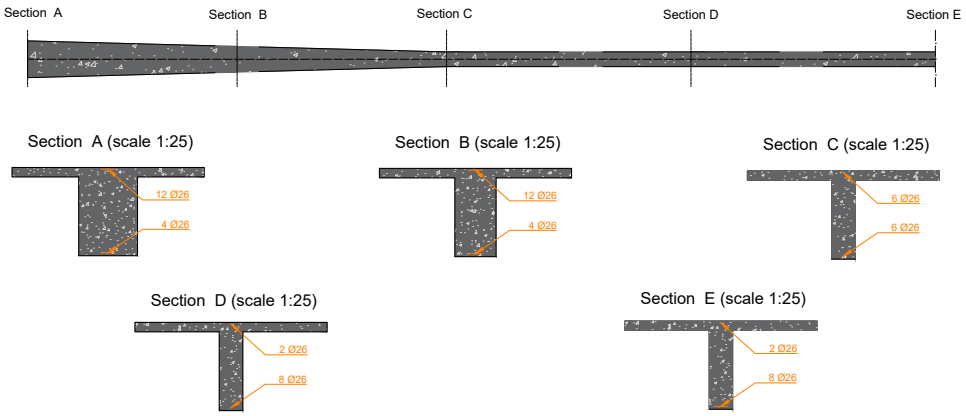

Figure 5.20: Longitudinal and transversal sections of the slab floor beams. From Drawing 2.

5.2.2.2 Columns

The four columns do not have a constant configuration with the increasing of the height of the building. Indeed, they change their shape by dividing in two at the height of 3,60 meters and reducing their thickness linearly. All the information regarding the shape of the columns is resumed in Drawing 3. Eventually, the reinforcement of the columns has been realized with circular smooth steel "Aq50"bars with a diameter of 30 millimetres. Nevertheless, the position of the bars is not indicated in the original documentation provided by the "Cittadella degli archivi di Milano".

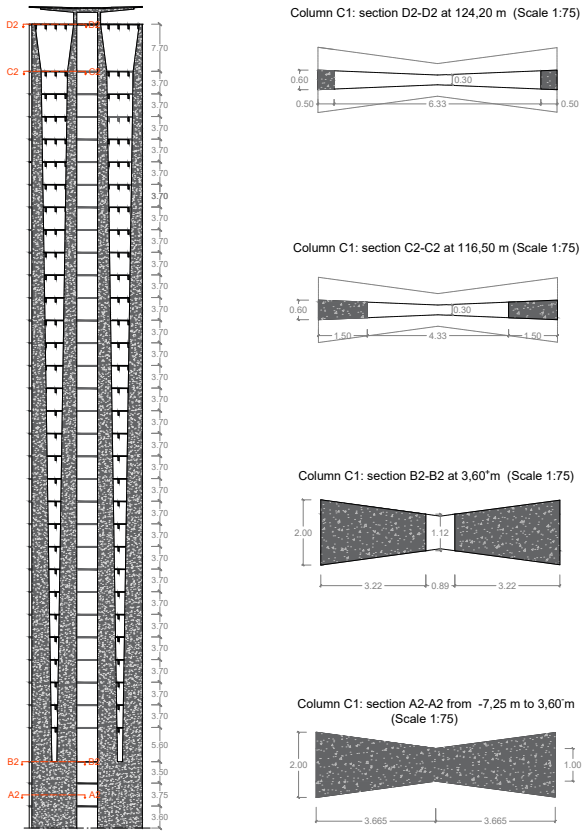

Figure 5.21: Longitudinal and transversal sections of the columns. From Drawing 3.

5.2.2.3 Triangular diaphragms

The thickness of the walls of the two lateral elements changes linearly, as shown in Drawing 4 and 5 and in Figures 5.22 and 5.23. The spaces enclosed by the walls of these elements are used for elevators and stairs, as represented in Drawing 1. The reinforcement of the triangular diaphragm walls has been realized with circular smooth steel “Aq50”bars with a diameter of 30, 22, 20 and 14 millimetres. As explained for the columns, even for these structural elements, the position of the bars was not present in the original documentation.

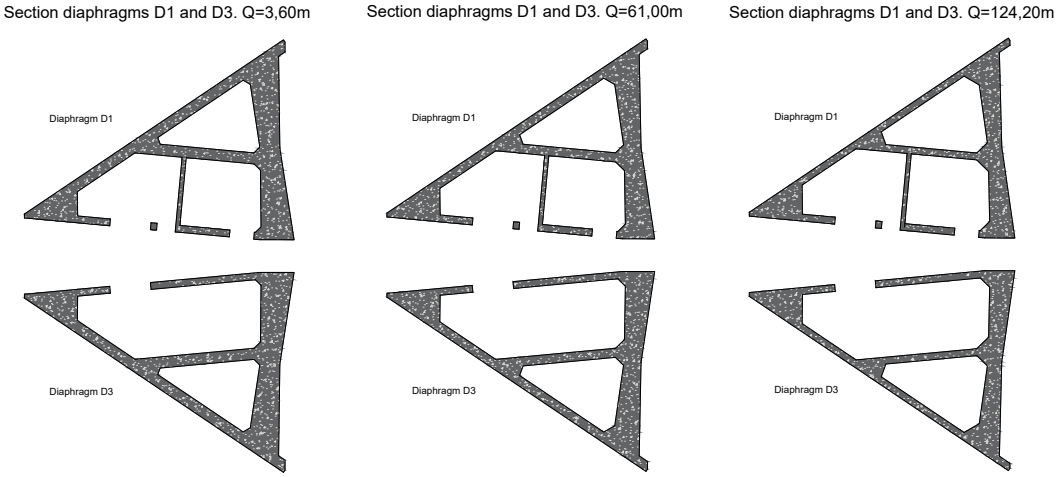

Figure 5.22: Transversal sections of the left triangular elements. From Drawing 4.

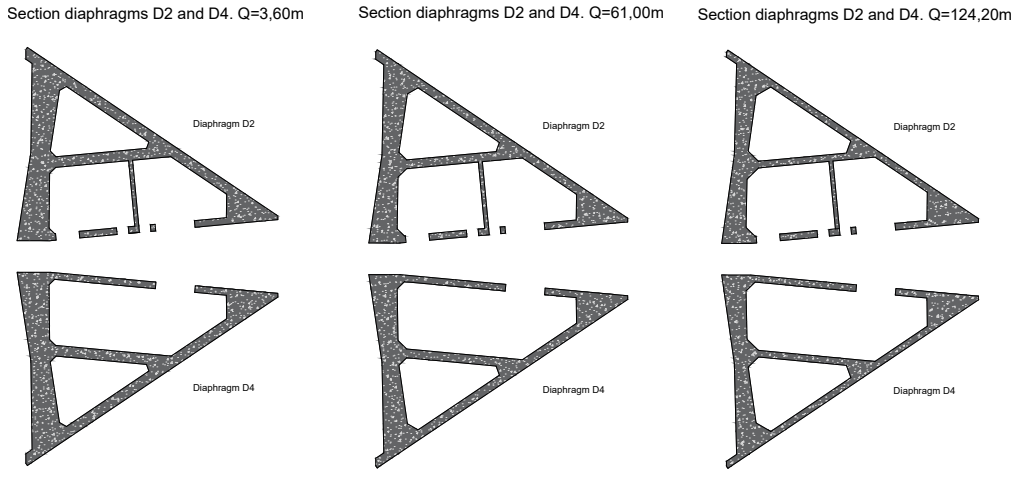

Figure 5.23: Transversal sections of the right triangular elements. From Drawing 5.

5.2.2.4 Central rectangular cores

The two rectangular cores have a constant thickness, and they join together in the last storey, as shown in Drawing 6 and 7 and in Fig. 5.24. The space between the internal walls of the two rectangular cores has been used for elevators and stairs that connect the central parts of the building. No information about the reinforcement of these elements has been found out.

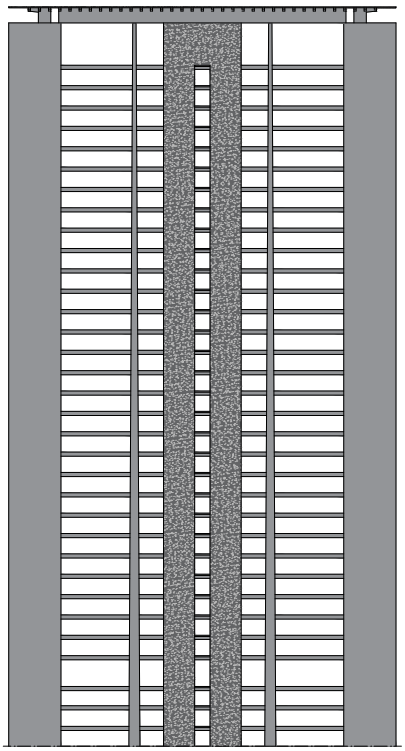

Figure 5.24: Longitudinal section of the central rectangular elements. From Drawing 7.

5.2.2.5 Top covering

The roofing of the building is a non-practicable covering, composed of two longitudinal walls that support a slab with a minimal inclination. Moreover, a reinforcing beams system has been used to strengthen the slab. The dimensions are illustrated in Drawing 8.

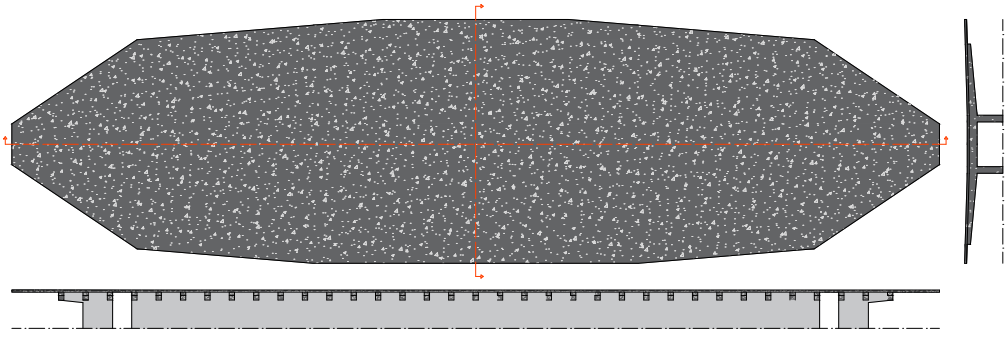

Figure 5.25: Plan view and sections of the covering. From Drawing 8.

5.3 Load analysis

In this section, the analysis of the loads that will be assigned to the various elements in the SAP2000 model is exposed.

5.3.1 Permanent structural loads G_1

The permanent structural loads will be obtained using the specific weight of the reinforced concrete $\gamma_c = 25\,KN/m^3$ and multiplying this value for the volume of the various elements.

5.3.1.1 Stairs permanent structural load

The stairs are located in the central cores and in the triangular walls (see Drawing 1). Therefore, they are supposed to consist of two and four slab ramps (depending on the inter-floor height) per floor, and they are interrupted by two or four staircase landings. In particular, the following characteristics shall be considered for each slab ramp:

- Ramp slab dimensions: Thickness: $20\,cm$, Width: $120\,cm$, Length: $280\,cm$;
- Ten steps for each ramp: Tread: $28\,cm$, Risers: Depends on the inter-storey, Width: $120\,cm$;
- Staircase landing dimensions: Thickness: $20\,cm$, Width: $300/220\,cm$, Length: $250/220\,cm$.

The total weight of the structural elements for the stairs located in the triangular elements is resumed in Table 5.2:

Table 5.2: Permanent structural loads of the stairs located in the triangular elements.

Share Q $[m]$	Element	Inter-storey $[m]$	$L \cdot W \cdot T$ $[m]$	Quantity	γ $[kN/m^3]$	G_1 $[kN]$
-7,25 to -3,65	Ramp slab	3,6	$2,8 \cdot 1,2 \cdot 0,20$	2	25	33,60
	Steps		$0,28 \cdot 1,2 \cdot 0,18$	20	25	30,24
	Staircase		$2,5 \cdot 3 \cdot 0,20$	1	25	37,5
					$G_{1,\,k}^{stairs}$ Total	101,34
-3,65 to 0,1	Ramp slab	3,75	$2,8 \cdot 1,2 \cdot 0,20$	2	25	33,60
	Steps		$0,28 \cdot 1,2 \cdot 0,19$	20	25	31,5
	Staircase		$2,5 \cdot 3 \cdot 0,20$	1	25	37,5
					$G_{1,\,k}^{stairs}$ Total	102,60
0,1 to 3,6	Ramp slab	3,5	$2,8 \cdot 1,2 \cdot 0,20$	2	25	33,60
	Steps		$0,28 \cdot 1,2 \cdot 0,18$	20	25	29,4
	Staircase		$2,5 \cdot 3 \cdot 0,20$	1	25	37,5
					$G_{1,\,k}^{stairs}$ Total	100,5
3,6 to 9,2	Ramp slab	5,6	$2,8 \cdot 1,2 \cdot 0,20$	4	25	67,20
	Steps		$0,28 \cdot 1,2 \cdot 0,14$	40	25	47,04
	Staircase		$2,5 \cdot 3 \cdot 0,20$	2	25	75
					$G_{1,\,k}^{stairs}$ Total	189,24
9,2 to 116,5	Ramp slab	3,7	$2,8 \cdot 1,2 \cdot 0,20$	2	25	33,60
	Steps		$0,28 \cdot 1,2 \cdot 0,19$	20	25	31,08
	Staircase		$2,5 \cdot 3 \cdot 0,20$	1	25	37,5
					$G_{1,\,k}^{stairs}$ Total	102,18
116,5 to 124,2	Ramp slab	7,7	$2,8 \cdot 1,2 \cdot 0,20$	4	25	67,20
	Steps		$0,28 \cdot 1,2 \cdot 0,19$	40	25	64,68
	Staircase		$2,5 \cdot 3 \cdot 0,20$	2	25	75
					$G_{1,\,k}^{stairs}$ Total	206,88

The determination of the total weight of the structural elements for the stairs located in the central part of the building is resumed in the following table:

Table 5.3: Permanent structural loads of the stairs located in the central part of the building.

Share Q $[m]$	Element	Inter-storey $[m]$	$L \cdot W \cdot T$ $[m]$	Quantity	γ $[kN/m^3]$	G_1 $[kN]$
-7,25 to -3,65	Ramp slab	3,6	$2,8 \cdot 0,8 \cdot 0,20$	2	25	22,40
	Steps		$0,28 \cdot 0,8 \cdot 0,18$	18	25	18,14
	Staircase		$2,2 \cdot 2,2 \cdot 0,20$	1	25	24,20
					$G_{1,k}^{stairs}$ Total	64,74
-3,65 to 0,1	Ramp slab	3,75	$2,8 \cdot 0,8 \cdot 0,20$	2	25	22,40
	Steps		$0,28 \cdot 0,8 \cdot 0,19$	18	25	18,9
	Staircase		$2,2 \cdot 2,2 \cdot 0,20$	1	25	24,2
					$G_{1,k}^{stairs}$ Total	65,5
0,1 to 3,6	Ramp slab	3,5	$2,8 \cdot 0,8 \cdot 0,20$	2	25	22,40
	Steps		$0,28 \cdot 0,8 \cdot 0,18$	18	25	17,64
	Staircase		$2,2 \cdot 2,2 \cdot 0,20$	1	25	24,2
					$G_{1,k}^{stairs}$ Total	64,24
3,6 to 9,2	Ramp slab	5,6	$2,8 \cdot 0,8 \cdot 0,20$	4	25	44,80
	Steps		$0,28 \cdot 0,8 \cdot 0,14$	36	25	28,22
	Staircase		$2,2 \cdot 2,2 \cdot 0,20$	2	25	48,4
					$G_{1,k}^{stairs}$ Total	121,42
9,2 to 116,5	Ramp slab	3,7	$2,8 \cdot 0,8 \cdot 0,20$	2	25	22,40
	Steps		$0,28 \cdot 0,8 \cdot 0,19$	18	25	18,65
	Staircase		$2,2 \cdot 2,2 \cdot 0,20$	1	25	24,2
					$G_{1,k}^{stairs}$ Total	65,25
116,5 to 124,2	Ramp slab	7,7	$2,8 \cdot 0,8 \cdot 0,20$	4	25	44,80
	Steps		$0,28 \cdot 0,8 \cdot 0,19$	36	25	38,09
	Staircase		$2,2 \cdot 2,2 \cdot 0,20$	2	25	48,4
					$G_{1,k}^{stairs}$ Total	132,01

5.3.2 Non structural permanent load G_2

Since no accurate details on the finishing of the floor slabs have been found (with the exception of the linoleum floor), a standard typology has been considered.

5.3.2.1 Inner floor slabs

Table 5.4: Table of permanent non-structural loads relative to the weight of the inner floor.

Material	γ $[KN/m^3]$	Thickness $[cm]$	$g_2^{s.int}$ $[KN/m^2]$
Cement screed	18	5	0,90
Linoleum floor	/	/	0,03
Plaster	20	1	0,20
		$g_2^{inner\ f}$ Total	1,13

5.3.2.2 Top floor slab

Table 5.5: Table of permanent non-structural loads relative to the weight of the roof slab.

Material	$\gamma\ [KN/m^3]$	Thickness [cm]	$g_2^{cov}\ [KN/m^2]$
Insulator	0,3	20	0,06
Cement screed	18	6	1,08
Floor	/	/	0,50
Plaster	20	1	0,20
		g_2^{cov} Total	1,84

5.3.2.3 Interior partitions

Also for the typology of the partitions, no precise information has been proportionated by the "Cittadella Degli Archivi di Milano". Therefore, a typical drywall partitions have been considered:

$$g_2^{drywall} = 0,8\,KN/m^2$$

5.3.2.4 Boundary facade load

The facade of the Pirelli Tower consists of a mix of glass and enamelled sheet metal. The detailed calculation of this load is resumed in the next table:

Table 5.6: Permanent non-structural loads relative to the weight of the main facade elements.

Main facade							
Share $Q\ [m]$	Portion	Interstorey $[m]$	Height $[m]$	THK [m]	$\gamma\ [kN/m^3]$	Area $[m^2]$	$g_2\ [kN/m]$
-7,25 to -3,65	Glass	3,6	3,36	0,02	25	0,050	1,26
	Metal	3,6	3,36	0,01	27	0,008	0,23
						$g_{2,k}^{facade}$ Total	1,49
-3,65 to 0,10	Glass	3,75	3,51	0,02	25	0,053	1,32
	Metal	3,75	3,51	0,01	27	0,009	0,24
						$g_{2,k}^{facade}$ Total	1,55
0,10 to 3,60	Glass	3,5	3,26	0,02	25	0,033	0,82
	Metal	3,5	3,26	0,01	27	0,016	0,44
						$g_{2,k}^{facade}$ Total	1,26
3,60 to 9,20	Glass	5,6	5,36	0,02	25	0,107	2,68
	Metal	5,6	5,36	0,01	27	0,000	0,00
						$g_{2,k}^{facade}$ Total	2,68
9,20 to 116,50	Glass	3,7	3,46	0,02	25	0,035	0,87
	Metal	3,7	3,46	0,01	27	0,017	0,47
						$g_{2,k}^{facade}$ Total	1,33
116,50 to 124,20	Glass	7,7	7,46	0,02	25	0,124	3,11
	Metal	7,7	7,46	0,01	27	0,012	0,34
						$g_{2,k}^{facade}$ Total	3,44

Table 5.7: Permanent non-structural loads relative to the weight of the rear facade elements.

Rear facade							
Share Q $[m]$	Portion	Interstorey $[m]$	Height $[m]$	THK [m]	γ $[kN/m^3]$	Area $[m^2]$	g_2 $[kN/m]$
-7,25 to -3,65	Glass	3,6	3,26	0,02	25	0,049	1,22
	Metal	3,6	3,26	0,01	27	0,008	0,22
						$g_{2,\,k}^{facade}$ Total	1,44
-3,65 to 0,10	Glass	3,75	3,41	0,02	25	0,051	1,28
	Metal	3,75	3,41	0,01	27	0,009	0,23
						$g_{2,\,k}^{facade}$ Total	1,51
0,10 to 3,60	Glass	3,5	3,16	0,02	25	0,032	0,79
	Metal	3,5	3,16	0,01	27	0,016	0,43
						$g_{2,\,k}^{facade}$ Total	1,22
3,60 to 9,20	Glass	5,6	5,26	0,02	25	0,105	2,63
	Metal	5,6	5,26	0,01	27	0,000	0,00
						$g_{2,\,k}^{facade}$ Total	2,63
9,20 to 116,50	Glass	3,7	3,36	0,02	25	0,034	0,84
	Metal	3,7	3,36	0,01	27	0,017	0,45
						$g_{2,\,k}^{facade}$ Total	1,29
116,50 to 124,20	Glass	7,7	7,36	0,02	25	0,123	3,07
	Metal	7,7	7,36	0,01	27	0,012	0,33
						$g_{2,\,k}^{facade}$ Total	3,40

5.3.2.5 Non structural stairs weight

Considering the dimensional specifications already presented in the previous sections and that the ramp has a plaster coating on the intrados, and floor on the extrados, the total non-structural weight can be calculated as follow:

Table 5.8: Non-structural weight of the stairs located in the triangular elements.

Element	γ $[kN/m^3]$	Thickness $[m]$	Area $[m^2]$	G_2 $[kN]$
Plaster	20	0,01	15,5	3,1
Pavement	15	0,02	15,5	4,65
			$g_{2,\,k}^{stairs}$ Total	7,75

Table 5.9: Non-structural weight of the stairs located in the central part of the building.

Element	γ $[kN/m^3]$	Thickness $[m]$	Area $[m^2]$	G_2 $[kN]$
Plaster	20	0,01	11	2,2
Pavement	15	0,02	11	3,35
			$g_{2,\,k}^{stairs}$ Total	5,5

5.3.3 Variable loads Q

5.3.3.1 Accidental loads

The building is used as an office, and therefore, as prescribed by Eurocode 1 [30], the building falls into category B. Thus the interior floors will have a load per unit area of $q_{catB} = 2\,KN/m^2$. For stairs and lifts instead, it is necessary to add 2 KN/m^2 to the previous value, then $q_{catB}^{stairs\,/\,lift} = 4\,KN/m^2$. The roof slab, also in accordance with the standard, being practicable only for maintenance, falls into category H and then has a load per unit area equal to 0,5 KN/m^2.

In Table 5.10 a resume of the accidental loads is presented.

Table 5.10: Table summarizing variable floor loads q_i.

Element	Specific use	$q_i\ [KN/m^2]$
Inner floors	Category B	2,00
Covering	Category H	0,50
Stairs and elevators	Category B	4,00

5.3.3.2 Snow loads

The building is located in Milan at an altitude of 120 meters above the sea level and has a top roof that can be approximated as flat. In agreement with the Eurocode 1 [30] and with the Italian National annex, the snow load can be determined as follow:

$$\text{Zone I Mediterranean} \quad \longrightarrow \quad a_s = 120\,m < 200\,m \quad \longrightarrow \quad q_{sk} = 1,50\,KN/m^2$$

and considering:

$$C_t = C_e = 1 \qquad\qquad \mu_1 = 0,8$$

the total snow load is:

$$q_{snow} = \mu_1 \cdot C_t \cdot C_e \cdot q_{sk} = 1,2\,KN/m^2$$

5.3.3.3 Wind action

The action of the wind against a skyscraper should be determined with precise analyses in the wind tunnel. However, this is not the purpose of this Thesis, and therefore, it will be determined following the indications reported in the EN-1991-1-4 [47] and the Italian National annex [48].

As can be seen in Figure N.A.1 of the Italian National annex [48], Milan is in zone 1. Therefore the Table N.A.1 indicates that the fundamental value of basic wind velocity is:

$$v_{b,\,0} = 25\,m/s \tag{5.12}$$

Considering the Directional factor C_{dir} and seasonal factor C_{season} equals to one (as recommended

by the standard) the basic wind velocity becomes:

$$v_b = C_{dir} \cdot C_{season} \cdot v_{b,\,0} = 25\,m/s \tag{5.13}$$

From Table N.A.3 and Figure N.A.2 of the National Annex [48] results that Milan is in:

- Roughness class A;
- Exposion category V.

That corresponds, as can be seen in Table N.A.2, to a roughness length of $z_0 = 0,7\,m$, a minimum height of $z_{min} = 12\,m$ and a terrain factor $k_r = 0,23$. Furthermore, considering $z_{max} = 200\,m$, as fixed by the Eurocode, it is possible to calculate the factor $C_r(z)$, that takes into account the variability of the mean wind velocity at the site of the structure, for various z:

$$C_r(z) = \begin{cases} k_r \cdot ln\left(\dfrac{z}{z_0}\right) & \text{for} \quad z_{min} \leq z \leq z_{max} \\ C_r(z_{min}) & \text{for} \quad z \leq z_{min} \end{cases} \tag{5.14}$$

Therefore, fixing the orography factor $C_0(z)$ equal to one (as recommended by the standard), it is possible to calculate the mean wind velocity for different z:

$$v_m(z) = C_r(z) \cdot C_0(z) \cdot v_b \tag{5.15}$$

Moreover, it is necessary to determinate the turbulence intensity factor I_v for different height:

$$I_v(z) = \begin{cases} \dfrac{\sigma_v}{v_m(z)} = \dfrac{k_l}{C_0(z) \cdot ln(z/z_0)} & \text{for} \quad z_{min} \leq z \leq z_{max} \\ I_v(z_{min}) & \text{for} \quad z \leq z_{min} \end{cases} \tag{5.16}$$

Where the turbulence factor k_l is normally taken equal to 1 as recommended by the standard.

Besides, considering the air density equal to $\rho_0 = 1,25\,Kg/m^3$, the basic velocity pressure become:

$$q_b = 0,5 \cdot \rho_0 \cdot v_b^2 = 0,391\,KPa \tag{5.17}$$

The exposure factor $C_e(z)$ can be calculated as follows:

$$C_e(z) = (1 + 7 \cdot I_v(z)) \cdot \frac{v_m(z)^2}{v_b^2} \tag{5.18}$$

Then, the peak velocity pressure $q_p(z)$, that includes mean and short-term velocity fluctuations, is:

$$q_p(z) = C_e(z) \cdot q_b \tag{5.19}$$

The coefficients described until now are summarized in Table 5.11, where have been determined for each storey.

Table 5.11: Coefficients $C_r(z)$, $v_m(z)$, $I_v(z)$, $C_e(z)$ and $q_p(z)$ for each storey of the building.

$z\ [m]$	$c_r(z)$	$v_m(z)\ [m/s]$	$I_v(z)$	$c_e(z)$	$q_p(z)\ [kN/m^2]$
0,10	0,65	16,34	0,35	1,48	0,58
3,60	0,65	16,34	0,35	1,48	0,58
9,20	0,65	16,34	0,35	1,48	0,58
12,90	0,67	16,75	0,34	1,53	0,60
16,60	0,73	18,20	0,32	1,70	0,67
20,30	0,77	19,36	0,30	1,85	0,72
24,00	0,81	20,32	0,28	1,97	0,77
27,70	0,85	21,15	0,27	2,08	0,81
31,40	0,87	21,87	0,26	2,17	0,85
35,10	0,90	22,51	0,26	2,26	0,88
38,80	0,92	23,09	0,25	2,34	0,91
42,50	0,94	23,61	0,24	2,41	0,94
46,20	0,96	24,09	0,24	2,48	0,97
49,90	0,98	24,53	0,23	2,54	0,99
53,60	1,00	24,94	0,23	2,60	1,02
57,30	1,01	25,33	0,23	2,66	1,04
61,00	1,03	25,69	0,22	2,71	1,06
64,70	1,04	26,03	0,22	2,76	1,08
68,40	1,05	26,35	0,22	2,81	1,10
72,10	1,07	26,65	0,22	2,85	1,11
75,80	1,08	26,94	0,21	2,90	1,13
79,50	1,09	27,21	0,21	2,94	1,15
83,20	1,10	27,47	0,21	2,98	1,16
86,90	1,11	27,72	0,21	3,02	1,18
90,60	1,12	27,96	0,21	3,05	1,19
94,30	1,13	28,19	0,20	3,09	1,21
98,00	1,14	28,41	0,20	3,12	1,22
101,70	1,15	28,63	0,20	3,15	1,23
105,40	1,15	28,83	0,20	3,19	1,24
109,10	1,16	29,03	0,20	3,22	1,26
112,80	1,17	29,22	0,20	3,25	1,27
116,50	1,18	29,41	0,20	3,28	1,28
124,20	1,19	29,78	0,19	3,34	1,30

With the coefficients resumed in Table 5.11 it is possible to calculate the wind pressure on external surfaces as:

$$w_e = q_p(z_e) \cdot C_{pe} \tag{5.20}$$

where z_e is the reference height and depends on the shape of the structure and c_{pe} the pressure coefficient that is different for every surface considered.

Eventually, the wind forces shall be determined as:

$$F_{w,e} = C_s \cdot C_d \cdot \sum_{elements} w_e \cdot A_{ref} \tag{5.21}$$

Where A_{ref} is the reference area i.e is the area correspondent to every floor.

Therefore, to determinate the values of $F_{w,e}$ for each storey of the building, it is still necessary to determinate z_e, C_{pe} and the structural factor $C_s \cdot C_d$. To do so, two perpendicular directions of wind should be considered:

1- Wind perpendicular to the long side of the building

Considering this direction of the wind respect of the Pirelli Tower, the dimensional characteristics of the building are the following:

$$h = 127,10\,m \qquad b = 70,38\,m \qquad d = 18,50\,m$$

Since the height of the building is greater than b (length of the building in the direction perpendicular to the wind action) but less than two times b, the Eurocode [47] states that the building may be considered to be in two parts as illustrated Fig. 5.26:

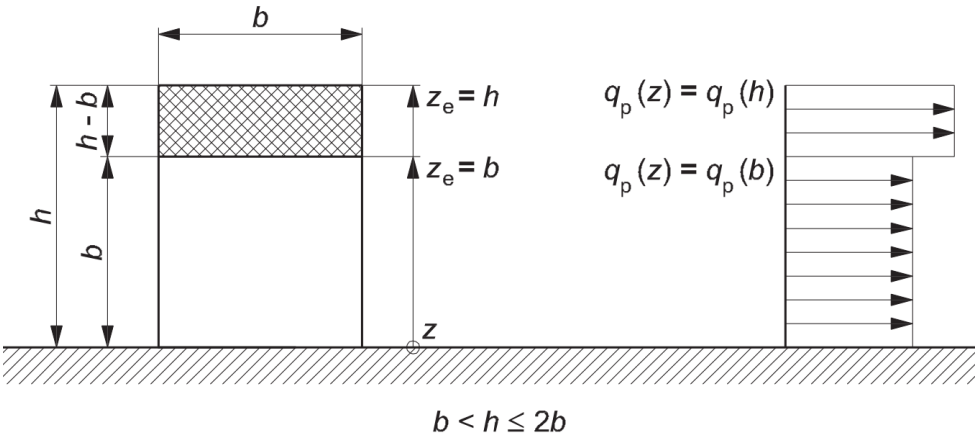

Figure 5.26: Reference height z_e depending on h and b and corresponding velocity pressure profile. From [47].

Thus, Fig. 5.26 indicates the reference height z_e for each considered z. Moreover, looking at Fig. 5.27 and at Table 7.1 of the Eurocode [47] it is possible to determinate the pressure coefficients:

$$\text{Zone D} \longrightarrow C_{pe,\,10} = 0,8 \qquad \text{Zone E} \longrightarrow C_{pe,\,10} = -0,7$$

where zones D and E correspond to the sides of the building perpendicular to the wind direction. The coefficient $C_s \cdot C_d$ can be approximated from the figure D.2 of the Eurocode [47], for a multistorey concrete building with $h = 127,10\,m$ and $b = 70,38\,m$. In this case results that $C_s \cdot C_d = 0,9$. However, Pressures against the short sides are negligible due to its relatively tiny dimensions, while the effect of the friction on the surface is negligible if $d < 4 \cdot b$:

$$d = 18,50\,m < 4 \cdot b = 4 \cdot 70,38 \; = 281,52\,m \tag{5.22}$$

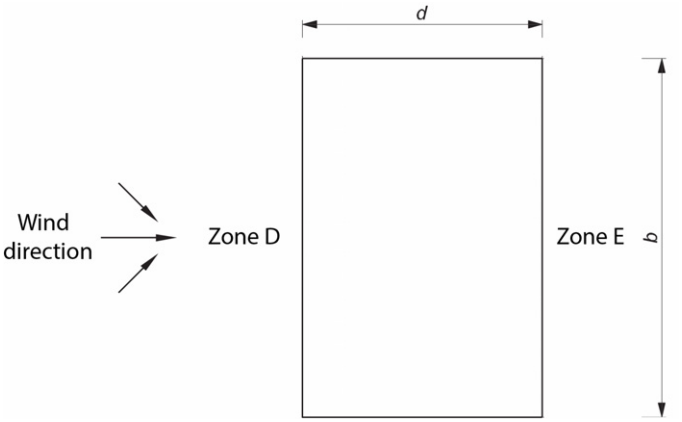

Figure 5.27: Building zone for the determination of the coefficients C_{pe}. From [47].

Therefore, the effects of wind friction on the surface can be disregarded. The values of wind force for each storey and zone are summarized in Table 5.12.

Table 5.12: Wind force for zones D and E considering an action perpendicular to the long side of the building.

				Zone D		Zone E	
$z\ [m]$	$z_e\ [m]$	$q_p(z_e)\ [kN/m^2]$	$A_{ref}(z)\ [m^2]$	$w_e(z_e)$	$F_{w,e}\ [kN]$	$w_e(z_e)$	$F_{w,e}\ [kN]$
0,10	70,38	1,11	130,20	0,88	103,70	-0,77	-90,74
3,60	70,38	1,11	320,23	0,88	255,05	-0,77	-223,17
9,20	70,38	1,11	327,27	0,88	260,65	-0,77	-228,07
12,90	70,38	1,11	260,41	0,88	207,40	-0,77	-181,48
16,60	70,38	1,11	260,41	0,88	207,40	-0,77	-181,48
20,30	70,38	1,11	260,41	0,88	207,40	-0,77	-181,48
24,00	70,38	1,11	260,41	0,88	207,40	-0,77	-181,48
27,70	70,38	1,11	260,41	0,88	207,40	-0,77	-181,48
31,40	70,38	1,11	260,41	0,88	207,40	-0,77	-181,48
35,10	70,38	1,11	260,41	0,88	207,40	-0,77	-181,48
38,80	70,38	1,11	260,41	0,88	207,40	-0,77	-181,48
42,50	70,38	1,11	260,41	0,88	207,40	-0,77	-181,48
46,20	70,38	1,11	260,41	0,88	207,40	-0,77	-181,48
49,90	70,38	1,11	260,41	0,88	207,40	-0,77	-181,48
53,60	70,38	1,11	260,41	0,88	207,40	-0,77	-181,48
57,30	70,38	1,11	260,41	0,88	207,40	-0,77	-181,48
61,00	70,38	1,11	260,41	0,88	207,40	-0,77	-181,48
64,70	70,38	1,11	260,41	0,88	207,40	-0,77	-181,48
68,40	70,38	1,11	260,41	0,88	207,40	-0,77	-181,48
72,10	127,10	1,31	260,41	1,05	245,90	-0,92	-215,16
75,80	127,10	1,31	260,41	1,05	245,90	-0,92	-215,16
79,50	127,10	1,31	260,41	1,05	245,90	-0,92	-215,16
83,20	127,10	1,31	260,41	1,05	245,90	-0,92	-215,16
86,90	127,10	1,31	260,41	1,05	245,90	-0,92	-215,16
90,60	127,10	1,31	260,41	1,05	245,90	-0,92	-215,16
94,30	127,10	1,31	260,41	1,05	245,90	-0,92	-215,16
98,00	127,10	1,31	260,41	1,05	245,90	-0,92	-215,16
101,70	127,10	1,31	260,41	1,05	245,90	-0,92	-215,16
105,40	127,10	1,31	260,41	1,05	245,90	-0,92	-215,16
109,10	127,10	1,31	260,41	1,05	245,90	-0,92	-215,16
112,80	127,10	1,31	260,41	1,05	245,90	-0,92	-215,16
116,50	127,10	1,31	401,17	1,05	378,82	-0,92	-331,47
124,20	127,10	1,31	279,96	1,05	255,87	-0,92	-223,89

2- Wind perpendicular to the short side of the building

Considering this direction of the wind, the dimensional characteristics of the building are:

$$h = 127,10\,m \qquad b = 18,50\,m \qquad d = 70,38\,m$$

In this case, the height of the building is greater than two times b so, the Eurocode [47], states that the building may be considered into multiple parts as illustrated Fig. 5.28:

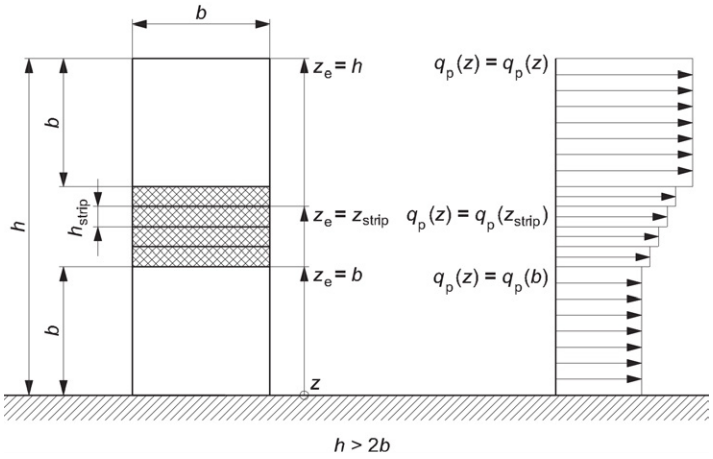

Figure 5.28: Reference height z_e depending on h and b and corresponding velocity pressure profile. From [47].

Differently to the previous situation, this time it is not possible to neglect the wind pressure against the lateral sides (in fact they are predominant), so the situations that should be considered is resumed in the next figure:

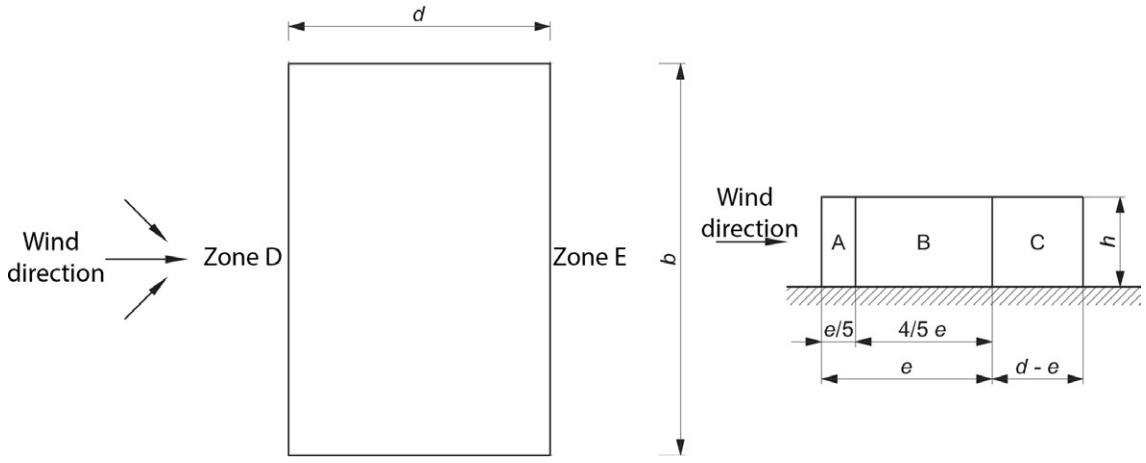

Figure 5.29: Building zone for the determination of the coefficients C_{pe}. From [47].

The value of e can be calculated as follow:

$$e = min(b,\, 2h) = 18,50\,m < d = 70,38\,m \tag{5.23}$$

With the value of e it is possible to determinate the zone A, B and C as illustrated in Fig. 5.29.

In the end, considering the ratio $h/d = 121,10/70,38 = 1,81$ and interpolating in table 7.1 of the Eurocode [47] it is possible to determinate the values of the coefficient C_{pe} for each zone:

$$\text{Zone D} \longrightarrow C_{pe,10} = 0,8 \qquad \text{Zone E} \longrightarrow C_{pe,10} = -0,54$$

$$\text{Zone A} \longrightarrow C_{pe,10} = -1,2 \qquad \text{Zone B} \longrightarrow C_{pe,10} = -0,8 \qquad \text{Zone C} \longrightarrow C_{pe,10} = -0,5$$

In this case, $C_s \cdot C_d$ can be assumed equal to 1. Considering the effects of wind friction on the surface we have:

$$d = 70,38\,m < 4 \cdot b = 4 \cdot 18,50\,m = 74,00\,m \tag{5.24}$$

Thus, also for this direction, the effects of the wind friction on the surface can be disregarded. The values of wind action for zone D and E are summarized in Table 5.13.

Table 5.13: Wind force for zones D and E considering an action perpendicular to the short side of the building.

				Zone D		Zone E	
$z\ [m]$	$z_e\ [m]$	$q_p(z_e)\ [kN/m^2]$	$A_{ref}(z)\ [m^2]$	$w_e(z_e)$	$F_{w,e}\ [kN]$	$w_e(z_e)$	$F_{w,e}\ [kN]$
0,10	18,50	0,70	34,23	0,56	19,03	-0,38	-12,86
3,60	18,50	0,70	84,18	0,56	46,81	-0,38	-31,62
9,20	18,50	0,70	86,03	0,56	47,84	-0,38	-32,31
12,90	18,50	0,70	68,45	0,56	38,07	-0,38	-25,71
16,60	18,50	0,70	68,45	0,56	38,07	-0,38	-25,71
20,30	20,30	0,72	68,45	0,58	39,50	-0,39	-26,68
24,00	24,00	0,77	68,45	0,62	42,14	-0,42	-28,46
27,70	27,70	0,81	68,45	0,65	44,44	-0,44	-30,02
31,40	31,40	0,85	68,45	0,68	46,50	-0,46	-31,40
35,10	35,10	0,88	68,45	0,71	48,35	-0,48	-32,66
38,80	38,80	0,91	68,45	0,73	50,05	-0,49	-33,80
42,50	42,50	0,94	68,45	0,75	51,60	-0,51	-34,85
46,20	46,20	0,97	68,45	0,77	53,05	-0,52	-35,83
49,90	49,90	0,99	68,45	0,79	54,40	-0,54	-36,74
53,60	53,60	1,02	68,45	0,81	55,66	-0,55	-37,59
57,30	57,30	1,04	68,45	0,83	56,85	-0,56	-38,39
61,00	61,00	1,06	68,45	0,85	57,97	-0,57	-39,15
64,70	64,70	1,08	68,45	0,86	59,04	-0,58	-39,87
68,40	68,40	1,10	68,45	0,88	60,05	-0,59	-40,56
72,10	72,10	1,11	68,45	0,89	61,02	-0,60	-41,21
75,80	75,80	1,13	68,45	0,90	61,94	-0,61	-41,83
79,50	79,50	1,15	68,45	0,92	62,83	-0,62	-42,43
83,20	83,20	1,16	68,45	0,93	63,68	-0,63	-43,01
86,90	86,90	1,18	68,45	0,94	64,49	-0,64	-43,56
90,60	90,60	1,19	68,45	0,95	65,28	-0,64	-44,09
94,30	94,30	1,21	68,45	0,96	66,04	-0,65	-44,60
98,00	98,00	1,22	68,45	0,98	66,78	-0,66	-45,10
101,70	101,70	1,23	68,45	0,99	67,48	-0,67	-45,58
105,40	105,40	1,24	68,45	1,00	68,17	-0,67	-46,04
109,10	127,10	1,31	68,45	1,05	71,82	-0,71	-48,50
112,80	127,10	1,31	68,45	1,05	71,82	-0,71	-48,50
116,50	127,10	1,31	105,45	1,05	110,64	-0,71	-74,72
124,20	127,10	1,31	71,23	1,05	74,73	-0,71	-50,47

Eventually, Table 5.14 resume the calculated wind actions in zone A, B and C.

Table 5.14: Wind force for zones A, B and C considering an action perpendicular to the short side of the building.

	Zone A			Zone B			Zone C		
z $[m]$	$w_e(z_e)$ /	$A_{ref}(z)$ $[m^2]$	$F_{w,e}$ $[kN]$	$w_e(z_e)$ /	$A_{ref}(z)$ $[m^2]$	$F_{w,e}$ $[kN]$	$w_e(z_e)$ /	$A_{ref}(z)$ $[m^2]$	$F_{w,e}$ $[kN]$
0,10	-0,83	6,85	-5,71	-0,56	27,38	-15,23	-0,35	95,98	-33,36
3,60	-0,83	16,84	-14,04	-0,56	67,34	-37,45	-0,35	236,05	-82,05
9,20	-0,83	17,21	-14,35	-0,56	68,82	-38,28	-0,35	241,24	-83,86
12,90	-0,83	13,69	-11,42	-0,56	54,76	-30,46	-0,35	191,96	-66,72
16,60	-0,83	13,69	-11,42	-0,56	54,76	-30,46	-0,35	191,96	-66,72
20,30	-0,87	13,69	-11,85	-0,58	54,76	-31,60	-0,36	191,96	-69,24
24,00	-0,92	13,69	-12,64	-0,62	54,76	-33,71	-0,38	191,96	-73,85
27,70	-0,97	13,69	-13,33	-0,65	54,76	-35,55	-0,41	191,96	-77,89
31,40	-1,02	13,69	-13,95	-0,68	54,76	-37,20	-0,42	191,96	-81,50
35,10	-1,06	13,69	-14,51	-0,71	54,76	-38,68	-0,44	191,96	-84,75
38,80	-1,10	13,69	-15,01	-0,73	54,76	-40,04	-0,46	191,96	-87,71
42,50	-1,13	13,69	-15,48	-0,75	54,76	-41,28	-0,47	191,96	-90,45
46,20	-1,16	13,69	-15,91	-0,77	54,76	-42,44	-0,48	191,96	-92,98
49,90	-1,19	13,69	-16,32	-0,79	54,76	-43,52	-0,50	191,96	-95,34
53,60	-1,22	13,69	-16,70	-0,81	54,76	-44,53	-0,51	191,96	-97,55
57,30	-1,25	13,69	-17,05	-0,83	54,76	-45,48	-0,52	191,96	-99,64
61,00	-1,27	13,69	-17,39	-0,85	54,76	-46,38	-0,53	191,96	-101,61
64,70	-1,29	13,69	-17,71	-0,86	54,76	-47,23	-0,54	191,96	-103,48
68,40	-1,32	13,69	-18,02	-0,88	54,76	-48,04	-0,55	191,96	-105,25
72,10	-1,34	13,69	-18,31	-0,89	54,76	-48,81	-0,56	191,96	-106,95
75,80	-1,36	13,69	-18,58	-0,90	54,76	-49,55	-0,57	191,96	-108,57
79,50	-1,38	13,69	-18,85	-0,92	54,76	-50,26	-0,57	191,96	-110,12
83,20	-1,40	13,69	-19,10	-0,93	54,76	-50,94	-0,58	191,96	-111,61
86,90	-1,41	13,69	-19,35	-0,94	54,76	-51,60	-0,59	191,96	-113,04
90,60	-1,43	13,69	-19,58	-0,95	54,76	-52,23	-0,60	191,96	-114,42
94,30	-1,45	13,69	-19,81	-0,96	54,76	-52,83	-0,60	191,96	-115,75
98,00	-1,46	13,69	-20,03	-0,98	54,76	-53,42	-0,61	191,96	-117,04
101,70	-1,48	13,69	-20,25	-0,99	54,76	-53,99	-0,62	191,96	-118,28
105,40	-1,49	13,69	-20,45	-1,00	54,76	-54,54	-0,62	191,96	-119,48
109,10	-1,57	13,69	-21,55	-1,05	54,76	-57,46	-0,66	191,96	-125,88
112,80	-1,57	13,69	-21,55	-1,05	54,76	-57,46	-0,66	191,96	-125,88
116,50	-1,57	21,09	-33,19	-1,05	84,36	-88,51	-0,66	295,72	-193,92
124,20	-1,57	14,25	-22,42	-1,05	56,98	-59,78	-0,66	199,74	-130,98

Chapter 6

FEM model in SAP2000

As mentioned in the previous chapters, the finite element program which has been used for the creation of the Pirelli Tower model is *SAP2000*. This software, produced by "Computers and Structures"(CSI) of Walnut Creek (California), is a finite element computing application created for Civil Engineering. *SAP2000* can perform static or dynamic, linear or non-linear analysis of structural systems. It is also a powerful design tool to design structures following many building codes. Therefore, it is a general instrument capable of analyzing structures with very different characteristics. The modelling, analysis and verification steps are integrated into a single graphics environment that makes the use of the program intuitive and easy to learn. It is currently used in more than 150 countries around the world and can boast the highest number of users in the industry.

Moreover, one of the most important reasons for which this program has been chosen for the purpose of this thesis, is that it is capable of generating and meshing highly complex models with more than a hundred thousand elements. The powerful 64-bit solver allows to perform non-linear analysis in step, P-Delta analysis and large displacements, buckling analysis, fast non-linear analysis (FNA) with dampers, base insulators, dissipative bearings, staged construction, progressive collapse analyses and much more. Therefore, to create the model, different types of objects have been used, to simulate in the most accurate way possible the real behaviour of the structure, within the limit of calculation of everyday computers. More in detail, between the various possibilities offered by the software, two different types of finite element have been used:

- **Frame objects:**

  These elements are commonly used for modelling beams, columns, braces, and trusses in planar and three-dimensional structures. Frames elements use a general, three-dimensional, formulation which includes the effects of biaxial bending, torsion, axial deformation, and biaxial shear deformations. Furthermore, they are modelled as a straight line connecting two points, and each element has its own local coordinate system for defining section properties and loads and also for interpreting the output. Therefore, these objects have been used to model the reinforcing beams of slab floors and top covering;

- **Shell objects:**

  These *Area objects* are used for the modelling of membranes, plates, and walls in planar and three-dimensional structures. The material of these elements may be homogeneous or layered through the thickness, and they can also consider material nonlinearity. The Shell

element is a three or four-node formulation that combines membrane and plate bending behaviour. Similarly to the frame elements, also each shell element has its own local coordinate system for defining material properties and loads, and for interpreting the output. Moreover, Two thickness formulations are available, which determine whether or not transverse shearing deformations are included in the plate-bending behaviour of a shell element: The Thick-Plate includes the effects of transverse shear deformation, and the Thin-Plate does not. Hence, to obtain the maximum accuracy possible, Shell-Thick elements have been used for modelling all the vertical load-bearing elements of the structure, which can clearly be considered walls, and the slabs of floors and top covering.

Thus, through the use of the previously described elements, the realised model, which can be seen in Fig 6.1, consists of:

- 114 667 joints of which 390 with Restraints;
- 113 850 Shell-Thick elements;
- 10 487 Frame elements;
- 360 Constraints.

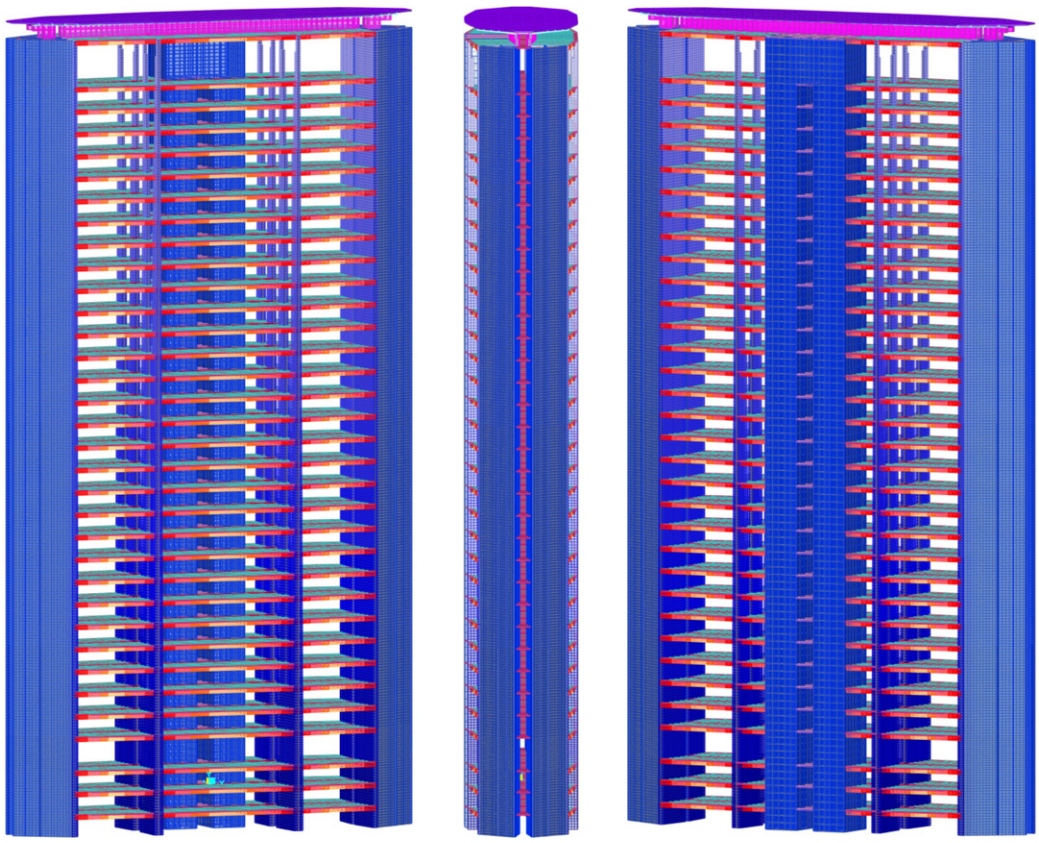

Figure 6.1: The model realized in Sap2000 of the Pirelli Tower.

In the next sections, a review of the most significant aspects of the model will be exposed.

6.1 Materials

The defined materials are the Concrete 400 and the steel used in the reinforcing bars of the slab floors, the RUMI LU3.

6.1.1 Concrete 400

This type of concrete has been used in the construction of the entire structure except for the foundation. The characteristics introduced in the program, which have been determined in section 5.2.1.1, are:

- Weight per unit volume: 25 KN/m^3;
- Modulus of elasticity: 31244 MPa;
- Coefficient of Poisson: 0,2;
- Coefficient of thermal expansion: $9,9 \cdot 10^{-6}\ ^{\circ}C^{-1}$;
- Specified compressive concrete strength: 13,7 MPa;
- Expected compressive concrete strength: 13,7 MPa.

This concrete type has been assigned to each section type defined in the model.

6.1.2 Steel RUMI LU3

This particular steel was used in the reinforcing bars of the slab floors. The parameters that have been introduced in the program are:

- Weight per unit volume: 76,9729 KN/m^3;
- Modulus of elasticity: 200000 MPa;
- Coefficient of thermal expansion: $1,17 \cdot 10^{-5}\ ^{\circ}C^{-1}$;
- Coefficient of Poisson: 0,2;
- Minimum yield stress: 440 MPa;
- Minimum tensile stress: 600 MPa;
- Expected yield stress: 457,5 MPa;
- Expected tensile stress: 640 MPa;

This steel type has been assigned to the reinforcing bars of the slab floors.

6.2 Modelling of the structural elements

6.2.1 Model organisation

To realize such a massive model, one of the most critical aspects concern the organization and the nomenclature used for the various elements. Indeed, if this preliminary step is not very well handled, could easily propitiate errors in the definition and assignment of properties to the various components. Hence, the vertical load-bearing elements of the building have been called with the code represented in Figure 6.2.

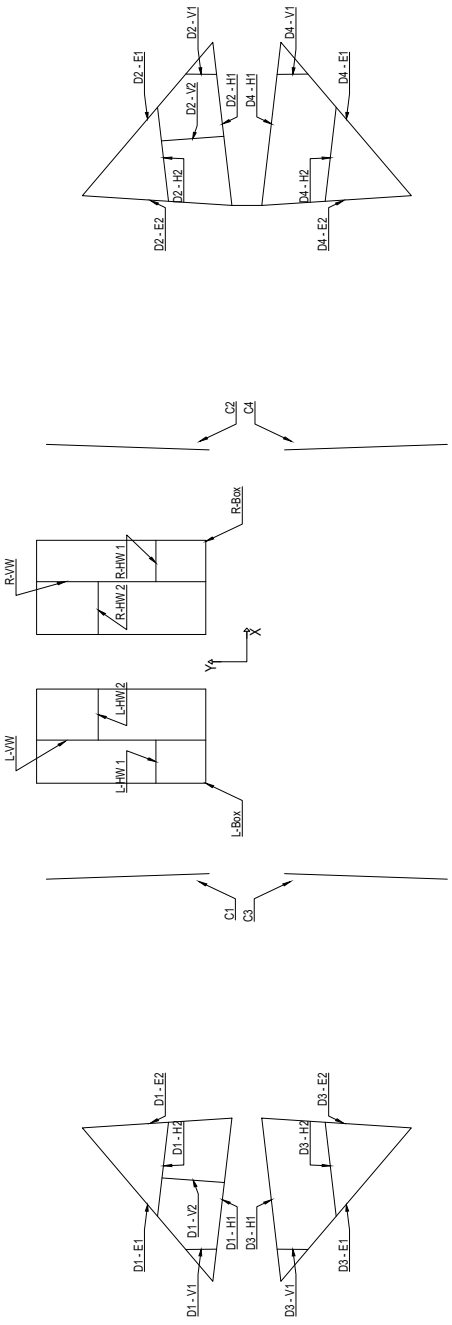

Figure 6.2: Nomenclature of the vertical elements.

6.2.2 Columns

6.2.2.1 Definition of the area sections

Since the hourglass shape of the columns was very complex to be well modelled and was not a significant aspect, the first step consisted of finding an equivalent rectangular shape that permits to have an equal transversal area of these elements. As the columns reduce their thickness with the height, the equivalent section has been determined at every storey level. Eventually, since the variation in thickness between each floor was very modest, the average value correspondent to every block formed by three storeys was used, and therefore twelve area sections have been determined:

- **C01 -7,25 m to 3,60 m**: Type: Shell-Thick, Membrane and bending thickness: $1,561\,m$, Material: Concrete 400;
- **C02 3,60 m to 16,60 m**: Type: Shell-Thick, Membrane and bending thickness: $1,510\,m$, Material: Concrete 400;
- **C03 16,60 m to 27,70 m**: Type: Shell-Thick, Membrane and bending thickness: $1,415\,m$, Material: Concrete 400;
- **C04 27,70 m to 38,80 m**: Type: Shell-Thick, Membrane and bending thickness: $1,324\,m$, Material: Concrete 400;
- **C05 38,80 m to 49,90 m**: Type: Shell-Thick, Membrane and bending thickness: $1,229\,m$, Material: Concrete 400;
- **C06 49,90 m to 61,00 m**: Type: Shell-Thick, Membrane and bending thickness: $1,132\,m$, Material: Concrete 400;
- **C07 61,00 m to 72,10 m**: Type: Shell-Thick, Membrane and bending thickness: $1,031\,m$, Material: Concrete 400;
- **C08 72,10 m to 83,20 m**: Type: Shell-Thick, Membrane and bending thickness: $0,927\,m$, Material: Concrete 400;
- **C09 83,20 m to 94,30 m**: Type: Shell-Thick, Membrane and bending thickness: $0,820\,m$, Material: Concrete 400;
- **C10 94,30 m to 105,40 m**: Type: Shell-Thick, Membrane and bending thickness: $0,710\,m$, Material: Concrete 400;
- **C11 105,40 m to 116,50 m**: Type: Shell-Thick, Membrane and bending thickness: $0,596\,m$, Material: Concrete 400;
- **C12 116,50 m to 124,20 m**: Type: Shell-Thick, Membrane and bending thickness: $0,559\,m$, Material: Concrete 400.

6.2.2.2 Modelling of the columns

The columns have been obtained using approximately square finite elements of 0,49 meters for each side. In this way, it was possible to model the narrowing of the column with the removal of one finite element in correspondence of levels located at $3,6\,m$, $20,3\,m$, $42,5\,m$, $75,8\,m$, $109,1\,m$, $121,4\,m$ and $124,2\,m$, minimizing the differences with the real shrinkage. The modelled columns can be seen in Fig. 6.3 and 6.4.

Figure 6.3: XY view of the modelled columns.

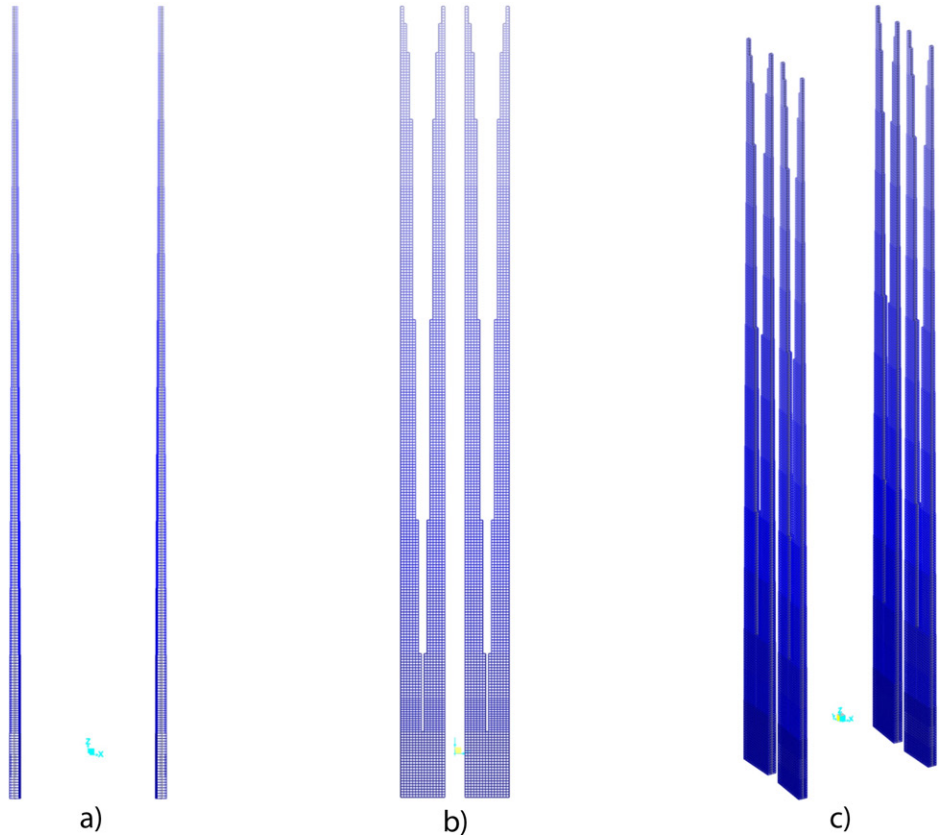

Figure 6.4: Different views of the modelled columns: a) XZ view, b) YZ view, c) 3D view.

6.2.3 Triangular diaphragms

6.2.3.1 Definition of the area sections

The triangular elements can be considered made up to two different parts, the inner walls D1-E2, D2-E2, D3-E2 and D4-E2 (see Fig. 6.2) with the same hourglass shape as the columns, and the other walls, which have a classic rectangular shape. For the former, a very similar procedure to the columns have been followed, defining twelve area sections equivalent to the original form, while the additional rectangular walls can be further subdivided: the elements D1-E1, D2-E1, D3-E1, D4-E1 and D1-H1, D2-H1, D3-H1, D4-H1 have a variable thickness with height while the remaining have a constant shape.

Equivalent rectangular walls for D1-E2, D2-E2, D3-E2, D4-E2 walls:

- **D01 -7,25 m to 3,60 m**: Type: Shell-Thick, Membrane and bending thickness: $0,960\,m$, Material: Concrete 400;
- **D02 3,60 m to 16,60 m**: Type: Shell-Thick, Membrane and bending thickness: $0,946\,m$, Material: Concrete 400;
- **D03 16,60 m to 27,70 m**: Type: Shell-Thick, Membrane and bending thickness: $0,920\,m$, Material: Concrete 400;
- **D04 27,70 m to 38,80 m**: Type: Shell-Thick, Membrane and bending thickness: $0,896\,m$, Material: Concrete 400;
- **D05 38,80 m to 49,90 m**: Type: Shell-Thick, Membrane and bending thickness: $0,872\,m$, Material: Concrete 400;
- **D06 49,90 m to 61,00 m**: Type: Shell-Thick, Membrane and bending thickness: $0,848\,m$, Material: Concrete 400;
- **D07 61,00 m to 72,10 m**: Type: Shell-Thick, Membrane and bending thickness: $0,824\,m$, Material: Concrete 400;
- **D08 72,10 m to 83,20 m**: Type: Shell-Thick, Membrane and bending thickness: $0,800\,m$, Material: Concrete 400;
- **D09 83,20 m to 94,30 m**: Type: Shell-Thick, Membrane and bending thickness: $0,776\,m$, Material: Concrete 400;
- **D10 94,30 m to 105,40 m**: Type: Shell-Thick, Membrane and bending thickness: $0,752\,m$, Material: Concrete 400;
- **D11 105,40 m to 116,50 m**: Type: Shell-Thick, Membrane and bending thickness: $0,729\,m$, Material: Concrete 400;
- **D12 116,50 m to 124,20 m**: Type: Shell-Thick, Membrane and bending thickness: $0,708\,m$, Material: Concrete 400.

Standard rectangular sections for D1-E1, D2-E1, D3-E1, D4-E1 and D1-H1, D2-H1, D3-H1, D4-H1 walls:

- **Wall 0,40 m**: Type: Shell-Thick, Membrane and bending thickness: $0,400\,m$, Material: Concrete 400, Height: -7,25 m to 24,00 m;
- **Wall 0,35 m**: Type: Shell-Thick, Membrane and bending thickness: $0,350\,m$, Material: Concrete 400, Height: 24,00 m to 61,00 m;
- **Wall 0,30 m**: Type: Shell-Thick, Membrane and bending thickness: $0,300\,m$, Material: Concrete 400, Height: 61,00 m to 101,70 m;
- **Wall 0,25 m**: Type: Shell-Thick, Membrane and bending thickness: $0,250\,m$, Material: Concrete 400, Height: 101,70 m to 124,20 m.

Standard rectangular section for D1-H2, D2-H2, D3-H2, D4-H2 walls:

- **Wall 0,35 m**: Type: Shell-Thick, Membrane and bending thickness: $0,350\,m$, Material: Concrete 400, Height: -7,25 m to 124,20 m.

Standard rectangular section for D1-V1, D2-V1, D3-V1, D4-V1 walls:

- **Wall 0,25 m**: Type: Shell-Thick, Membrane and bending thickness: $0,250\,m$, Material: Concrete 400, Height: -7,25 m to 124,20 m.

Standard rectangular section for D1-V2, D2-V2, D3-V2, D4-V2 walls:

- **Wall 0,15 m**: Type: Shell-Thick, Membrane and bending thickness: $0,150\,m$, Material: Concrete 400, Height: -7,25 m to 124,20 m.

6.2.3.2 Modelling of the triangular diaphragms

The diaphragms have been obtained proceeding in a very similar way regard what has been done for the columns. The finite elements are approximately square and have various dimensions to allow a good precision of the model. Moreover, using the command *Area object-joint offset in thickness direction* with the elements D1-E2, D2-E2, D3-E2, D4-E2 and D1-H2, D2-H2, D3-H2, D3-H2, the offset of the component, with reference to the drawn line, has been moved sideways of half the thickness of the various parts to guarantee that the variation in thickness of these elements is only in the inner part of the building. The modelled triangular walls can be seen in Figures 6.5 and 6.6.

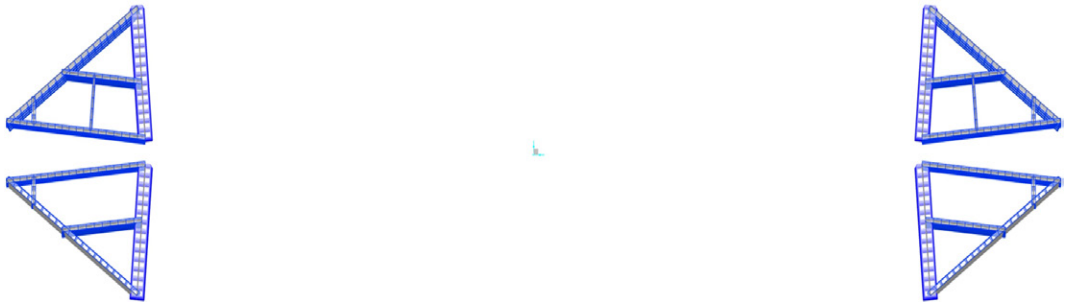

Figure 6.5: XY view of the modelled triangular walls.

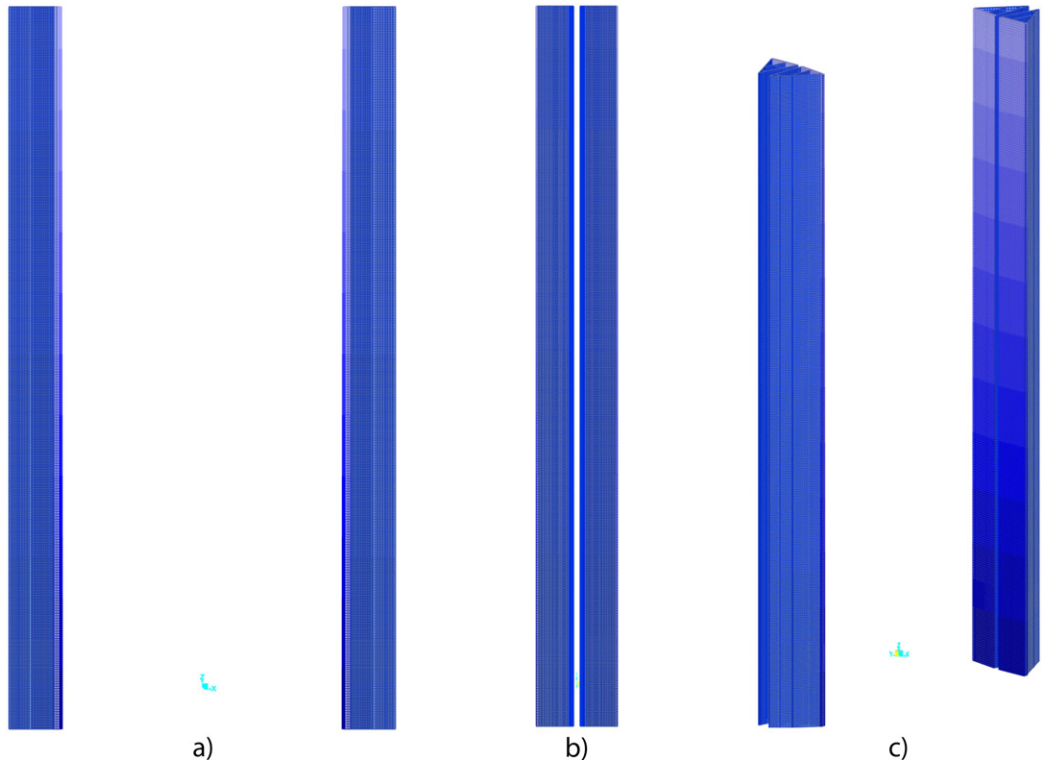

Figure 6.6: Different views of the modelled triangular walls: a) XZ view, b) YZ view, c) 3D view.

6.2.4 Rectangular cores

6.2.4.1 Definition of the area sections

All the elements of this structural part have a constant thickness with height. The area sections defined to model these objects are the following:

Standard rectangular wall for L-Box and R-Box:

- **Wall 0,30 m**: Type: Shell-Thick, Membrane and bending thickness: $0,300\,m$, Material: Concrete 400, Height: -7,25 m to 124,20 m.

Standard rectangular wall for L-VW and R-VW:

- **Wall 0,20 m**: Type: Shell-Thick, Membrane and bending thickness: $0,200\,m$, Material: Concrete 400, Height: -7,25 m to 124,20 m.

Standard rectangular wall for L-HW1, L-HW2, R-HW1, R-HW2:

- **Wall 0,15 m**: Type: Shell-Thick, Membrane and bending thickness: $0,150\,m$, Material: Concrete 400, Height: -7,25 m to 124,20 m.

6.2.4.2 Modelling of the rectangular cores

As done previously, the finite elements are approximately square and have various dimensions to guarantee a good precision of the model. The Figures 6.7 and 6.8 show the modelled cores.

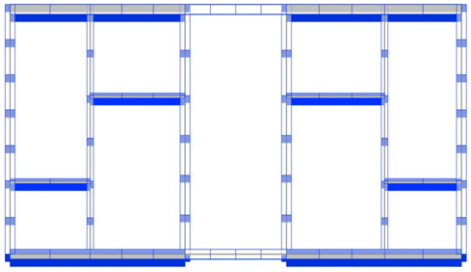

Figure 6.7: XY view of the modelled rectangular cores.

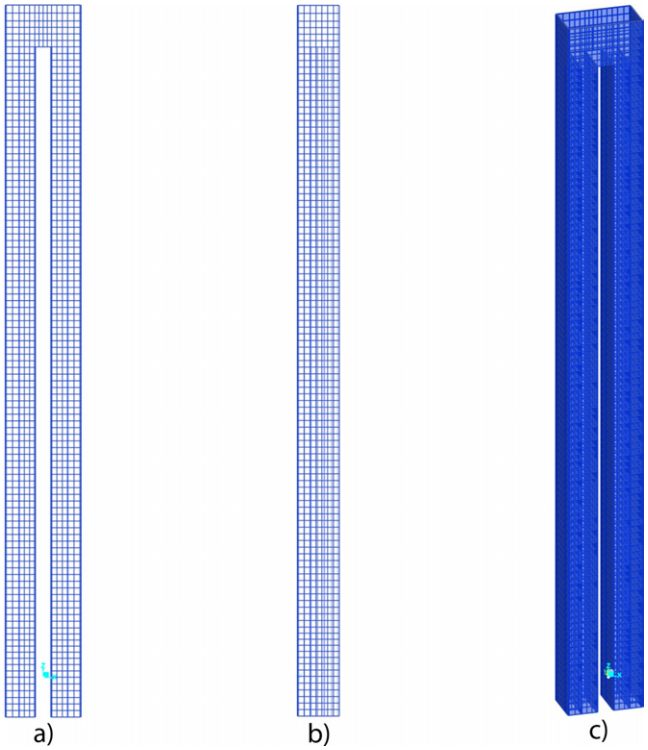

Figure 6.8: Different views of the modelled rectangular cores: a) XZ view, b) YZ view, c) 3D view.

6.2.5 Slab floors

The slab floors have been modelled trying to replicate the originals structural plans as faithfully as possible. More in detail, the "T"beams, represented in Drawing 2, have been decomposed in two elements, a rectangular beam joined to a slab in the upper portion. Therefore, to replicate the thickness variability of the slab and beams, numerous elements have been defined.

6.2.5.1 Frame elements

First of all, four rectangular sections of the primary beams plus the one related to the secondary beams have been determined:

- **SF-SA**: Depth$= 0,67\,m$, width$= 0,50\,m$, Material: Concrete 400;
- **SF-SB**: Depth$= 0,67\,m$, width$= 0,35\,m$, Material: Concrete 400;
- **SF-SC**: Depth$= 0,67\,m$, width$= 0,20\,m$, Material: Concrete 400. Concrete 400;
- **SF-SD**: Depth$= 0,67\,m$, width$= 0,20\,m$, Material: Concrete 400;
- **SF-SE**: Depth$= 0,67\,m$, width$= 0,50\,m$, Material: Concrete 400;
- **Secondary beams**: Depth$= 0,67\,cm$, width$= 0,18\,cm$, Material: Concrete 400.

As should be noticed, sections SF-SA, SF-SB, SF-SC, SF-SD represent the rectangular portion of the "T"sections represented in Drawing 2. Subsequently, four beams with a variable section have been defined with the following characteristics:

- **1-Variable section E-D**: Start section: SF-SE, End section: SF-SD, Length: 1, Length type: variable, EI33 variation: Linear, EI22 variation: Cubic, Color: yellow ocher;
- **2-Variable section D-C**: Start section: SF-SD, End section: SF-SC, Length: 1, Length type: variable, EI33 variation: Linear, EI22 variation: Cubic, Color: orange;
- **3-Variable section C-B**: Start section: SF-SC, End section: SF-SB, Length: 1, Length type: variable, EI33 variation: Linear, EI22 variation: Cubic, Color: light red;
- **4-Variable section B-A**: Start section: SF-SB, End section: SF-SA, Length: 1, Length type: variable, EI33 variation: Linear, EI22 variation: Cubic, Color: red.

Thus, it was necessary to pay particular attention drawing the beams keeping the same local axes for each one. Eventually, using the command *Assign-frame-insertion point* was possible to modify the position of the beams respect to the drawn line. Most in detail, the drawn line was moved upwards by 0,335 cm, ensuring that the beams and the slab that will be described in the next section, would join together correctly. The group of beams obtained is represented in Fig. 6.9.

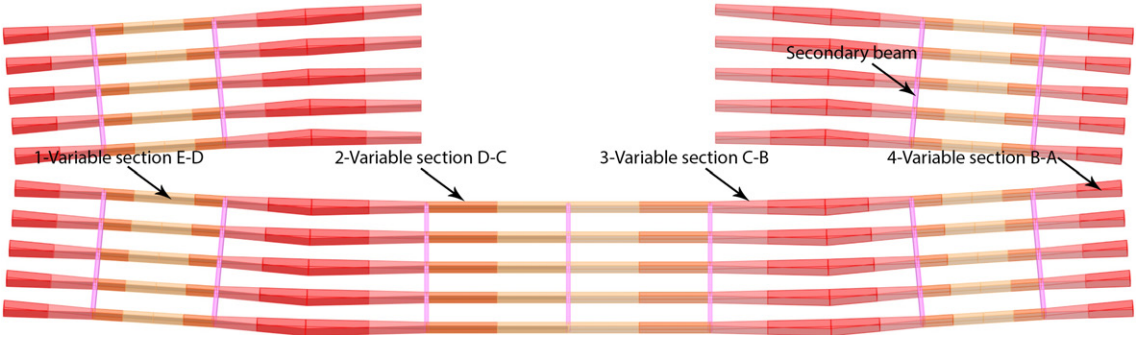

Figure 6.9: 3D view of the modelled slab floor beams.

6.2.5.2 Shell elements

As indicated in Drawing 1, three different thickness of the slab have been used in the Pirelli Tower. Therefore, three different Shell-Thick elements have been defined:

- **SF1**: Membrane thickness $= 0,08\,m$, Bending thickness $= 0,08\,m$, Material: Concrete 400;
- **SF2**: Membrane thickness $= 0,12\,m$, Bending thickness $= 0,12\,m$, Material: Concrete 400;
- **SF3**: Membrane thickness $= 0,22\,m$, Bending thickness $= 0,22\,m$, Material: Concrete 400.

The various shell elements of the slab have been drawn paying attention to use the existing joints of the slab floor beams, ensuring so the monolithic behaviour of these two components of the floor. Moreover, as done for some other shell elements, with the command *Area object joint offset in thickness direction* the offset of the component, with reference to the drawn line, has been moved downwards of half the thickness of the various slab. The final aspect of the slab floor is represented if Fig. 6.10.

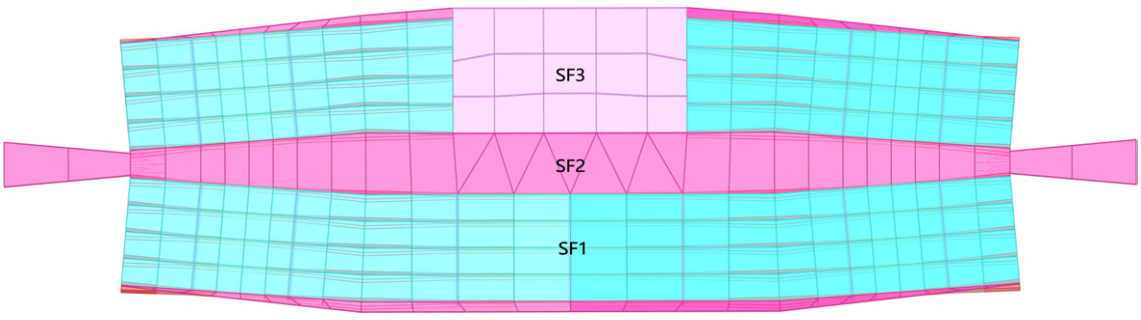

Figure 6.10: 3D view of the modelled slab floor in SAP2000.

It should be noticed that the portion of the *SF3* slab is present only in the last two storeys, while in the others this section of the building is used for elevators and stairs.

6.2.6 Roof slab

The roof consists of two walls with two openings, and a top slab reinforced with beams of variable thickness.

6.2.6.1 Frame elements

Similarly to what realized with the slab floors beam, two rectangular sections have been defined:

- **Covering-SA**: Depth$= 0,25\,m$, width$= 0,40\,m$, Material: Concrete 400;
- **Covering-SB**: Depth$= 0,60\,m$, width$= 0,40\,m$, Material: Concrete 400.

Therefore a beam with a variable section has been defined with the following characteristics:

- **Covering variable section**: Start section: Covering-SB, End section: Covering-SA, Length: 1, Length type: variable, EI33 variation: cubic, EI22 variation: linear, Color: azure.

Eventually, as did before, with the command *Assign-frame-insertion point* the position of the beams respect to the drawn line has been modified, ensuring that the beams and the slab would join together correctly.

6.2.6.2 Shell elements

Two area sections have been defined, one for the walls and another for the covering slab:

- **Covering**: Membrane thickness $= 0,15\,m$, Bending thickness $= 0,15\,m$, Material: Concrete 400;
- **Covering wall**: Membrane thickness $= 0,5\,m$, Bending thickness $= 0,5\,m$, Material: Concrete 400.

The various shell elements of the slab have been drawn paying attention to use the existing joints of the slab floor beams, ensuring so the monolithic behaviour of these two components of the floor. Also for the covering slab, the element offset has been moved downwards of half the thickness of the slab. In the end, in Figures 6.12 and 6.11, different views of the covering can be observed.

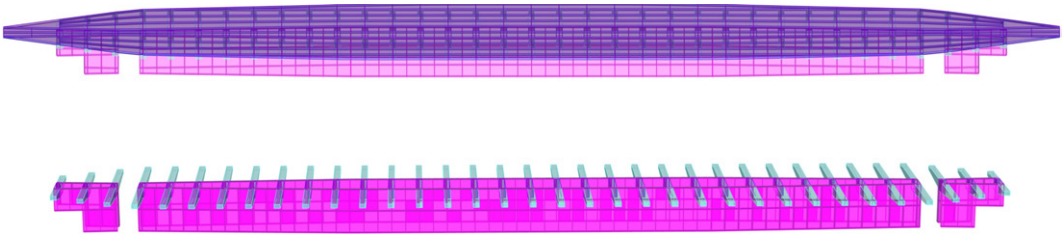

Figure 6.11: Roofing with the top slab (up) and without (down).

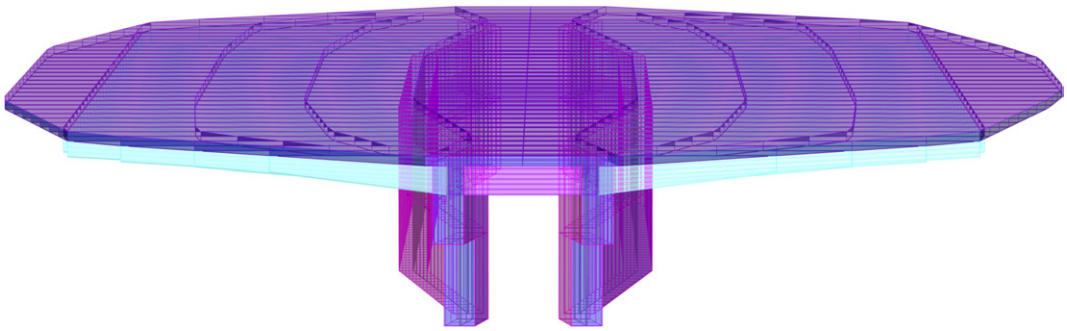

Figure 6.12: 3D view of the modelled roof.

6.3 Restraints

The model is characterized by 390 restraints entirely assigned to the joints at the base of the building. The assigned restraints limit the following movements:

Translation 1: Blocked	Rotation about 1: Blocked
Translation 2: Blocked	Rotation about 2: Blocked
Translation 3: Blocked	Rotation about 3: Blocked

Figure 6.13 shows two view of the assigned restraints.

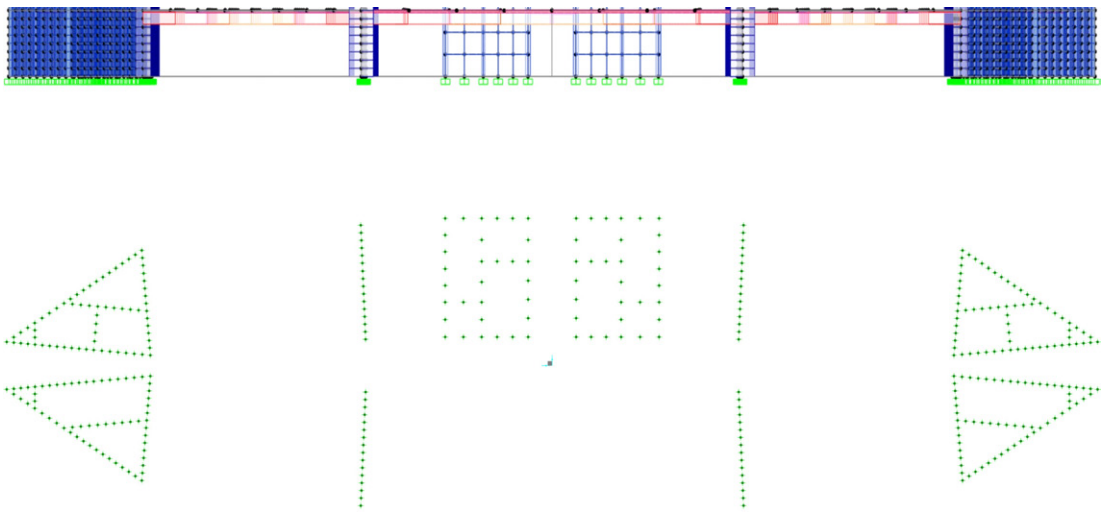

Figure 6.13: View of the restraints assigned to the joints at the base of the building.

6.4 Constraints between floors and vertical elements

Between the elements belonging to the slab floors and the vertical elements, 340 constraints (ten for each storey) have been defined guaranteeing the correct behaviour of the structure. More in detail, depending on the storeys, two different types of constraints have been assigned:

- First floor to fourth $\longrightarrow$ XY-Hinge;
- Fourth floor to last floor $\longrightarrow$ XY-Lock;

Where XY represents a code of two numbers assigned as follows:

- **X:**

  Number of the considered floor (1 to 35);

- **Y:**

  Number of the intersection between vertical elements and slab floor components in each storey, counterclockwise;

In the next sections, a description of the main features of the defined constraints is presented.

6.4.1 First floor to fourth

As said before, the first four floors are simply supported by the vertical structural elements.

Therefore, the constraints defined and assigned between the lateral joints of the slab floors and the vertical elements have the following characteristics:

Translation X: Free	Rotation X: Free
Translation Y: Free	Rotation Y: Free
Translation Z: Blocked	Rotation Z: Free

6.4.2 Fifth floor to the last

Differently to the previous floors, the constraints defined and assigned between the lateral joints of the slab floors and the vertical elements of the upper storeys have the following properties:

Translation X: Blocked	Rotation X: Blocked
Translation Y: Blocked	Rotation Y: Blocked
Translation Z: Blocked	Rotation Z: Blocked

6.5 Loads

The first step required for implementing the loads was the definition of the *Load patterns*:

- **DEAD:** Type: Dead, Self weight multiplier: 1;
- **G1:** Type: Other, Self weight multiplier: 0;
- **G2:** Type: Other, Self weight multiplier: 0;
- **Overload_B:** Type: Other, Self weight multiplier: 0;
- **Overload_H:** Type: Other, Self weight multiplier: 0;
- **Snow** Type: Other, Self weight multiplier: 0;
- **Wind_Y** Type: Other, Self weight multiplier: 0;
- **Wind_-Y** Type: Other, Self weight multiplier: 0;
- **Wind_X** Type: Other, Self weight multiplier: 0;
- **Wind_-X** Type: Other, Self weight multiplier: 0.

Secondly, depending on the load type, two different approaches have been used to implement the loads in the model:

- Floor finishings, partitions, overload for B and H category in the slab floors and snow have been implemented as *area loads* assigning to each shell element the correspondent uniform load in KN/m^2;
- Structural and non-structural stairs loads, category B overload of the stairs, facade loads and the wind action have been assigned to the correspondent joints that delimit the shell elements interested by the actions.

6.5.1 Area loads

6.5.1.1 Floor finishings

For this loads, at each shell element forming part of the inner slab floors, has been assigned an area loads with the following characteristics:

- Load pattern: G2;
- Coordinate system: Global;
- Load direction: Gravity;
- Uniform load: 1,13 KN/m^2.

While for the last floor on top of the building, the assigned area load was:

- Load pattern: G2;
- Coordinate system: Global;
- Load direction: Gravity;
- Uniform load: 1,84 KN/m^2.

6.5.1.2 Partitions

As did for the previous load, at each shell element was assigned the following uniform area load:

- Load pattern: G2;
- Coordinate system: Global;
- Load direction: Gravity;
- Uniform load: 0,8 KN/m^2.

6.5.1.3 Overloads for categories B and H

The assigned *uniform area load* assigned at each shell elements of the slab floor was:

- Load pattern: Overload_B;
- Coordinate system: Global;
- Load direction: Gravity;
- Uniform load: 2 KN/m^2.

and for the covering:

- Load pattern: Overload_H;
- Coordinate system: Global;
- Load direction: Gravity;
- Uniform load: 0,5 KN/m^2.

6.5.1.4 Snow loads

The last *uniform area load* assigned to the covering was related to the snow:

- Load pattern: Snow;
- Coordinate system: Global;
- Load direction: Gravity;
- Uniform load: 1,2 KN/m^2.

6.5.2 Joint loads

The forces assigned to each joint were determined, dividing the resultant force between the total number of joints affected by the action.

6.5.2.1 Structural stairs loads

The determination of the forces assigned to the joints is summarized in Tables 6.1 and 6.2.

Table 6.1: Permanent structural loads for each joint of the stairs located in the triangular elements.

Height Q $[m]$	Inter-storey $[m]$	G_1 $[kN]$	Joints	$G_{1,\,joints}$ $[kN]$
-7,25 to -3,65	3,60	101,34	38	2,67
-3,65 to 0,10	3,75	102,60	38	2,70
0,10 to 3,60	3,50	100,50	38	2,64
3,60 to 9,20	5,60	189,24	38	4,98
9,20 to 116,50	3,70	102,18	38	2,69
116,50 to 124,20	7.70	206,88	38	5,44

Table 6.2: Permanent structural loads for each joint of the stairs located in the rectangular cores.

Height Q $[m]$	Inter-storey $[m]$	G_1 $[kN]$	Joints	$G_{1,\,joints}$ $[kN]$
-7,25 to -3,65	3,60	64,74	13	4,98
-3,65 to 0,10	3,75	65,50	13	5,04
0,10 to 3,60	3,50	64,24	13	4,94
3,60 to 9,20	5,60	121,42	13	9,34
9,20 to 116,50	3,70	65,25	13	5,02
116,50 to 124,20	7.70	132,01	13	10,15

Through the command *Assign joint loads* the forces have been assigned to each joint with the following characteristics:

- Load pattern: G1;
- Coordinate system: Global;
- Force global Z: value depends on the storey.

6.5.2.2 G2 stairs loads

The determination of this load is summarized in Table 6.3 while the assigned *joint loads* have the following properties:

- Load pattern: G2;
- Coordinate system: Global;
- Force global Z: value depends on the storey.

Table 6.3: Permanent non-structural loads for each joint of the stairs.

Stairs in the triangular diaphragms			
Height Q $[m]$	Load $[kN]$	Joints	Q_{joint} $[kN]$
-7,25 to 124,20	7,75	38	0,2
Stairs rectangular cores of the building			
Height Q $[m]$	Load $[kN]$	Joints	Q_{joint} $[kN]$
-7,25 to 124,20	5,5	13	0,42

6.5.2.3 Overload stairs load

The last load that has to be assigned to the stairs joints is the overload for category B:

Table 6.4: Category B overloads for each joint of the stairs.

Stairs in the triangular diaphragms					
Height Q $[m]$	Load $[kN/m^2]$	Area $[m^2]$	Q $[kN]$	Joints	Q_{joint} $[kN]$
-7,25 to 124,20	4,00	15,50	62,00	38	1,63
Stairs in the central part of the building					
Height Q $[m]$	Load $[kN/m^2]$	Area $[m^2]$	Q $[kN]$	Joints	Q_{joint} $[kN]$
-7,25 to 124,20	4,00	11,00	44,00	13	3,38

The assigned *joint load* was:

- Load pattern: Overload_B;
- Coordinate system: Global;
- Force global Z: Depends on the stairs location.

6.5.2.4 G2 facade loads

The facade, at each storey, can be divided into three areas: the main facade, the rear one between the two rectangular cores and the two parts at the sides of the rectangular cores. Therefore, the facade loads were assigned to joints belonging ate the perimeter of each floor.

Table 6.5: Facade loads for each peripheral joint of the slab floors.

Inter-storey height $[m]$	Main facade $F_{G2,\,joint}$ $[KN]$	lateral Rear facade $F_{G2,\,joint}$ $[KN]$	Central rear facade $F_{G2,\,joint}$ $[KN]$
3,75	2,66	2,04	2,34
3,50	2,15	1,65	1,89
5,60	4,59	3,52	4,08
3,7 Locked	2,28	1,75	2,01
3,7 supported	2,83	2,38	2,01
7,70	7,32	6,17	5,27

The assigned load had the following characteristics:

- Load pattern: G2;
- Coordinate system: Global;
- Force global Z: Depends on the storeys and location of the joints.

6.5.2.5 Wind load

The wind loads have been assigned considering the four directions Y, -Y, X and -X. Moreover, the loads have been attributed to the external joints of the structure and correspondent to each floor.

Wind in direction Y

Considering this direction of the wind, the applied forces to each joint have been summarized in Table 6.6:

Table 6.6: Wind loads for the external joints belonging to zone D and E of the building. Direction Y.

	Zone D		Zone E	
z $[m]$	Joints	$F_{w,e,\,joint}$ $[kN]$	Joints	$F_{w,e,\,joint}$ $[kN]$
0,10	71	1,46	80	-1,13
3,60	71	3,59	80	-2,79
9,20	71	3,67	80	-2,85
12,90	65	3,19	72	-2,52
16,60	65	3,19	72	-2,52
20,30	65	3,19	72	-2,52
24,00	65	3,19	72	-2,52
27,70	65	3,19	72	-2,52
31,40	65	3,19	72	-2,52
35,10	65	3,19	72	-2,52
38,80	65	3,19	72	-2,52
42,50	65	3,19	72	-2,52
46,20	65	3,19	72	-2,52
49,90	65	3,19	72	-2,52
53,60	65	3,19	72	-2,52
57,30	65	3,19	72	-2,52
61,00	65	3,19	72	-2,52
64,70	65	3,19	72	-2,52
68,40	65	3,19	72	-2,52
72,10	65	3,78	72	-2,99
75,80	65	3,78	72	-2,99
79,50	65	3,78	72	-2,99
83,20	65	3,78	72	-2,99
86,90	65	3,78	72	-2,99
90,60	65	3,78	72	-2,99
94,30	65	3,78	72	-2,99
98,00	65	3,78	72	-2,99
101,70	65	3,78	72	-2,99
105,40	65	3,78	72	-2,99
109,10	65	3,78	72	-2,99
112,80	65	3,78	72	-2,99
116,50	65	5,83	72	-4,60
124,20	65	3,94	72	-3,11

The load assignment has been accomplished in the following form:

- Load pattern: Wind_Y;
- Coordinate system: Global;
- Force global Y: Depends on the storeys and location of the joints.

Wind in direction -Y

This case is the opposite of the previous. The zone D and E are inverted regard the case considered in the previous section.

Table 6.7: Wind loads for the external joints belonging to zone D and E of the building. Direction -Y.

	Zone D		Zone E	
z $[m]$	Joints	$F_{w,e,\,joint}$ $[kN]$	Joints	$F_{w,e,\,joint}$ $[kN]$
0,10	80	1,30	71	-1,28
3,60	80	3,19	71	-3,14
9,20	80	3,26	71	-3,21
12,90	72	2,88	65	-2,79
16,60	72	2,88	65	-2,79
20,30	72	2,88	65	-2,79
24,00	72	2,88	65	-2,79
27,70	72	2,88	65	-2,79
31,40	72	2,88	65	-2,79
35,10	72	2,88	65	-2,79
38,80	72	2,88	65	-2,79
42,50	72	2,88	65	-2,79
46,20	72	2,88	65	-2,79
49,90	72	2,88	65	-2,79
53,60	72	2,88	65	-2,79
57,30	72	2,88	65	-2,79
61,00	72	2,88	65	-2,79
64,70	72	2,88	65	-2,79
68,40	72	2,88	65	-2,79
72,10	72	3,42	65	-3,31
75,80	72	3,42	65	-3,31
79,50	72	3,42	65	-3,31
83,20	72	3,42	65	-3,31
86,90	72	3,42	65	-3,31
90,60	72	3,42	65	-3,31
94,30	72	3,42	65	-3,31
98,00	72	3,42	65	-3,31
101,70	72	3,42	65	-3,31
105,40	72	3,42	65	-3,31
109,10	72	3,42	65	-3,31
112,80	72	3,42	65	-3,31
116,50	72	5,26	65	-5,10
124,20	72	3,55	65	-3,44

The load assignment was the following:

- Load pattern: Wind_-Y;

- Coordinate system: Global;
- Force global Y: Depends on the storeys and location of the joints.

Wind in direction X

The last case considered concern the wind acting in direction X. In this circumstance, the detachment of the vortices causes a non-negligible action against the principal and rear facade. For this reason, also the zones A, B and C have been considered, and the loads that have been applied to each joint are summarized in Tables 6.8 and 6.9. For direction -X, it will be sufficient to change the sign of forces in Tables Tables 6.8 and 6.9.

Table 6.8: Wind loads for the external joints belonging to zone D, E and A of the building. Direction X.

	Zona D		Zona E		Zona A - Main and rear f.	
z $[m]$	joints	$F_{w,e,\,joint}$ $[kN]$	joints	$F_{w,e,\,joint}$ $[kN]$	joints	$F_{w,e,\,joint}$ $[kN]$
0,10	42	0,45	42	-0,31	9	-0,63
3,60	42	1,11	42	-0,75	9	-1,56
9,20	42	1,14	42	-0,77	9	-1,59
12,90	42	0,91	42	-0,61	9	-1,27
16,60	42	0,91	42	-0,61	9	-1,27
20,30	42	0,94	42	-0,64	9	-1,32
24,00	42	1,00	42	-0,68	9	-1,40
27,70	42	1,06	42	-0,71	9	-1,48
31,40	42	1,11	42	-0,75	9	-1,55
35,10	42	1,15	42	-0,78	9	-1,61
38,80	42	1,19	42	-0,80	9	-1,67
42,50	42	1,23	42	-0,83	9	-1,72
46,20	42	1,26	42	-0,85	9	-1,77
49,90	42	1,30	42	-0,87	9	-1,81
53,60	42	1,33	42	-0,90	9	-1,86
57,30	42	1,35	42	-0,91	9	-1,89
61,00	42	1,38	42	-0,93	9	-1,93
64,70	42	1,41	42	-0,95	9	-1,97
68,40	42	1,43	42	-0,97	9	-2,00
72,10	42	1,45	42	-0,98	9	-2,03
75,80	42	1,47	42	-1,00	9	-2,06
79,50	42	1,50	42	-1,01	9	-2,09
83,20	42	1,52	42	-1,02	9	-2,12
86,90	42	1,54	42	-1,04	9	-2,15
90,60	42	1,55	42	-1,05	9	-2,18
94,30	42	1,57	42	-1,06	9	-2,20
98,00	42	1,59	42	-1,07	9	-2,23
101,70	42	1,61	42	-1,09	9	-2,25
105,40	42	1,62	42	-1,10	9	-2,27
109,10	42	1,71	42	-1,15	9	-2,39
112,80	42	1,71	42	-1,15	9	-2,39
116,50	42	2,63	42	-1,78	9	-3,69
124,20	42	1,78	42	-1,20	9	-2,49

Table 6.9: Wind loads for the external joints belonging to zone B, C of the building. Direction X.

	Zona B - Main and rear f.		Zona C - Main f.		Zona C - Rear f.	
z $[m]$	joints	$F_{w,e,\,joint}$ $[kN]$	joints	$F_{w,e,\,joint}$ $[kN]$	joints	$F_{w,e,\,joint}$ $[kN]$
0,10	18	-0,85	44	-0,76	53	-0,63
3,60	18	-2,08	44	-1,86	53	-1,55
9,20	18	-2,13	44	-1,91	53	-1,58
12,90	17	-1,79	39	-1,71	46	-1,45
16,60	17	-1,79	39	-1,71	46	-1,45
20,30	17	-1,86	39	-1,78	46	-1,51
24,00	17	-1,98	39	-1,89	46	-1,61
27,70	17	-2,09	39	-2,00	46	-1,69
31,40	17	-2,19	39	-2,09	46	-1,77
35,10	17	-2,28	39	-2,17	46	-1,84
38,80	17	-2,36	39	-2,25	46	-1,91
42,50	17	-2,43	39	-2,32	46	-1,97
46,20	17	-2,50	39	-2,38	46	-2,02
49,90	17	-2,56	39	-2,44	46	-2,07
53,60	17	-2,62	39	-2,50	46	-2,12
57,30	17	-2,68	39	-2,55	46	-2,17
61,00	17	-2,73	39	-2,61	46	-2,21
64,70	17	-2,78	39	-2,65	46	-2,25
68,40	17	-2,83	39	-2,70	46	-2,29
72,10	17	-2,87	39	-2,74	46	-2,32
75,80	17	-2,91	39	-2,78	46	-2,36
79,50	17	-2,96	39	-2,82	46	-2,39
83,20	17	-3,00	39	-2,86	46	-2,43
86,90	17	-3,04	39	-2,90	46	-2,46
90,60	17	-3,07	39	-2,93	46	-2,49
94,30	17	-3,11	39	-2,97	46	-2,52
98,00	17	-3,14	39	-3,00	46	-2,54
101,70	17	-3,18	39	-3,03	46	-2,57
105,40	17	-3,21	39	-3,06	46	-2,60
109,10	17	-3,38	39	-3,23	46	-2,74
112,80	17	-3,38	39	-3,23	46	-2,74
116,50	17	-5,21	39	-4,97	46	-4,22
124,20	17	-3,52	39	-3,36	46	-2,85

In the end, the last load assignments were:

- Load pattern: Wind_X;
- Coordinate system: Global;
- Force global X: Depends on the storeys and location of the joints;
- Force global Y: Depends on the storeys and location of the joints.

And for direction -X:

- Load pattern: Wind_-X;
- Coordinate system: Global;
- Force global X: Depends on the storeys and location of the joints;
- Force global Y: Depends on the storeys and location of the joints.

6.6 Validation of the model

Once the model was completed with the load assignments, it was possible to control the accuracy of the same. In particular, to validate the model, three aspects were examined:

- The comparison between the results obtained from the load tests carried out in floor slabs at heights $Q = 16,60\,m$ and $Q = 90,60\,m$ and described in the testing report and the results of the analogue analyses carried out in the model;
- The behaviour of the structure with regards to a quasi-permanent combination;
- The behaviour of the structure against the wind action.

Therefore, several static simulations were run in the model, and the results have been summarized in the next sections.

6.6.1 Slab floors load tests

Before evaluating the response of the model and compare it with the testing report, some considerations need to be made:

- The testing report shows the deformation of the slab floors starting from zero. Thus, to compare the results accurately, it would be necessary to realize a *Staged Construction* analysis, but this is not the purpose of this Thesis;
- Since the position of the instruments is reported only with schematic draws, the experimental results will be compared with the displacements of the joints that seem to be more close to the instrument location.

6.6.1.1 Slab floor at Q=16,60 m

The comparison will be realized only considering the distributed load of 3,8 KN/m^2 assigned, as shown in Figure 6.14, which also indicates the position of the instrumentation:

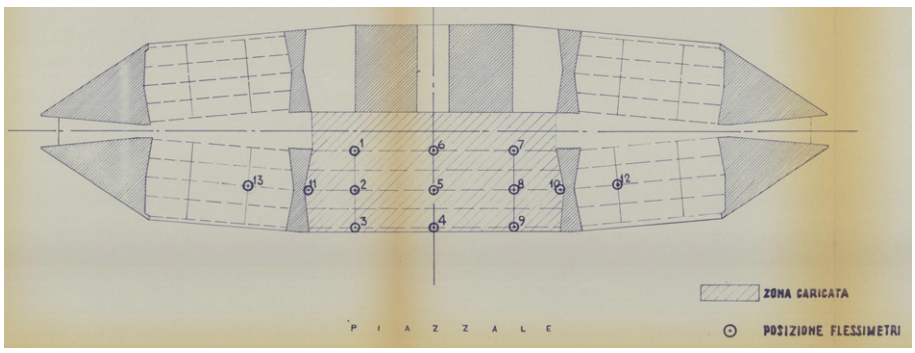

Figure 6.14: Location of the instrumentation and distyributed load. From Table 577 [44].

Table 6.10 summarized the displacements values obtained with the simulation in the model and the results of the testing report (resumed in Table Ia of the testing report [44]) for locations 1 to 9.

Table 6.10: Comparison between vertical displacement in the testing report and in the model with a distributed load of 3,8 KN/m^2. Slab floor at $= 16,60\,m$. Experimental measurements from Table Ia of the testing report [44].

Vertical displacement $[mm]$			
Instrument location	Testing report	Model	Difference $[mm]$
1	1,95	2,6	0,7
2	3,9	4,5	0,6
3	2,55	5,7	3,2
4	7,85	12	4,2
5	8,85	9,7	0,9
6	6,45	6,9	0,5
7	3,05	2,6	-0,5
8	4,15	4,5	0,4
9	2,85	5,7	2,9

As can be seen, the model provides the vertical displacement of the same order of magnitude as the testing report. The very modest differences are probably due to the fact that the joints are not in the same exact location as the instrumentation used. Thus, the model accuracy can be considered satisfactory.

6.6.1.2 Slab floor at Q=90,60 m

In this slab floor, the applied uniform load was 6 KN/m^2 and was distributed in a different way, respect what was described in the previous section. The locations of the uniform load and instrumentation are indicated in the next figure:

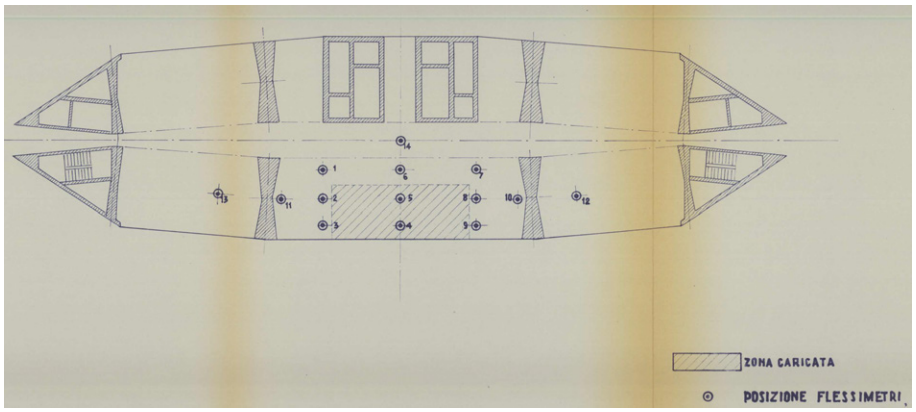

Figure 6.15: Location of the instrumentation and load. From Table 578 [44].

As done for the previous floor, the comparison between the model and the testing report is resumed in Table 6.11:

Table 6.11: Comparison between vertical displacements in the testing report and in the model with a distributed load of 6 KN/m^2. Slab floor at $= 90,60\,m$. Experimental measurements from Table 4 of the testing report [44].

Vertical displacement $[mm]$			
Instrument location	Testing report	Model	Difference $[mm]$
1	1,5	2,2	0,7
2	3,94	3,4	-0,5
3	5,21	4,7	-0,5
4	12,07	10,3	-1,8
5	8,59	7,5	-1,1
6	3,2	4,8	1,6
7	1,41	2,2	0,8
8	4,17	3,4	-0,8
9	5,26	4,7	-0,6

Like the previous comparison, the results have the same order of magnitude and differ at maximum 1,6 millimetres. Therefore, it can be concluded that the slab floors have been reproduced very accurately.

6.6.2 Quasi permanent combination

In addition to the previous check, to evaluate the accuracy of the model, and verify that no mistakes have been made during creation phases, the response of the exceptional 24 span meters slab floor has been examined. To this purpose, the following quasi-permanent combination, that maximize the vertical load, has been considered:

$$\sum_{j\geq 1} G_{1,j} + \sum_{j\geq 1} G_{2,j} + \sum_{i\geq 1} \Psi_{2,i} Q_{k,i} \tag{6.1}$$

Where the coefficients Ψ_2, for the various accidental loads, are:

- Category B overload: $\Psi_2 = 0,3$;
- Category H overload: $\Psi_2 = 0$;
- Snow: $\Psi_2 = 0$;
- Wind: $\Psi_2 = 0$.

In Figure 6.16, the deformed shape of the structure with the previous load combination is represented. Moreover, Table 6.12, summarize the vertical displacement of the central joints of each 24 meters slab floors, comparing it with the actual limitation of the Italian standards [49] for a quasi-permanent combination, that is:

$$U_{3max} = L/250 = \frac{24}{250} = 0,096\,m = 9,6\,cm \tag{6.2}$$

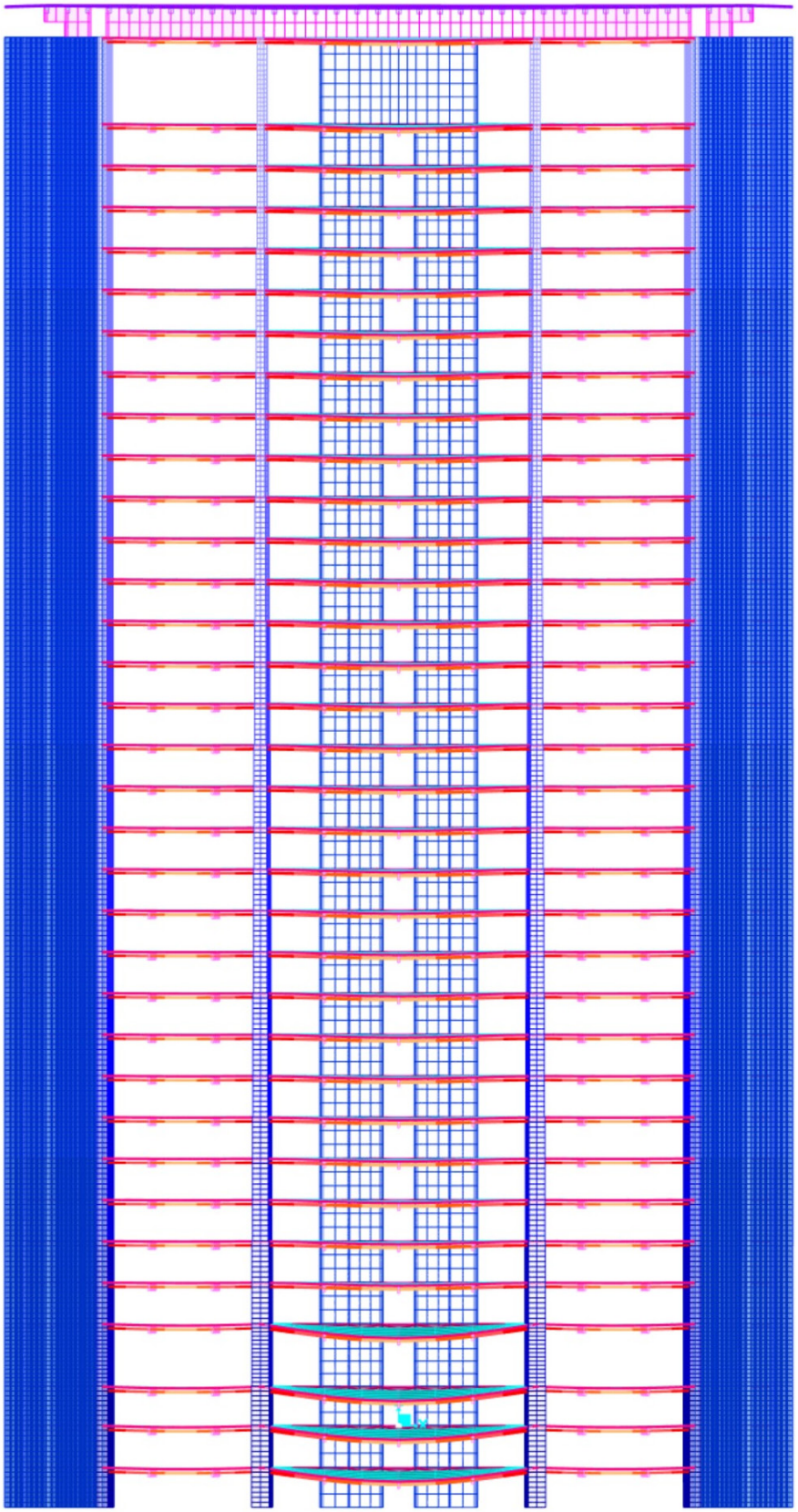

Figure 6.16: Deformed shape of the structure with a quasi-permanent combination. Scaling=20.

Table 6.12: U_3 displacement of the central and most external joint of each 24 meters slab floor.

Floor	Height $[m]$	Joint	$U_{3\,lim}$ $[cm]$	U_3 $[cm]$
1	-3,65	97507	9,60	12,55
2	0,10	97491	9,60	12,59
3	3,60	97798	9,60	12,97
4	9,20	98068	9,60	12,77
5	12,90	98338	9,60	2,88
6	16,60	98608	9,60	2,91
7	20,30	98878	9,60	2,98
8	24,00	99148	9,60	3,05
9	27,70	99418	9,60	3,11
10	31,40	99688	9,60	3,18
11	35,10	99958	9,60	3,24
12	38,80	100228	9,60	3,30
13	42,50	100498	9,60	3,38
14	46,20	100768	9,60	3,45
15	49,90	101038	9,60	3,52
16	53,60	101308	9,60	3,59
17	57,30	101578	9,60	3,65
18	61,00	101848	9,60	3,71
19	64,70	102118	9,60	3,78
20	68,40	102338	9,60	3,84
21	72,10	102658	9,60	3,90
22	75,80	102928	9,60	3,99
23	79,50	103198	9,60	4,05
24	83,20	103468	9,60	4,12
25	86,90	103738	9,60	4,20
26	90,60	104008	9,60	4,25
27	94,30	104278	9,60	4,32
28	98,00	104548	9,60	4,40
29	101,70	104818	9,60	4,42
30	105,40	105088	9,60	4,52
31	109,10	105358	9,60	4,67
32	112,80	105628	9,60	4,65
33	116,50	105898	9,60	5,04
34	124,20	106168	9,60	3,78

Looking at Table 6.12 and Figure 6.16 some consideration can be done:

- **Embedded floors: from Q=12,90 m to 124,20 m:**

  For these slab floors, the maximum vertical displacement is always far inferior that the actual limits. Moreover, it should be noticed that the displacement increase in value with height as the constraint become less effective due to the narrowing of the vertical elements. These fantastic results, underline the incredible design work that Nervi and his crew have done to avoid the use of the prestressing.

- **Simply supported floors: from Q=-3,65 m to 9,20 m**

  Differently to the previous slab floors, these four have a slightly more significant vertical displacement than the actual limits. Considering that the loss of rigidity in these four storeys was an intentional objective sought by the designers to prevent the thermal issues during the construction phases, the fact that the model is capable of representing this behaviour, emphasises the accuracy of the same.

Even in this simulation, the model has shown excellent reliability, giving the expected results.

6.6.3 Behavior of the structure against the wind action

The last check, to ensure that the model has been correctly realized, consist of verifying the lateral deformation respect to the wind force. Figure 6.17 shows the deformed shape of the building due to the envelope load combination that considers the different direction of the wind force.

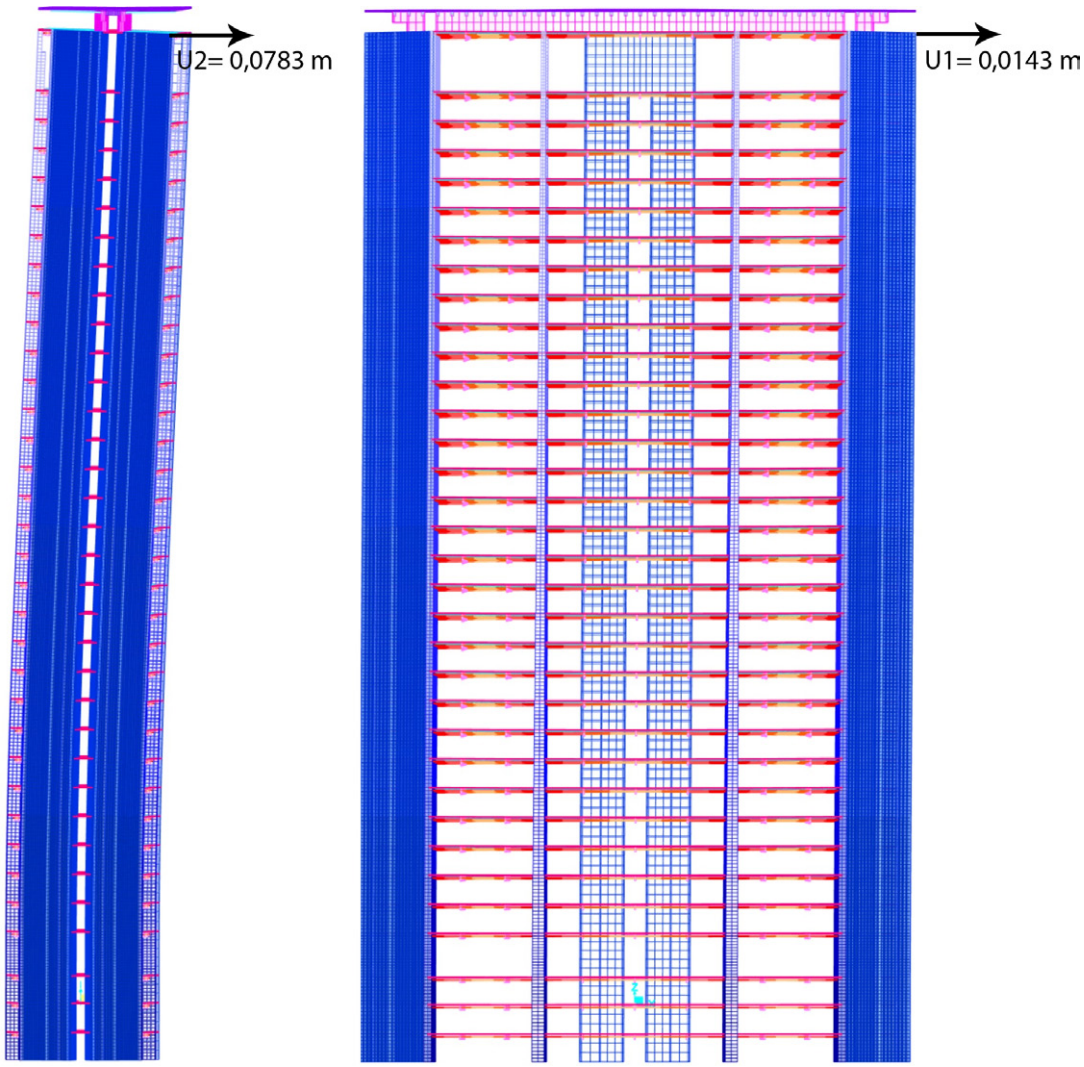

Figure 6.17: Deformed shape of the structure with the envelope wind action. Scaling=50.

Since the Pirelli Tower resistant mechanism is entirely made up of diaphragm walls, the expected deformed shape due to horizontal actions should be a cantilever type. As can be seen in the left image in Figure 6.17, the output of the program complies the expectation representing precisely this type of deformed shape. Moreover, it is possible to compare the maximum displacement on top of the building with the reference limit value of:

$$U_{limit} = H/1000 = 127/1000 = 0,127\,m \tag{6.3}$$

Considering the values of displacement on top, due to the wind in direction Y and X, reported in the previous figure, we have:

$$U2 = 0,0783\,m < 0,127\,m \qquad\qquad U1 = 0,0143\,m < 0,127\,m$$

Therefore, also the behaviour against horizontal load, reproduced by the model, seems to be absolutely reasonable.

6.6.4 Final consideration above the accuracy of the model

Considering what documented in the previous sections, it is possible to state that the model has excellent accuracy that allows reproducing with a high level of confidence the behaviour of the slab floors (comparing it with the experimental results of the original testing report the measures have only a few millimetres of difference). Moreover, since the performance of the structure against vertical and horizontal loads match precisely the expectations, we can exclude the presence of notable errors in the model.

6.7 S22 stress in the accidental combination

An important parameter that will be used to understand the behaviour of the structure during the dynamic analyses, that will be described in the next sections, is the distribution of compressive S22 stress. More in detail, to have a reference scenario useful to compare the results of the local failures scenarios, the accidental combination in the undamaged configuration has been considered. The expression of the accidental combination is the following:

$$\sum_{j\geq 1} G_{1,j} + \sum_{j\geq 1} G_{2,j} + A_d + \sum_{i\geq 1} \Psi_{2,i} Q_{k,i} \tag{6.4}$$

Where the coefficients Ψ_2, for the various loads, are:

- Category B overload: $\Psi_2 = 0,3$;
- Category H overload: $\Psi_2 = 0$;
- Snow: $\Psi_2 = 0$;
- Wind: $\Psi_2 = 0$.

While A_d has not been considered at this level. Therefore, the compression stresses in the central structural elements obtained running a static analysis, are represented in Figure 6.18. As can be seen, the design resistance of the concrete, that was determined in the previous chapter and is equal to 13,7 MPa, is far to be reached. More in detail, the maximum stresses are localized in some finite elements belonging to in the highest sections of the columns and are inferior to 8 MPa. In the rest of the structure, the compression stresses are lower than this value and uniformly distributed. Keeping in mind this distribution of stresses, in the next chapter, the variation of S22 stresses due to local failures will be described.

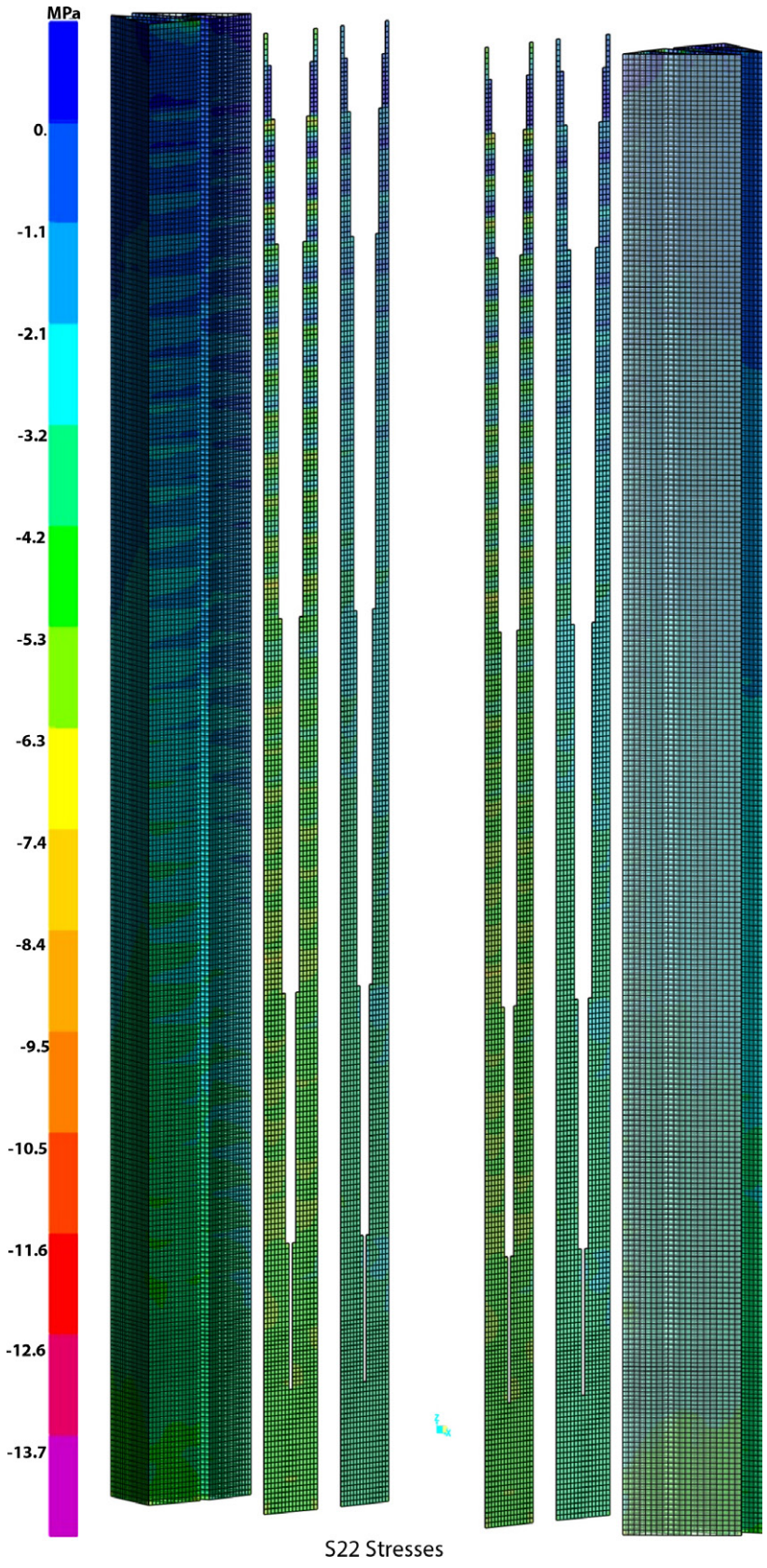

Figure 6.18: S22 stresses in the vertical load-bearing elements with the accidental combination.

Chapter 7

Analyses and conclusions

This chapter has the purpose of evaluating the structural robustness of the Pirelli Tower, following the indications of the Eurocode summarized in Chapter 4, and employing the "Thread Independent Approach". This method considers the elimination of a part of the vertical load bearings elements due to an unknown cause. However, since the Eurocode prescriptions are still lacking in some aspect, the American standard "General services administration - Alternate path analysis & design guidelines for progressive collapse resistance"[50], has been consulted. More further, the most interesting prescriptions of the GSA standard can be summarized as follow:

- The minimum extent of damage that should be applied to the vertical load-bearing elements is equal to the inter-storey height;
- The local damage should be applied to the elements located at the same level as the road, simulating the scenario created by the impact of a vehicle or a bomb explosion;
- The local damage should be applied in the most critical locations, such as external corners or where the structure has any vertical load discontinuity.

These prescriptions, together with the indications of the Eurocode, such as maximum notional section removal equal to 2,25 H (that has to be applied to one element at a time), have been used to determinate the local failure extent and location. In the next sections, the considered scenarios will be described in detail.

7.1 Relevant considerations

An important concept that should be kept in mind is that the analyses which will be presented have the purpose of evaluating the structural robustness of the tower. However, the investigations are not able to predict whether the tower would collapse as a result of an explosion or not. Though, since a building characterized by excellent structural robustness is capable of opposing to phenomena of progressive or disproportionate collapse, the results of the analyses can give an idea of the behaviour that the building would have. Moreover, the extent of the local failure that will be considered in the two scenarios would be caused by extraordinary events that clearly would produce damages all around the structure. Nevertheless, since the objective of this thesis is the assessment of the structural robustness in agreement with the standards, and as no other procedures have been defined until now, the damage will be represented exclusively by the partial removal of vertical load-bearing elements.

7.2 Description of the analyses type

The software SAP2000 offers various options: linear static, non-linear static, dynamic linear and non-linear dynamic analyses. Since the structural progressive collapse phenomenon involves significant dynamic inertial effects, an advanced dynamic analysis is strongly recommended. Furthermore, between a dynamic linear or non-linear analyses, other considerations should be done: a non-linear investigation could better represent local behaviour but, also being very sensitive to the modelling assumptions, it would take a quantity of time not manageable with standard computers (in the order of thousands of hours). Hence, the best option consists of dynamic linear analyses. In the next sections, the detailed procedure followed in carrying out these advanced simulations will be explained in detail.

7.2.1 Description of the procedure

The procedure which needs to be followed in these kinds of analyses in SAP2000 can be resumed in three steps:

1- Creating the model ("Model 1") which contains the entire structure, including the vertical load-bearing elements that will be removed and run a static analysis. These results are needed to obtain the internal forces of the structural parts which will be eliminated;

2- Creating a second model ("Model 2") in which the selected portions of the load-bearing element are removed. The presence of the eliminated regions is simulated by applying the internal forces, obtained during the analysis of the "Model 1", transmitted by these sections;

3- Simulating the sudden removal of the vertical load-bearing element in "Model 2", by running a time-history analysis in which these equivalent element forces are reduced to zero over a short amount of time by applying opposite forces that appear instantaneously.

The procedure summarized above will be described in detail applied to the considered scenarios.

7.2.2 Solution type and damping

For this kind of linear dynamic time-history load case, the most suitable solution's type that can be selected in SAP2000 are the following:

- **Modal superposition method:** this solution considers the structural displacement as a linear combination of orthogonal vibration modes. This method is very commonly used to calculate the dynamic response for linear dynamic analysis of large structures as it has a little computational cost. Nevertheless, the accuracy of the total response strongly depends on the number of modes used in the calculation;
- **Direct integration method:** This solution type integrates the dynamic equilibrium equations of motion directly as the structure is subjected to dynamic loading. This method is susceptible to the time step used.

The main differences between these two solution types are summarized in Table 7.1.

Table 7.1: Different characteristics between Modal superposition and Direct integration methods.

Aspects	Direct Integration	Modal Superposition
Analysis time	Long analysis time	Short analysis time
Details	Time step dependant	Number of considered modes dependant
Model size	Adequate for small models	Adequate for large models
Analysis accuracy	Long analysis time but highly accurate	Accuracy errors if the considered modes are not sufficient

Examining the characteristics resumed in Table 7.1 and considering the massive dimension of the model, the modal superposition method has been selected. The number of modes necessary to an accurate analysis was determined running various simulations considering an increasing number of modes: 20, 50, 100, 150, 200 and 400. The results demonstrated that the solutions became more precise until the 200 modes and did not change increasing this quantity. Therefore, the modal analyses have been run considering 200 vibration modes.

Another relevant aspect concern the value of the modal damping that in a dynamic analysis assumes crucial importance. For a progressive collapse analysis, the *csiamerca* website [51] suggest a modal damping value inferior to one or even zero. Since the site has not proportioned any more information useful to the determination of the damping value, some test has been realized focused on understanding the effect of different values of this parameter. The results have shown that a dumping rate of one strongly reduces the dynamic effects. Therefore, since there were not more precise information, and to stay on the safe side, the damping coefficient has been defined as zero.

7.2.3 Accidental load combination

Since the "Threat independent approach"has been applied, the accidental load combination that should be considered is the following:

$$\sum_{j\geq 1} G_{1,j} + \sum_{j\geq 1} G_{2,j} + A_d + \sum_{i\geq 1} \Psi_{2,i} Q_{k,i} \tag{7.1}$$

Where the accidental action A_d is represented by the removal of the structural element and the coefficients Ψ_2, for the various loads, are:

- Category B overload: $\Psi_2 = 0,3$;
- Category H overload: $\Psi_2 = 0$;
- Snow: $\Psi_2 = 0$;
- Wind: $\Psi_2 = 0$.

7.3 Considered local damage scenarios

As said before, in this thesis work, the local failure scenarios are focused on lateral triangular walls. Obviously, the most interesting scenario to be investigated is the most unfavourable. Therefore,

observing the structure, it should be noticed how whatever local failure concerning the lateral walls in the main facade (Diaphragms D3 and D4 in Drawing 1) would represent a worse situation than a local failure affecting the structural elements in the rear part of the building. This difference in the behaviour of the structure is clearly due to the lack of rectangular cores in the main facade. Hence, the localized damage should be located regardless in Diaphragm D3 or D4 as the structure is symmetric respect to the axis X. Taking into account what said until now, two scenarios, called Scenario A and B, have been considered, both concerning the element D3 (see Fig. 7.1). In the next sections, a complete explanation of both scenarios will be exposed.

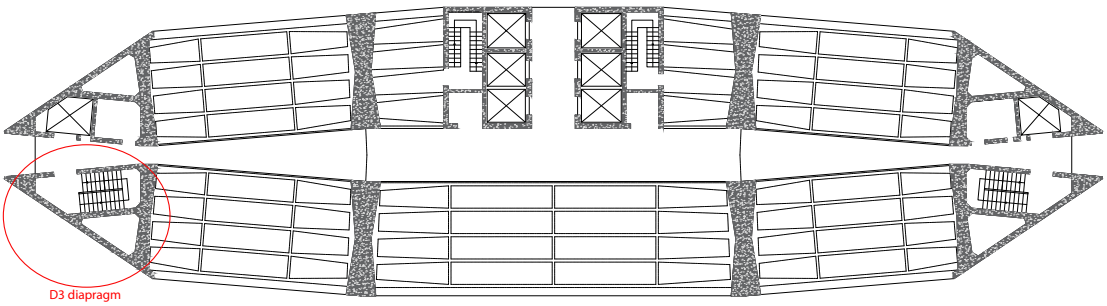

Figure 7.1: D3 element location in the plan view of the building.

7.3.1 Scenario A

Taking into account what prescribed by the American GSA standard [50], the damage will be included in the model at the ground level, in other words in correspondence of the entrance floor, where the inter-storey height is equal to 5,6 meters. Since the triangular elements are composed by massive walls which work together, to create a dangerous situation, the considered local failure should be, at least, very close to the maximum indicated by the Eurocode that, in this case, is equal to:

$$L_{max\,local\,failure} = 2,25 \cdot H = 1,25 \cdot 5,60\,m = 12,60\,m \tag{7.2}$$

Moreover, to consider the worst possible scenario, the failure should include the external corner and a large part of the D3-E2 element (see Fig. 6.2) that is the thickest wall of the Diaphragm D3.

Therefore, the total length of the removed wall, that has been determined considering all the aspect described above, and consisting in the removal of 24 finite elements, is equal to:

$$L_{local\,failure} = 11,96\,m < L_{max\,local\,failure} = 12,60\,m \tag{7.3}$$

Eventually, the local damage has been extended along the entire height of the first floor as represented in Figure 7.2.

In the next section, the entire procedure necessary to carry out a dynamic modal analysis will be explained.

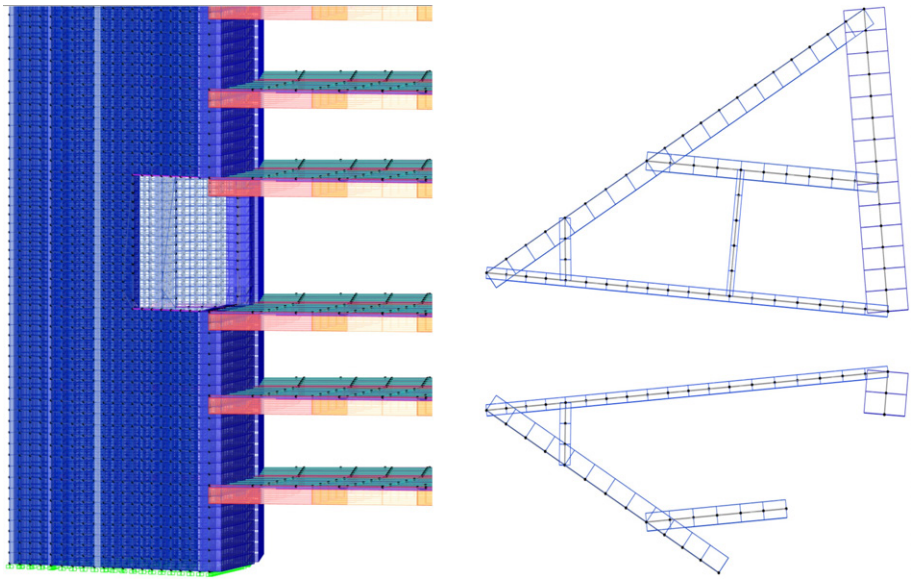

Figure 7.2: Considered local failure in the scenario A. Total length of removed wall=11,96 m.

7.3.1.1 Assessment of the internal forces concerning the removed finite elements

As said before, the first step to carry on a progressive collapse dynamic analysis is to assess the internal forces transmitted by the element that will be removed. Since the triangular walls have been modelled entirely with Shell-Thick finite elements, and to evaluate the internal forces with the maximum precision possible, a *Section cut* for each peripheral shell element of the removed section has been defined. Therefore, to correctly set up the *Section cuts*, 48 new groups were created in the model, 24 for the top finite element of the removed sector and 24 for the bottom, as shown in Figure 7.3. Subsequently, each group were assigned to the correspondent *Section cut* as can be seen in Figure 7.4.

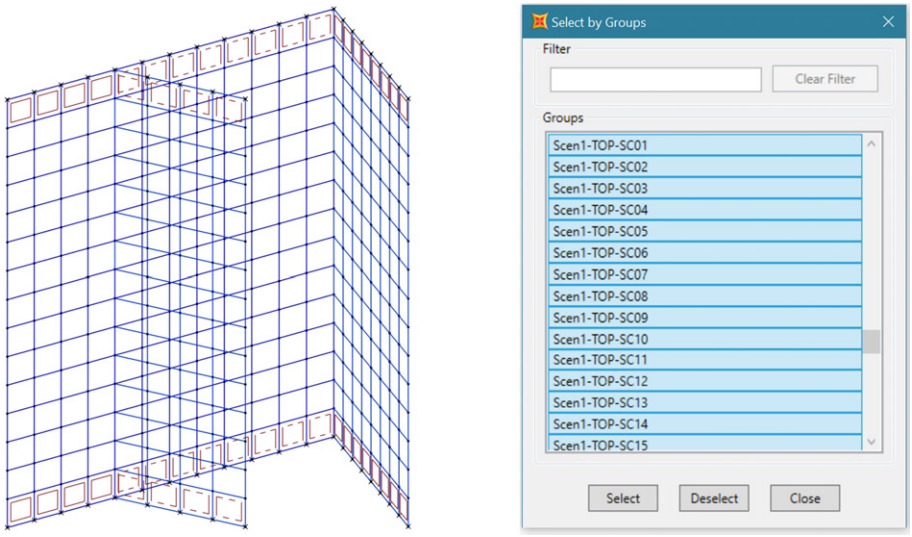

Figure 7.3: Assignment of finite elements to the new groups.

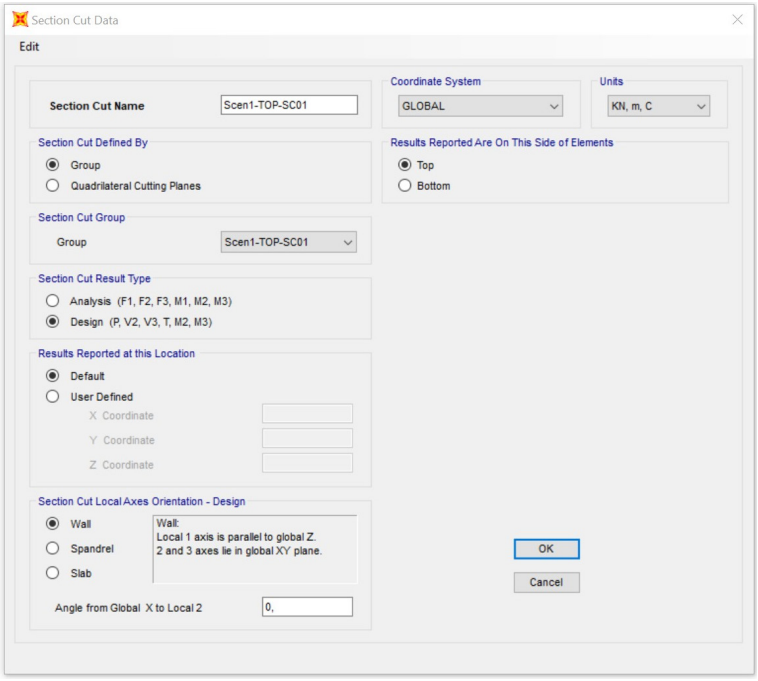

Figure 7.4: Definition of a *Section cut*.

Therefore, considering the accidental combination represented in Eq.7.1, and running a static analysis, it has been possible to obtain the internal forces on the top and bottom of the structural part that will be removed. In Table 7.2, the forces obtained through the *Section cut*, previously defined, are listed.

7.3.1.2 Set up of the dynamic modal analysis in the "Model 2"

Once the internal forces have been assessed, it is possible to work in the "Model 2". First of all, in this new copy of the model, the local damage represented in Fig 7.2 has been created eliminating the correspondent finite elements. Consequently, two new *Load Patterns* were created:

- **D3 equivalent:** Type: Other, Self weight multiplier: 0;
- **Sudden D3 loss:** Type: Other, Self weight multiplier: 0;

Where, the former will be used to apply the loads that simulate the presence of the removed wall sections and the latter to apply the instantaneous loads, opposite to the previous, that simulate the sudden removal of the walls. Since in SAP2000 it is not possible to apply these loads directly on the Shell-Thick elements and assign them on joints also would be very complicated (due to the tremendous number of joints in the model), a third option was considered. A new type of *frame section* was defined, characterized by the dimensions represented in Figure 7.5 and the *property modifiers* listed below:

- Cross-section Area: $1 \cdot 10^{-9}$;
- Shear Area in 2 direction: $1 \cdot 10^{-9}$;

- Shear Area in 3 direction: $1 \cdot 10^{-9}$;
- Torsional Constant: $1 \cdot 10^{-9}$;
- Moment of inertia about 2 axis: $1 \cdot 10^{-9}$;
- Moment of inertia about 3 axis: $1 \cdot 10^{-9}$;
- Mass: 0;
- Weight: 0.

This *frame section* type were called “Fake beams”as it was used only like an expedient to apply in an easy way the loads and does not have any structural capacity. Therefore, 48 frames element were positioned precisely in the position where the equivalent forces will have applied, as represented in Figure 7.5. Thus, dividing the loads in Table 7.2 by the length of each frame element and assigning the load in KN/m importing an Excel file, properly compiled, the loads belonging to the “D3 equivalent”were correctly set. The same procedure was used for the loads belonging to the load pattern “D3 sudden loss”but changing the sign of the forces appropriately. Figure 7.6 shows the loads applied for the two load patterns, “D3 equivalent”and “D3 sudden loss”.

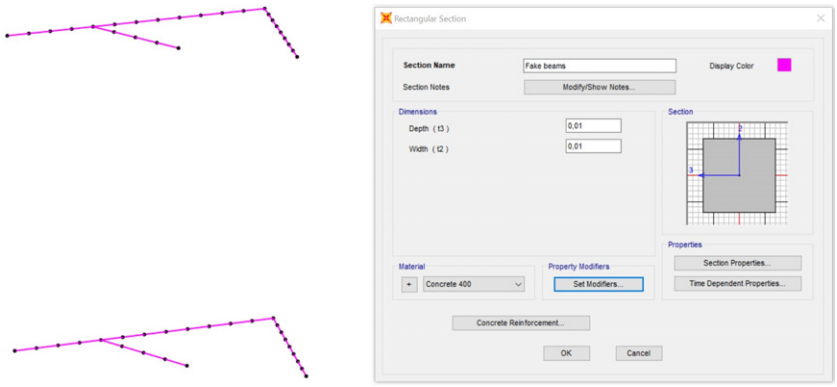

Figure 7.5: The “Fake beams”inserted in the model to allow an easy assignment of the equivalent forces.

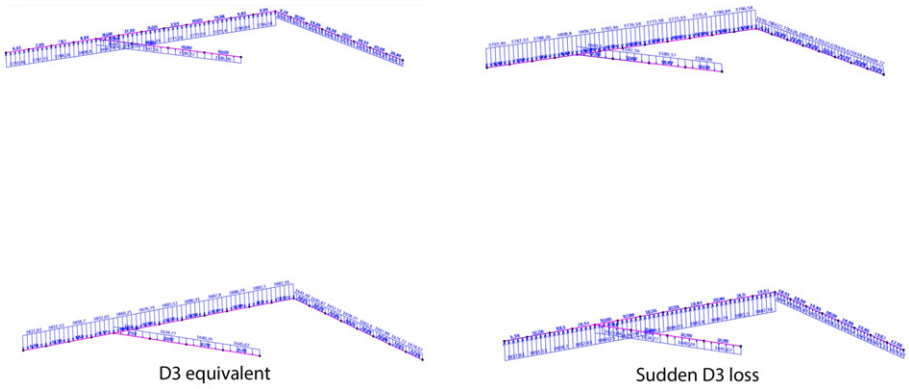

Figure 7.6: Forces and moments per unit length applied on the “Fake beams”frames.

Table 7.2: Internal forces determined through the defined *Section cuts* for the accidental combination in the "Model 1".

SectionCut	OutputCase	$P\ [KN]$	$V_2\ [KN]$	$V_3\ [KN]$	$T\ [KNm]$	$M_2\ [KNm]$	$M_3\ [KNm]$
Scen1-BOT-SC01	AC	-1832,564	-3,119	-2,761	5,2422	-0,3382	-5,8802
Scen1-BOT-SC02	AC	-1839,104	-1,775	-5,852	3,5344	-1,2559	-2,7173
Scen1-BOT-SC03	AC	-1842,531	-1,492	-8,834	3,248	-1,5976	-0,6641
Scen1-BOT-SC04	AC	-1839,64	-1,194	-9,711	2,2553	-1,7318	0,8694
Scen1-BOT-SC05	AC	-1878,011	-0,806	-6,787	2,6701	-1,8818	1,3076
Scen1-BOT-SC06	AC	-1886,059	-0,965	-8,337	1,9219	-1,852	1,115
Scen1-BOT-SC07	AC	-1889,334	-1,106	-9,126	1,5884	-1,8902	0,8212
Scen1-BOT-SC08	AC	-1890,984	-1,242	-9,737	1,0762	-1,9293	0,485
Scen1-BOT-SC09	AC	-1891,417	-1,364	-10,188	0,7304	-1,9336	0,1232
Scen1-BOT-SC10	AC	-1890,898	-1,477	-10,432	0,3807	-1,9217	-0,2477
Scen1-BOT-SC11	AC	-1889,322	-1,605	-10,654	-0,0135	-1,8732	-0,6206
Scen1-BOT-SC12	AC	-1888,67	-1,701	-9,551	-0,1829	-1,7684	-1,0257
Scen1-BOT-SC13	AC	-828,128	-7,523	5,303	2,942	138,393	91,1794
Scen1-BOT-SC14	AC	-830,343	-9,377	6,755	3,4748	139,1307	90,9976
Scen1-BOT-SC15	AC	-833,693	-9,812	7,044	3,2563	139,6958	91,2953
Scen1-BOT-SC16	AC	-836,589	-10,04	7,159	3,2592	140,1531	91,5616
Scen1-BOT-SC17	AC	-839,185	-10,071	7,135	2,9722	140,5358	91,8351
Scen1-BOT-SC18	AC	-841,445	-9,92	6,991	2,916	140,8386	92,1043
Scen1-BOT-SC19	AC	-843,384	-9,585	6,725	2,5667	141,0676	92,3712
Scen1-BOT-SC20	AC	-845,024	-9,061	6,34	2,4585	141,2256	92,6401
Scen1-BOT-SC21	AC	-860,463	-13,285	-1,154	-0,7886	-0,3265	-2,7702
Scen1-BOT-SC22	AC	-865,286	-15,438	-1,396	-0,8334	-0,4254	-2,9901
Scen1-BOT-SC23	AC	-868,192	-16,087	-1,445	-0,902	-0,4293	-3,1152
Scen1-BOT-SC24	AC	-871,025	-16,308	-1,435	-0,9378	-0,4262	-3,1457
Scen1-TOP-SC01	AC	-1811,376	3,064	1,101	7,5052	0,3706	-9,0222
Scen1-TOP-SC02	AC	-1808,451	0,992	3,785	9,5006	-0,1528	-4,8959
Scen1-TOP-SC03	AC	-1808,893	0,478	3,653	9,309	-0,8259	-2,0824
Scen1-TOP-SC04	AC	-1818,7	0,592	4,217	9,452	-1,3423	-0,0566
Scen1-TOP-SC05	AC	-1851,907	0,799	12,766	8,8836	-1,8125	1,0146
Scen1-TOP-SC06	AC	-1840,653	-0,345	13,23	8,1806	-2,4201	1,5197
Scen1-TOP-SC07	AC	-1837,11	-1,279	12,771	6,2319	-2,4673	1,7141
Scen1-TOP-SC08	AC	-1835,75	-1,94	11,627	5,62	-2,2779	1,6863
Scen1-TOP-SC09	AC	-1835,658	-2,352	9,595	3,9907	-1,9247	1,492
Scen1-TOP-SC10	AC	-1836,73	-2,512	6,976	3,3249	-1,4284	1,1706
Scen1-TOP-SC11	AC	-1839,38	-2,468	4,111	1,9152	-0,9371	0,7237
Scen1-TOP-SC12	AC	-1847,037	-2,395	1,504	0,9784	-0,7099	0,1645
Scen1-TOP-SC13	AC	-815,665	-3,701	2,126	1,2781	135,1105	91,867
Scen1-TOP-SC14	AC	-818,664	-6,779	4,524	1,9244	135,2066	92,8352
Scen1-TOP-SC15	AC	-820,41	-9,816	6,684	2,463	135,0422	93,6772
Scen1-TOP-SC16	AC	-820,378	-12,269	8,406	3,1003	134,6554	94,1688
Scen1-TOP-SC17	AC	-819,122	-13,977	9,594	3,3536	134,1624	94,3575
Scen1-TOP-SC18	AC	-817,1	-14,92	10,247	3,6549	133,6436	94,2928
Scen1-TOP-SC19	AC	-814,682	-15,18	10,431	3,5592	133,1503	94,0443
Scen1-TOP-SC20	AC	-812,105	-14,879	10,235	3,5392	132,7068	93,6655
Scen1-TOP-SC21	AC	-847,676	-25,053	-1,503	0,4456	0,0016	5,0802
Scen1-TOP-SC22	AC	-842,94	-26,828	-2,056	0,0935	0,1429	5,1033
Scen1-TOP-SC23	AC	-841,255	-26,027	-2,061	0,0949	0,1155	4,9862
Scen1-TOP-SC24	AC	-839,502	-24,76	-1,952	-0,3037	0,0983	4,7151

Once assigned the loads in the "Model 2"it has been necessary to define the Time History Functions which will govern the behaviour of the loads. Therefore, two different functions were defined, both represented in Figure 7.7. The first, called "Constant loads"will be assigned to each load that

would be present in normal conditions while the second, named “Sudden D3 loss”will influence only the loads that represent the abrupt local failure. As can be seen, the sudden loss will appear in 0,001 seconds.

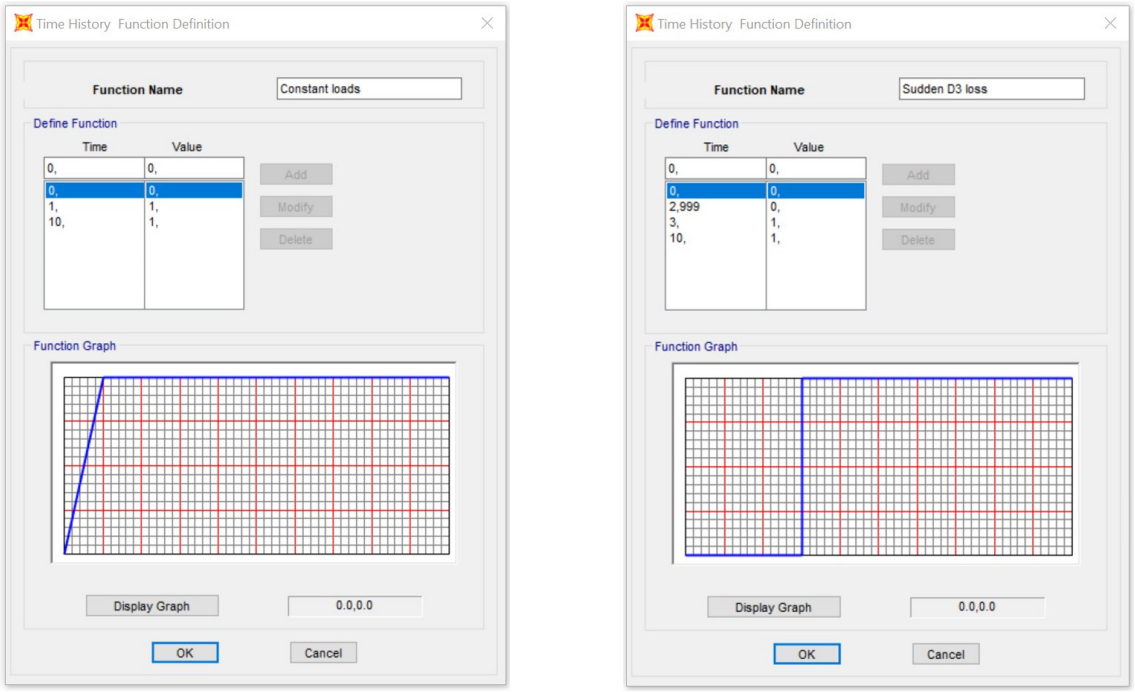

Figure 7.7: Time history functions defined.

The last step that needs to be set before running the dynamic analysis consists of defining the *load cases* for each *load pattern* that appears in the accidental combination (with a coefficient $\Psi_2 \neq 0$)specified in Eq. 7.1. More in detail, the loads can be divided into three groups depending on the settings of the individual load cases. The three groups are the following:

- **Group 1:**

  Dead, G1, G2, Overload_B and D3 equivalent.

- **Group 2:**

  Sudden D3 loss.

- **Group 3:**

  Modal.

In Figures 7.8, 7.9 and 7.10 an example of the setting for each group is presented. As should be noticed, the only difference between Group 1 and 2, lies in the function that governs the behaviour of the loads while Group 3 is formed only by the “MODAL”*load case*. Since the total duration of the simulation was set to 10 seconds, and the time step to 0,01, the analysis will includes1000 steps.

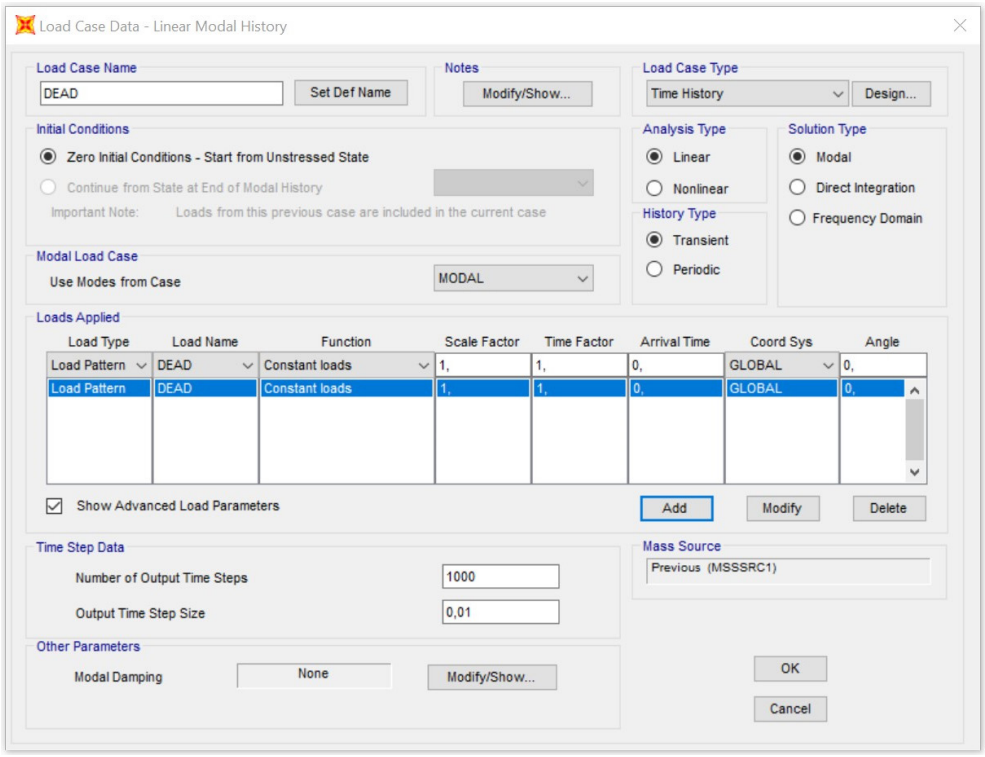

Figure 7.8: Load case setting for Group 1 loads.

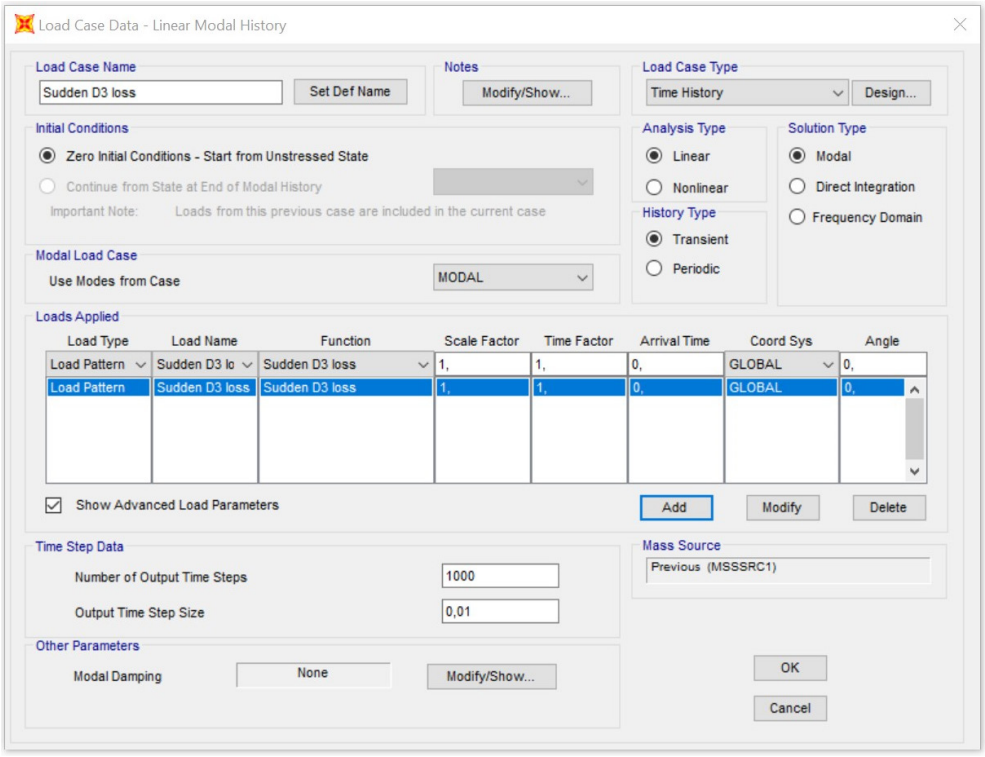

Figure 7.9: Load case setting for Group 2 loads.

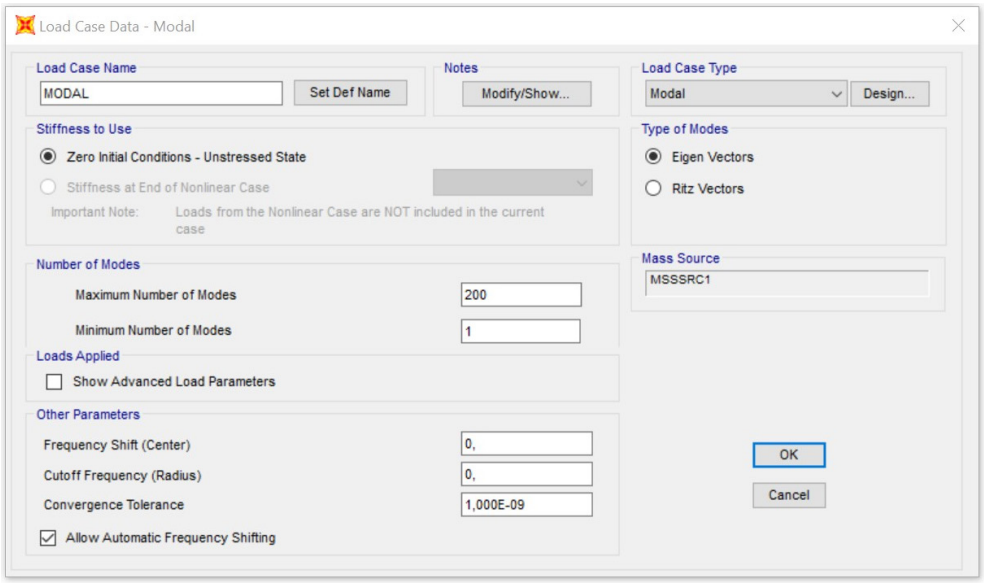

Figure 7.10: Load case setting for Group 3 loads.

Eventually, after all these steps were possible to run the dynamic analysis. The entire calculation took almost one hour, as shown in the analysis report shown in Fig. 7.11.

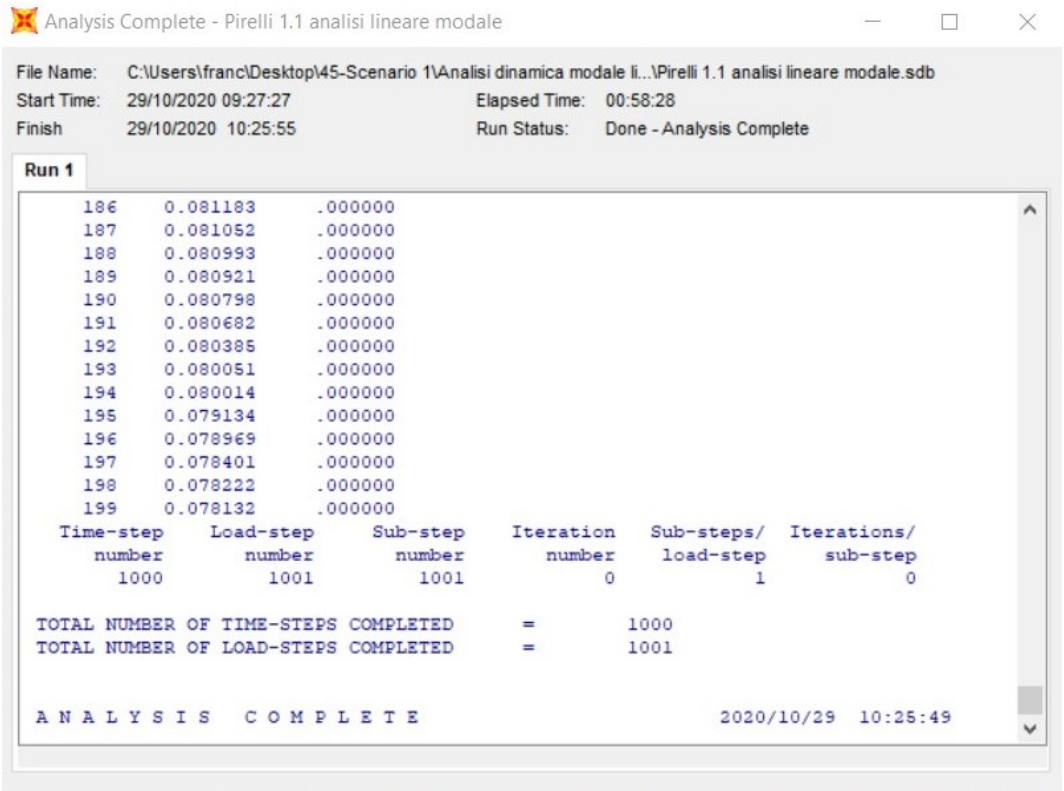

Figure 7.11: Analysis report of the modal linear analysis.

7.3.1.3 Analysis and results of Scenario A

As said before, the damage imposed at the structure reached 11,96 meters, and it is very close to the maximum indicated by the Eurocode, 12,60 meters. Moreover, although the location of the damage tries to create the worst possible situations, including the external corner and the major part of the massive wall D3-E2, the set of walls makes the triangular diaphragm so massive and rigid, that also such a considerable loss of do not cause large deformations and significant dynamic effects in the building. Indeed, Figure 7.12 shows the comparison between the structural deformation of the dynamic analysis with the one resulting from the static calculation of the undamaged structure. As can be seen, the increment in the displacement of the top joint of the Diaphragm D3 is very modest:

$$\Delta_{U1}^{joint\,12379} = 0,0049\,m \qquad \Delta_{U2}^{joint\,12379} = 0,0233\,m \qquad \Delta_{U3}^{joint\,12379} = 0,0016\,m$$

The same considerations can be done comparing the structural deformation in the area surrounding the local damage in between the damaged and undamaged situations. Figure 7.13, shows the small differences between the two cases.

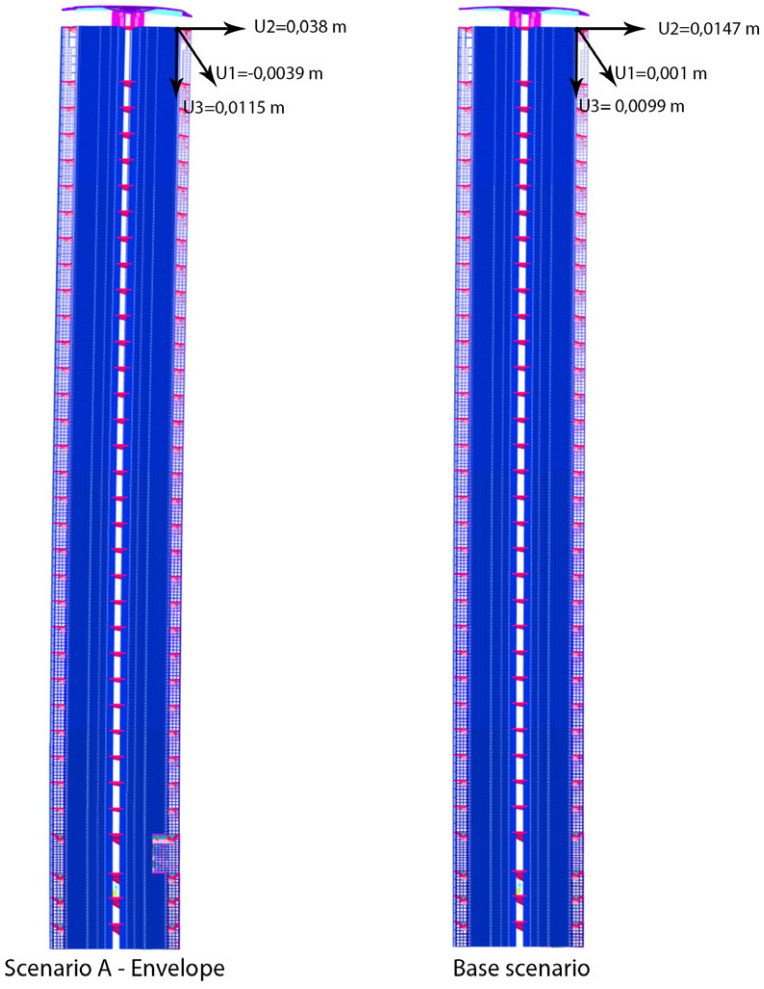

Figure 7.12: Structural deformation from side. Displacements for joint 12379. Scaling value=50.

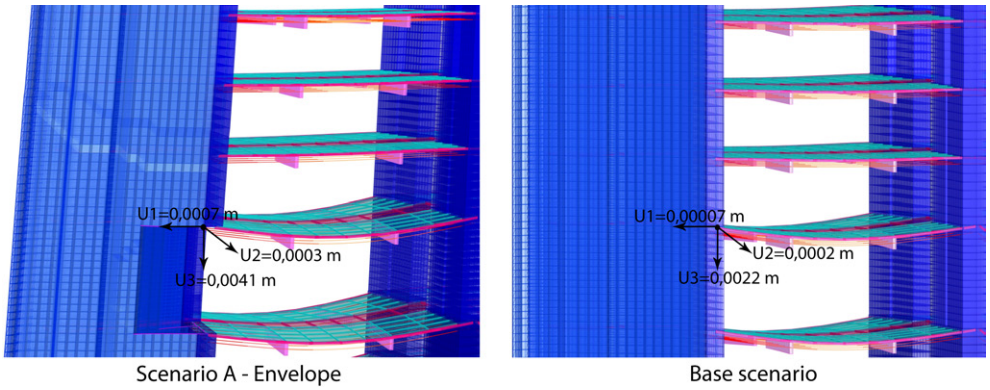

Figure 7.13: Displacements values of joint 393. Scaling value=50.

The variations in the displacements of the joint 393, above the local damage, are:

$$\Delta_{U1}^{joint\,393} = 0,00063\,m \qquad \Delta_{U2}^{joint\,393} = 0,0001\,m \qquad \Delta_{U3}^{joint\,393} = 0,0019\,m$$

Moreover, the vertical deformation of the structure is not sufficient to appreciate the Viereendel alternative load path created by the slab floors. Indeed, as can be seen in Figure 7.14, the slabs floor do not present the typical double curvature, and the deformed shape of the slabs is the same in both cases.

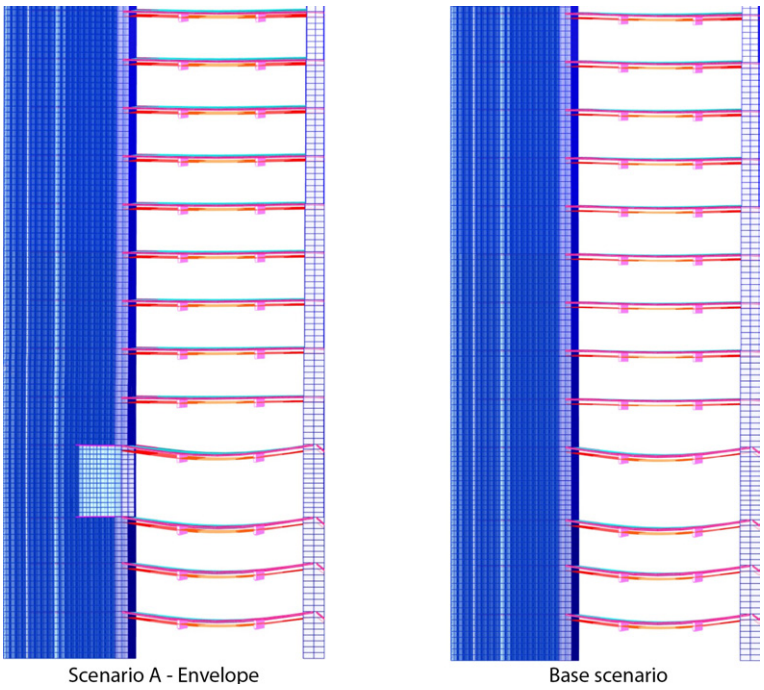

Figure 7.14: Slab floors deformations in the two cases. Scaling value=50.

Considering the redistribution of stresses after the local damage, Figure 7.15 shows how there is a dramatic but localized increasing in compression in the remaining section of the wall D3-E2, very close to the local damage. Moreover, Figure 7.16 shows in detail the damaged area comparing it with the base scenario.

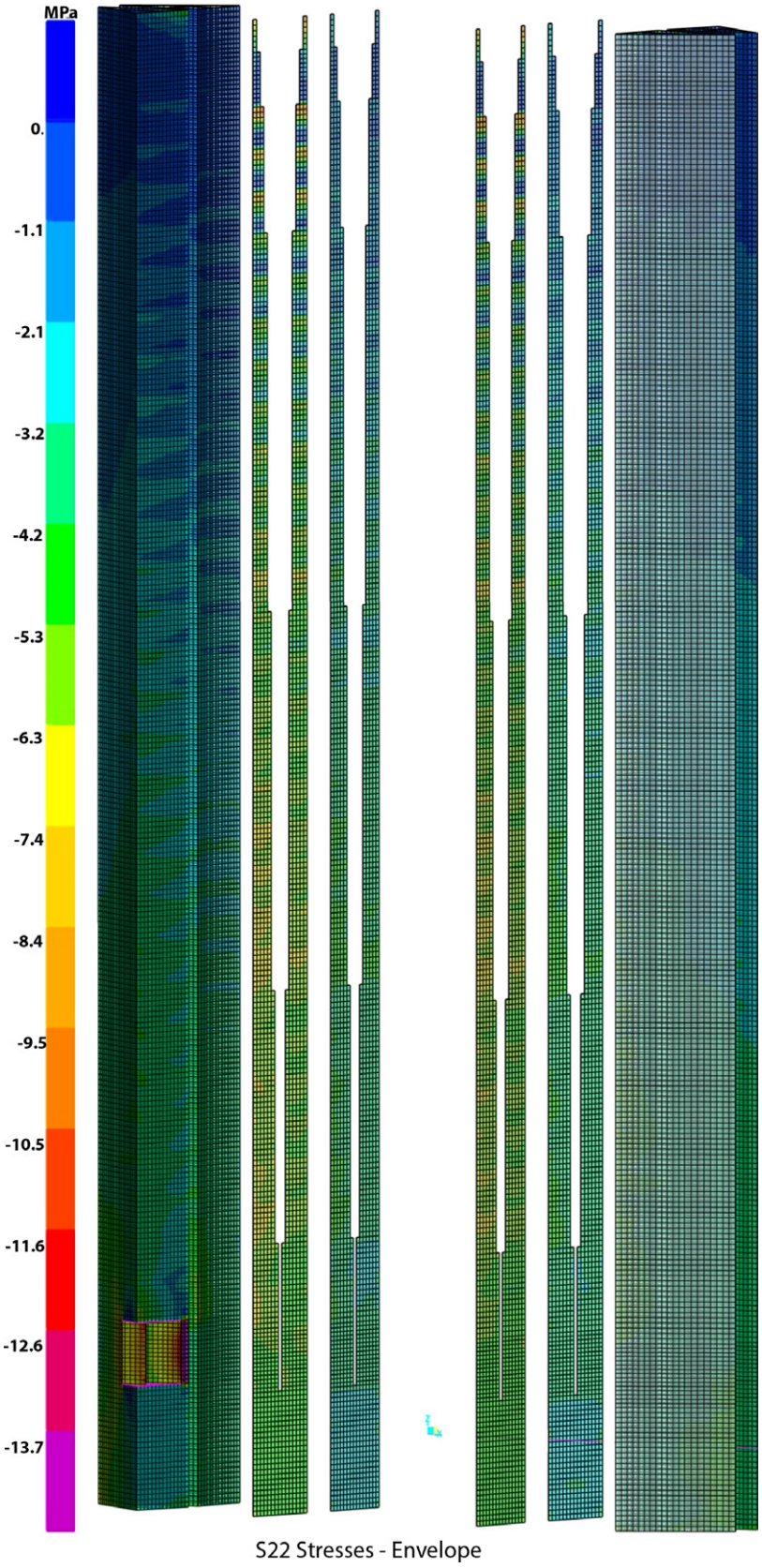

Figure 7.15: S22 envelope compression stresses in Scenario A.

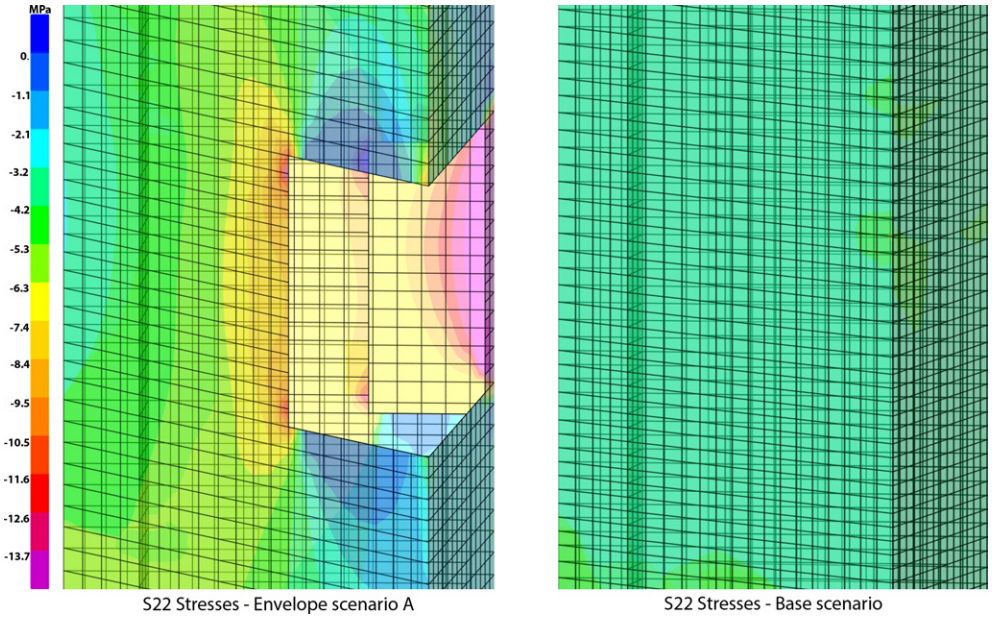

Figure 7.16: Comparison between the S22 stresses in the two cases.

As can be seen, in the areas coloured in violet, the compressive stress is higher than the design resistance of the concrete, that is 13,7 MPa. This means that if the prescriptions of the Eurocode are strictly followed, those parts break. However, since we are considering an exceptional event, we can refer to the characteristic resistance of the concrete, that, as calculated in Chapter 5, is equal to 24,2 MPa. Thus, rearranging the previous stress map with a different contour range, that reaches the value of 24,2 MPa, we obtain what represented in the next figure:

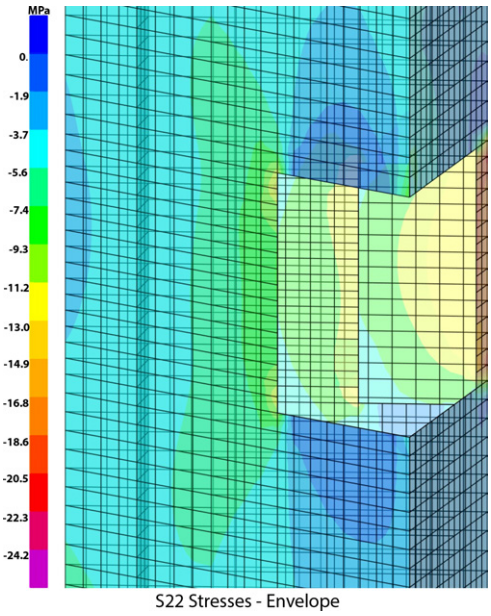

Figure 7.17: S22 stresses with a color contour range that reach 24,2 MPa.

As can be seen, there are not regions where the characteristic resistance of the concrete is exceeded. Moreover, it would be important carrying out a nonlinear analysis, also taking into ac-

count the action of the reinforcing bars. However, since the location of the bars is not known and considering the enormous computational costs of this analysis type, this check could not be realized.

7.3.2 Scenario B

Since with the scenario A the prescriptions of the Eurocode have been applied, with this new Scenario B a considerable more severe loss has been considered: the complete removal of the walls in the first floor of the diaphragm D3. In this way, it will be possible to see the response of the building against a local failure way more prominent than every standard requirement. However, it should be kept in mind that such a loss, in a real situation, would damage the entire structure and not only a portion of it, but, as said before, no other procedures have been developed until now to evaluate the structural robustness. Figure 7.18 represents the local failure considered in this new scenario:

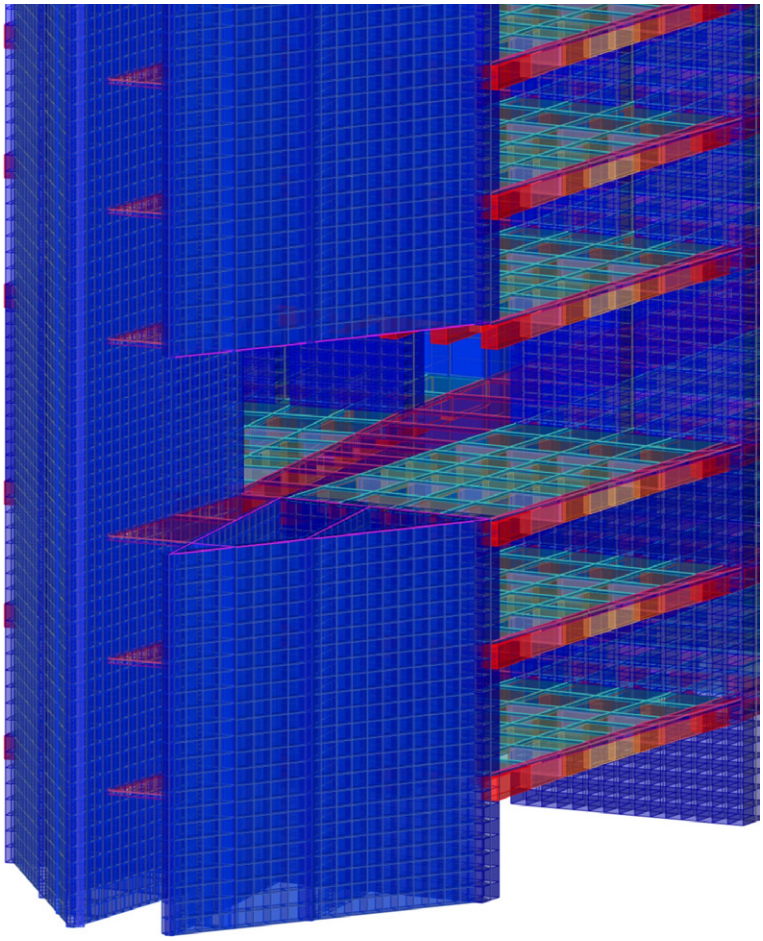

Figure 7.18: Considered local failure in the scenario B. Total length of removed walls = 33,33 m.

The adopted procedure was the same as the one followed in the previous scenario, with the only exception consisting in the amount of *section cut* defined that this time was 132. Therefore, the procedure will not be described in detail, focusing on the main results of this new case.

7.3.2.1 Analysis and results of Scenario B

In this scenario, that represents a dramatic local failure, much more severe than whatever standards requirements, it is possible to observe very well the behaviour of the structure and the different load paths activated by the local damage. First of all, Figure 7.19 shows the deflection of Tower, focusing in the displacements of joint 12379. In this circumstance, the increments in displacements, respect the undamaged case, are very substantial, along each direction:

$$\Delta_{U1}^{joint\,12379} = 0,004\,m \qquad \Delta_{U2}^{joint\,12379} = 0,1143\,m \qquad \Delta_{U3}^{joint\,12379} = 0,0264\,m$$

The same can be said with regards to the displacements of joint 393, shown in Figure 7.20, that is just above to the damaged area.

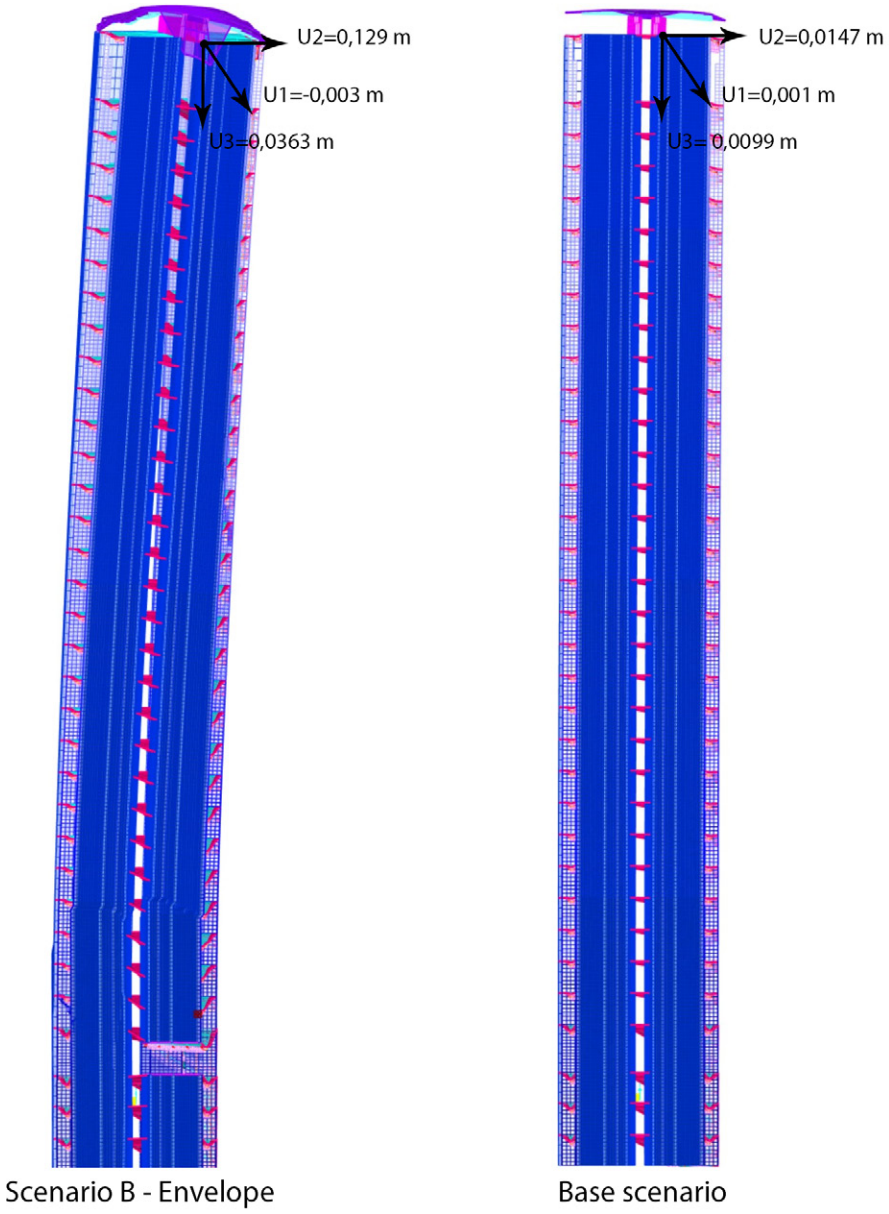

Figure 7.19: Displacements of joint 12379. Scaling value=50.

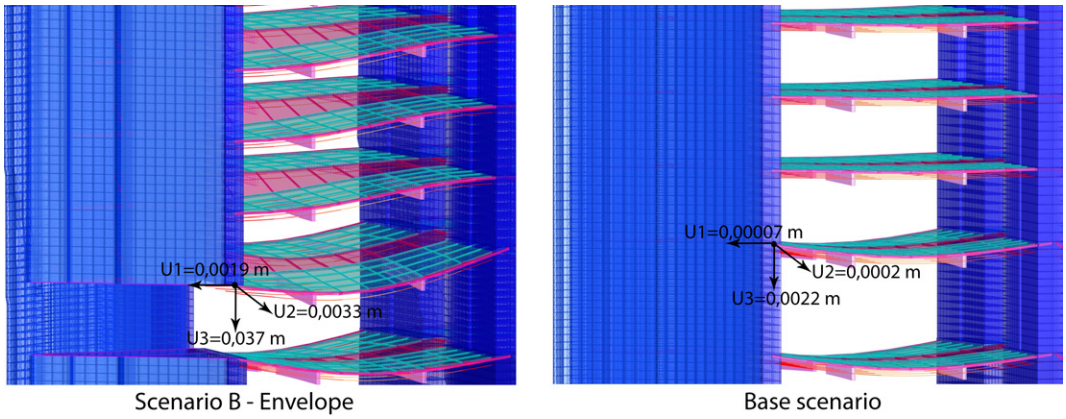

Figure 7.20: Displacements of joint 393. Scaling value=50.

The increments in displacements of joint 393 are:

$$\Delta_{U1}^{joint\,393} = 0,00183\,m \qquad \Delta_{U2}^{joint\,393} = 0,0031\,m \qquad \Delta_{U3}^{joint\,393} = 0,0348\,m$$

In this scenario, the displacements are sufficient to recognise the alternative load path consisting of the behaviour of the floors as Vierendeel beams. This mechanism is noticeable in the left image of Figure 7.21, where the slab floors have the typical double curvature of a Vierendeel beam. It is crucial to emphasise that this behaviour can appear only in high rise building, where the high number of floor permits to sustain the damaged vertical element, otherwise, in standard residential construction, the number of floors is not sufficient.

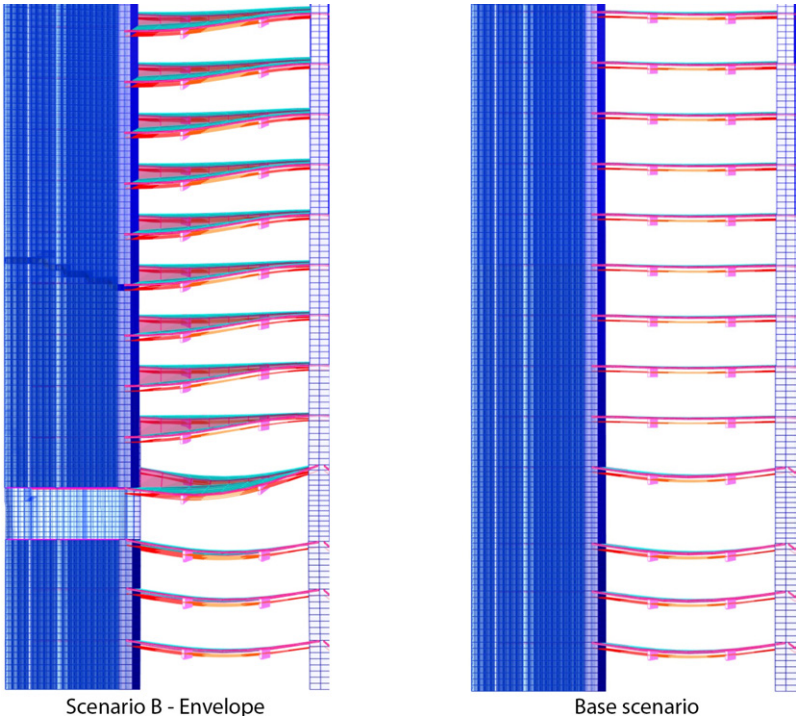

Figure 7.21: Slab floors deformations in the two cases. In the left image, the behaviour like Viereendel beam of the slab floors can be observed. Scaling value=50.

An additional resistant mechanism, that permits the building to oppose the progressive collapse, consists of the tridimensional effect that can see in Figure 7.22. Indeed, the slab floors, besides linking the triangular elements to the column acting like Vierendeel beams, bind the structural components in the front part of the structure to the ones in the rear, ensuring the sharing of loads in the entire building.

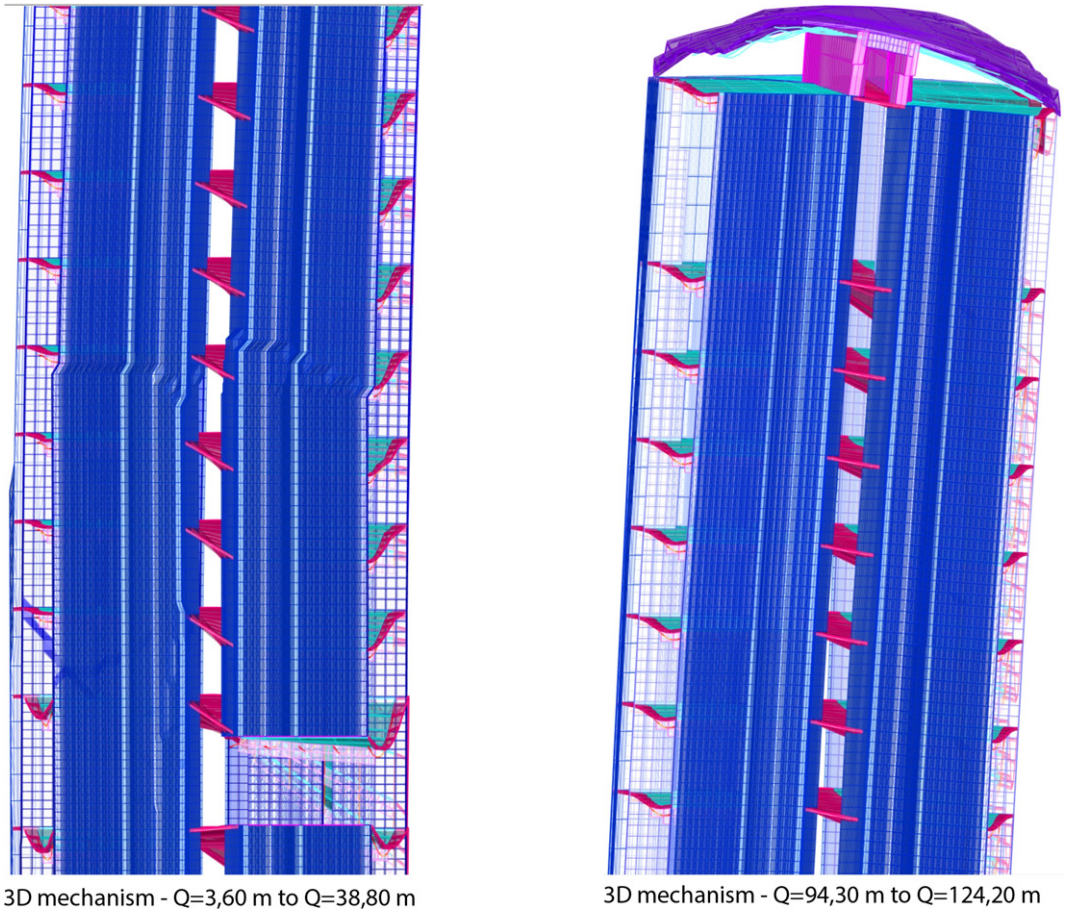

Figure 7.22: 3D resistant mechanism. Scaling value=50.

In analogy with what did for the previous scenario, the last aspect that has been evaluated is the distribution of compressive stress in the vertical structural elements, after the local failure. Figure 7.23 shows the envelope of the S22 stress in the structure. Differently to what has been observed in Scenario A, the increment in strains is much more diffused in the building. Moreover, this redistribution of tensions in the entire structure confirms the effectiveness of the functioning like Vierendeel beams of the slab floors. Looking at 7.24, that shows a magnification of the most solicited structural elements it should be noticed that some parts of the Diaphragm D1 and Columns C3 and C4 have compressive stress higher than the design resistance of the concrete (13,7 MPa). Eventually, as done for the previous case, Figure 7.25 shows the same three elements considering a different contour range, doing reference to the characteristic resistance of the concrete (24,2 MPa). Therefore, despite that this scenario assumes a massive local failure, only a few finite elements of the thin terminal sections of column C3 present stresses higher than 24,2 MPa.

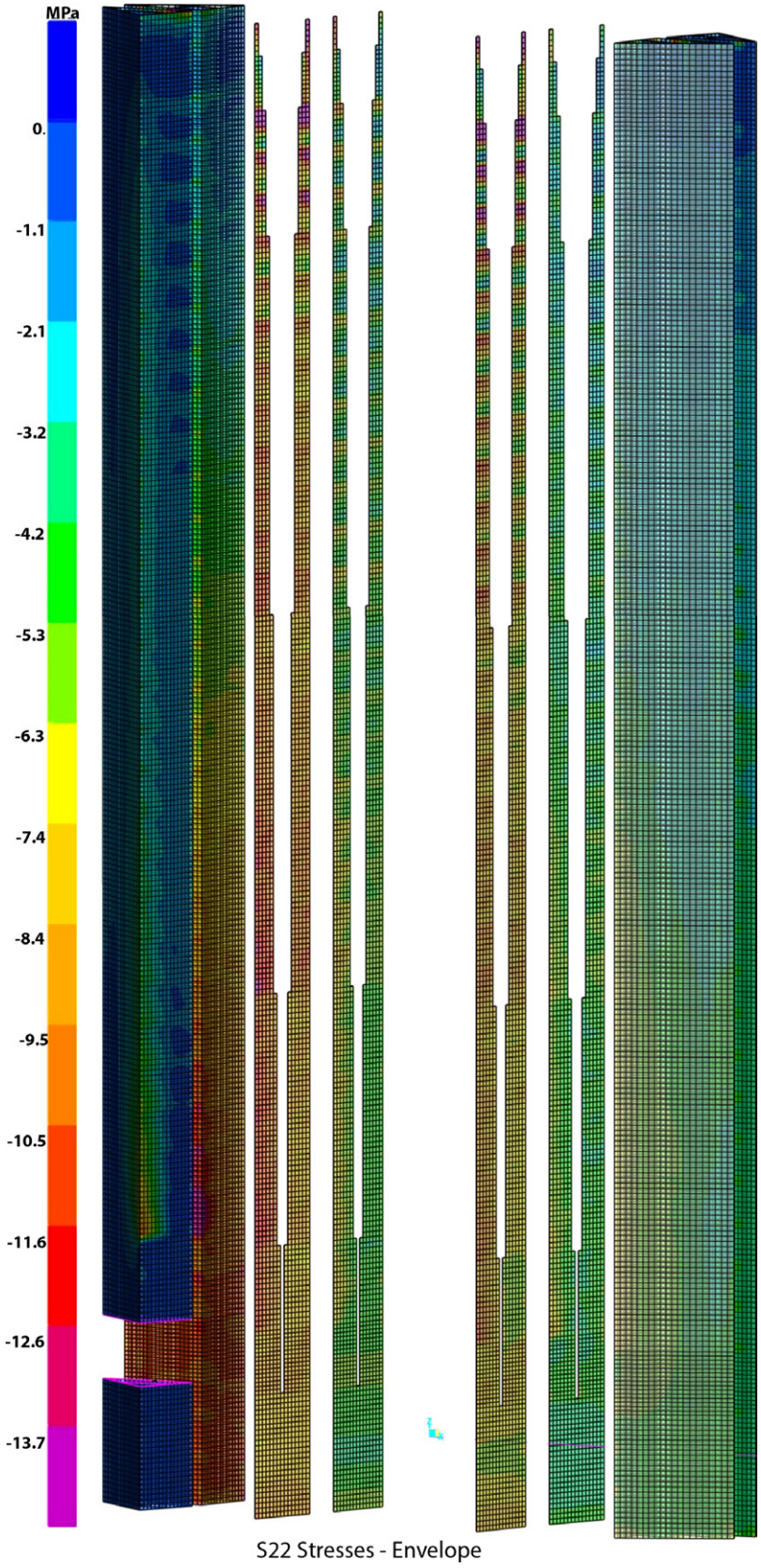

Figure 7.23: S22 envelope compression stresses in Scenario B.

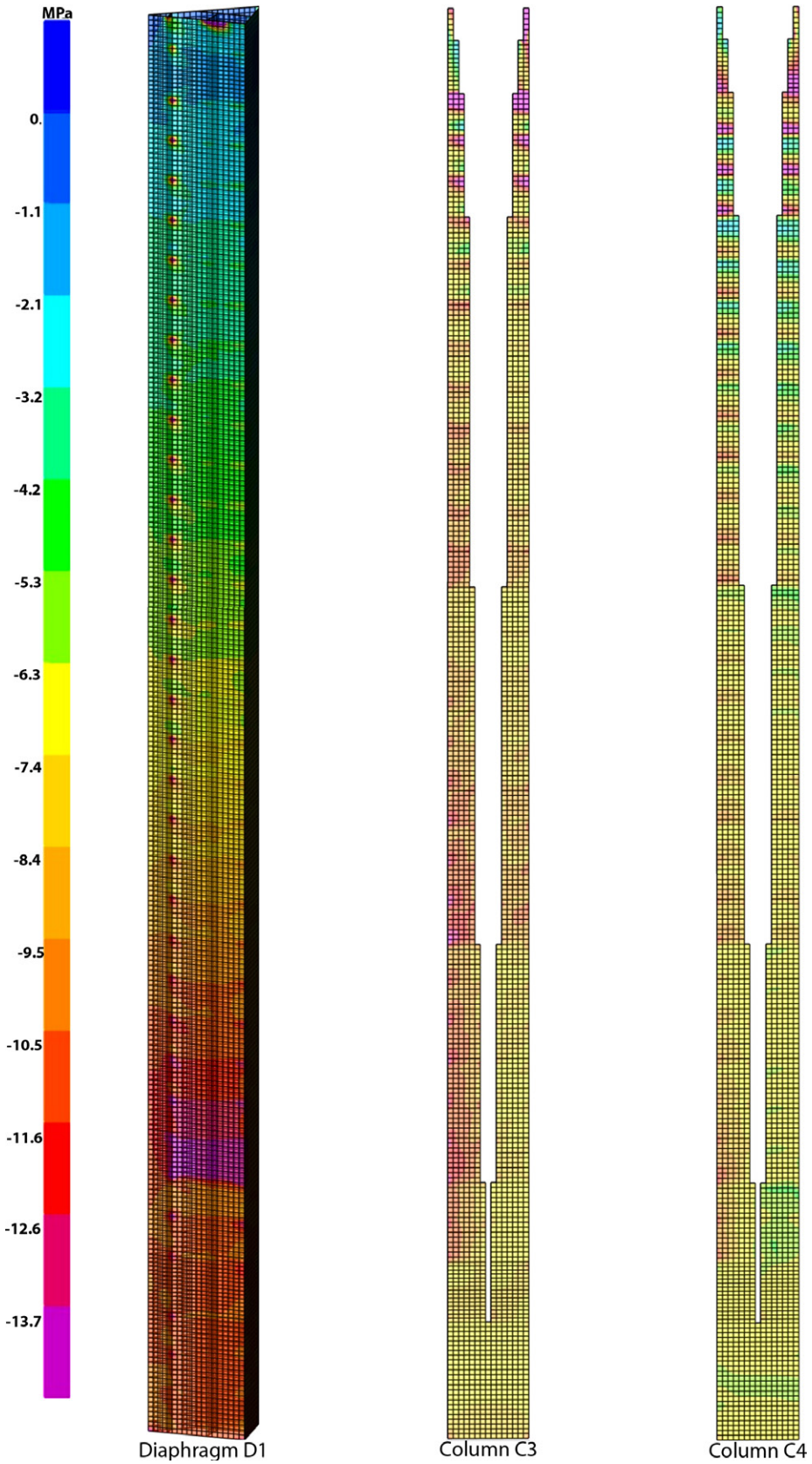

Figure 7.24: S22 envelope compression stresses in elements D1, C3 and C4.

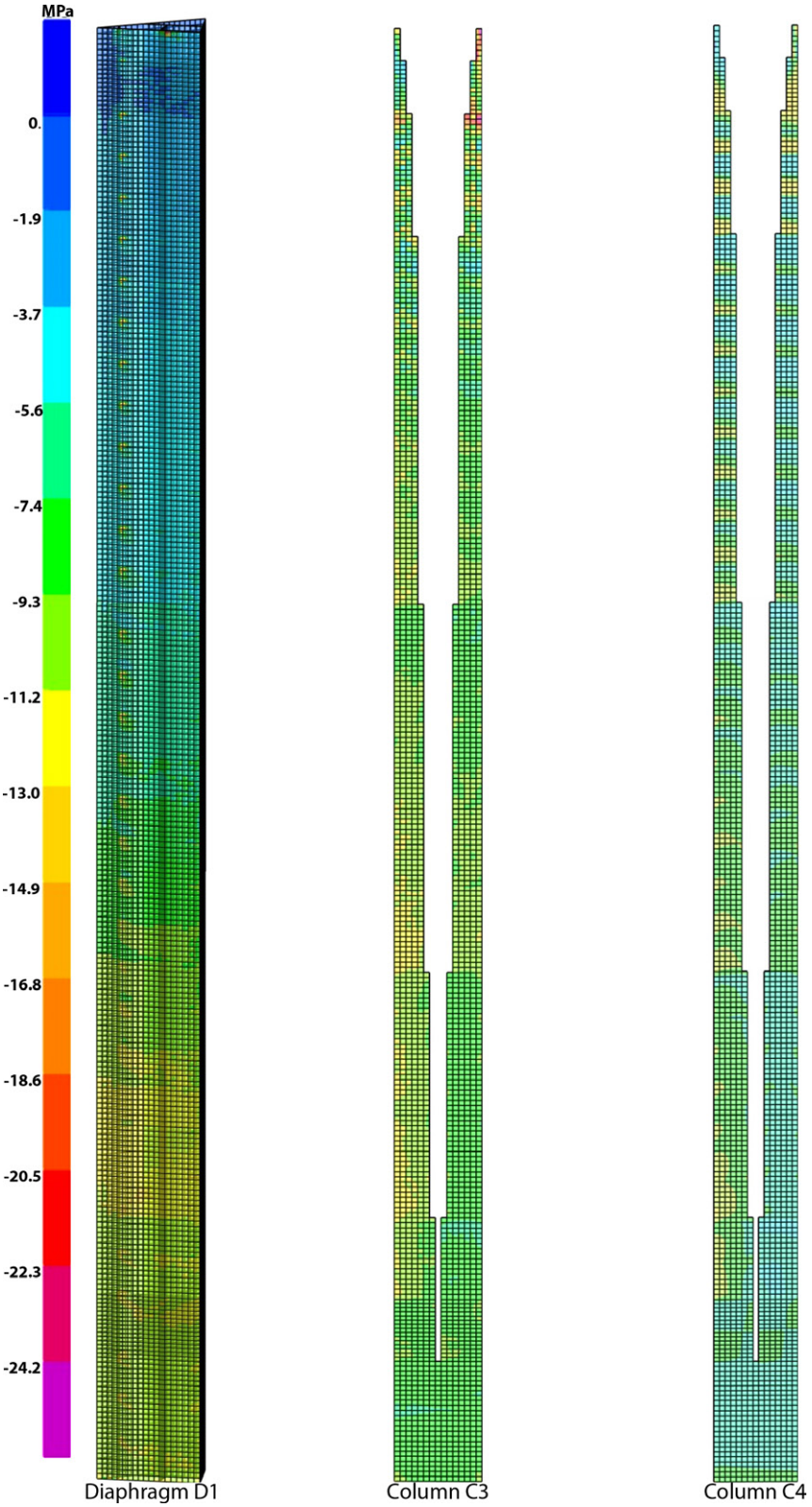

Figure 7.25: S22 envelope compression stresses in elements D1, C3 and C4 with a different contour range that reach the characteristic resistance of the concrete, 24,2 MPa.

7.4 Conclusions

This thesis has the aim to assess the structural robustness of the Pirelli Tower, following the existing standards and the "Threat Independent Approach", analyzing various local failure scenarios focused on the lateral walls. As said before, it is not possible to foresee if the Pirelli Tower will survive accidental situations like the ones described in this work, but, considering the previous results of the analyses, we can understand if the building has or not sufficient structural robustness. For this purpose, a summary of what has been observed is useful:

- **Scenario A:**

  In this case, the amount of removed walls is 11,96 meters, very close to the maximum states by the Eurocode [31] and clearly higher than the minimum indicated by the GSA American Standard [50]. The results have been excellent. The displacements were relatively modest, and the increment in vertical stresses was localized in the area close to the local failure and inferior to the characteristic resistance of the concrete.

- **Scenario B:**

  To test more thoroughly the building, in this scenario a more massive damage has been considered, much more severe than whatever prescription of any standards. With this damage, the behaviour of the slabs floor such as Vierendeel beams has become apparent, and the redistribution of stresses has interested the entire building.

Therefore, keeping in mind what said so far, it can be concluded that, although the building has been designed and built in an era where structural robustness was not yet considered, and no advanced calculation tools were available, the Pirelli Tower has demonstrated a fantastic response. The building has shown a tremendous aptitude to redistribute the stresses and opposing very efficiently to the progressive collapse. Thus, this Nervi's masterpiece has proved one more time the intuition of one of the best European engineer of all time, so able to realize a structure capable of satisfying even the most modern standards requirements.

Appendix A

Drawings

This appendix contains the entire collection of drawings accomplished in AutoCAD. As said before, these drawings have been realized from scratch with all the structural information obtained thanks to the “Cittadella degli Archivi di Milano”.

Plan view of a generic storey (scale 1:200)

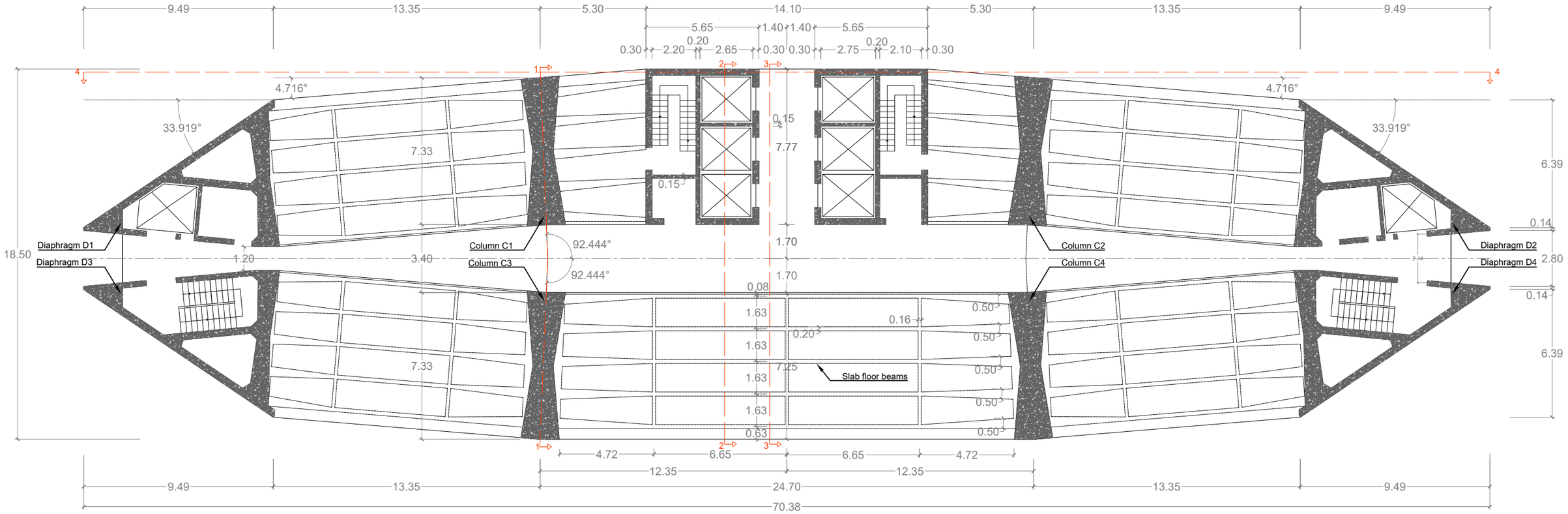

Transversal section 2-2 of the slab floor (scale 1:50)

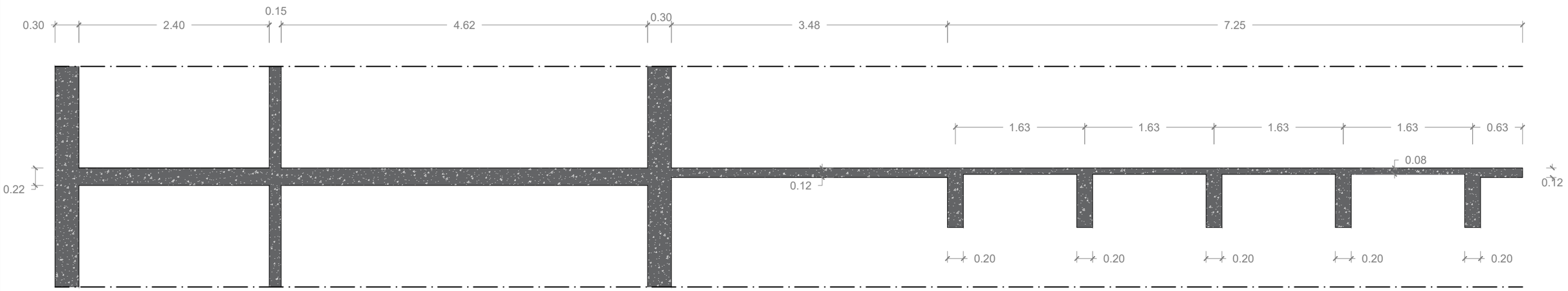

UNIVERSITAT POLITÈCNICA DE VALÈNCIA
Escuela Técnica Superior de Caminos, Canales y Puertos

Advisors: José Miguel Adam Martínez
Marco Ballerini

Student: Francesco Da Rif

Master Thesis: "Structural robustness assessment of the Pirelli Tower in Milan. Consequences of local failures in lateral walls."

Object: Drawing 1, Plan view of a generic storey and transversal section of the slab floor.

UNIVERSITY OF TRENTO
Master Degree in Civil Engineering, Double Degree Program

Longitudinal section of the slab floor beams (scale 1:40)

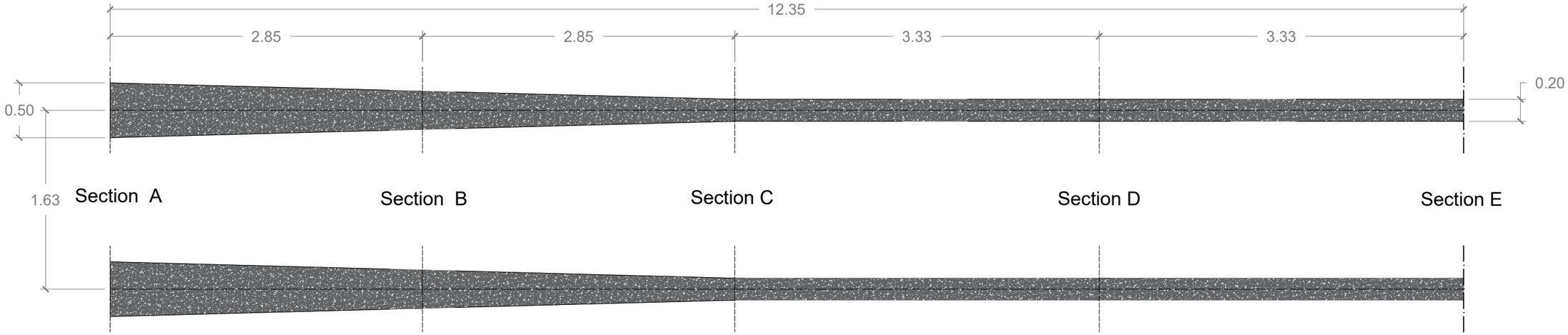

Section A (scale 1:25)

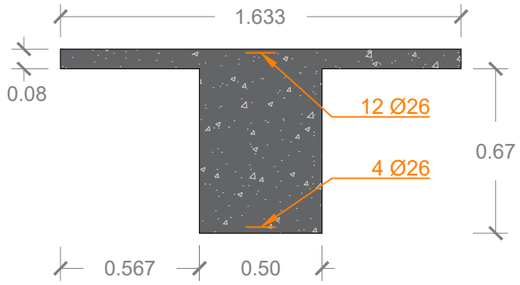

Section B (scale 1:25)

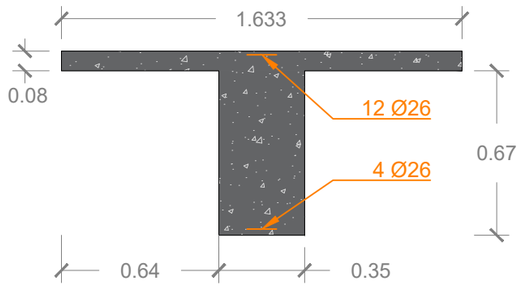

Section C (scale 1:25)

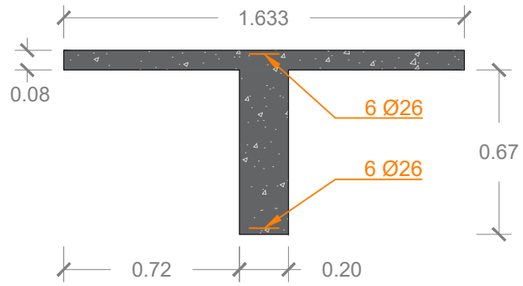

Section D (scale 1:25)

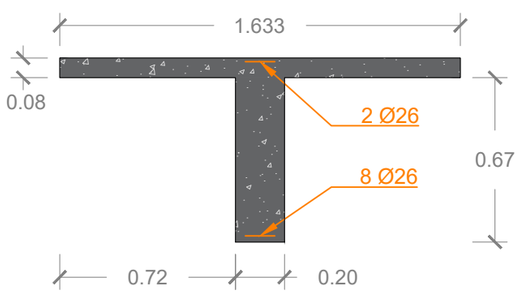

Section E (scale 1:25)

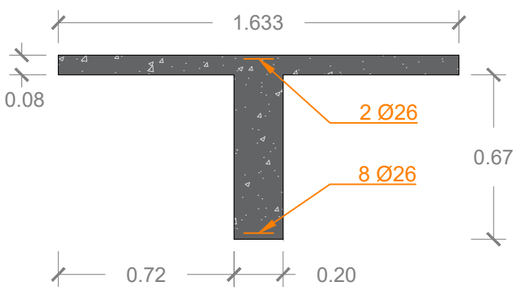

UNIVERSITAT POLITÈCNICA DE VALÈNCIA
Escuela Técnica Superior de Caminos, Canales y Puertos

Advisors: José Miguel Adam Martínez
Marco Ballerini

Student: Francesco Da Rif

Master Thesis: "Structural robustness assessment of the Pirelli Tower in Milan. Consequences of local failures in lateral walls."

Object: Drawing 2, Slab floor beam longitudinal and transversal sections.

UNIVERSITY OF TRENTO
Master Degree in Civil Engineering, Double Degree Program

Transversal section 1-1 (scale 1:400)

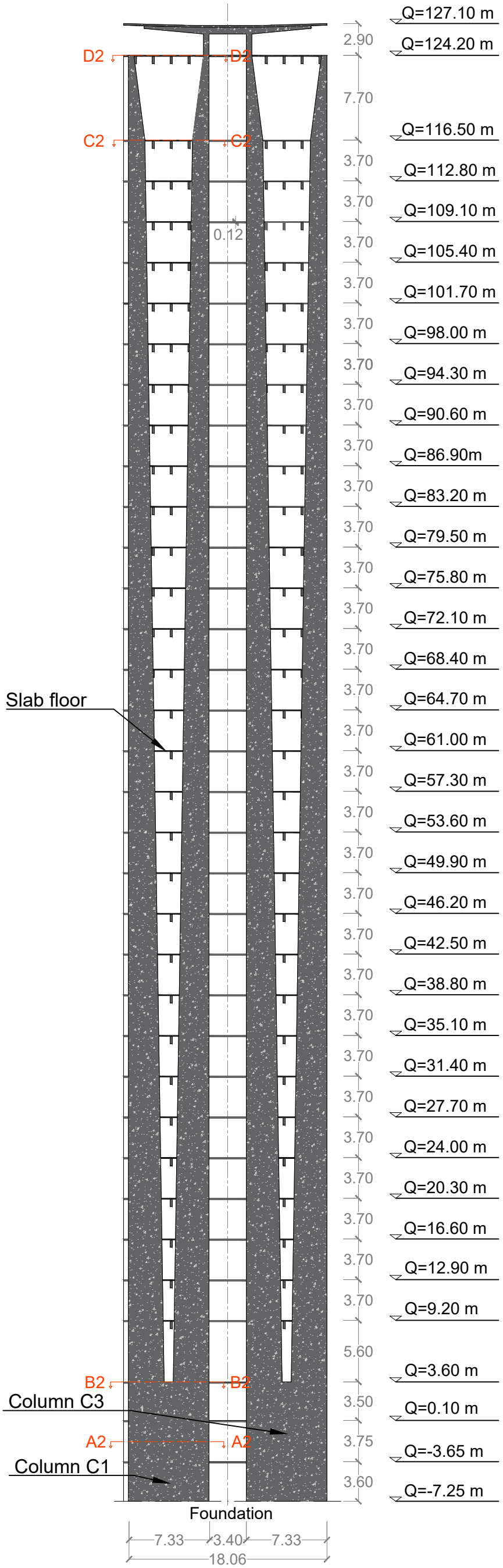

Column C1: section D2-D2 at 124,20 m (Scale 1:75)

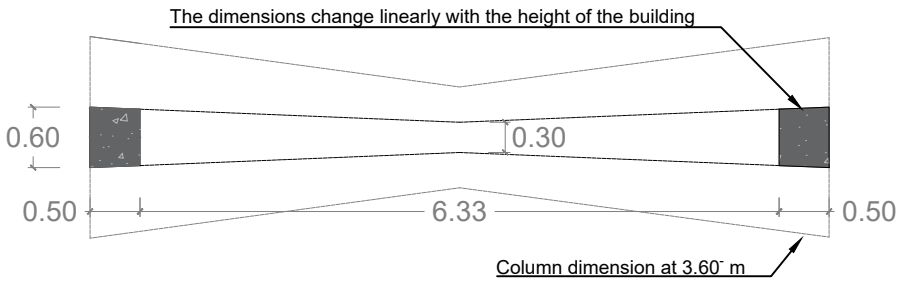

Column C1: section C2-C2 at 116,50 m (Scale 1:75)

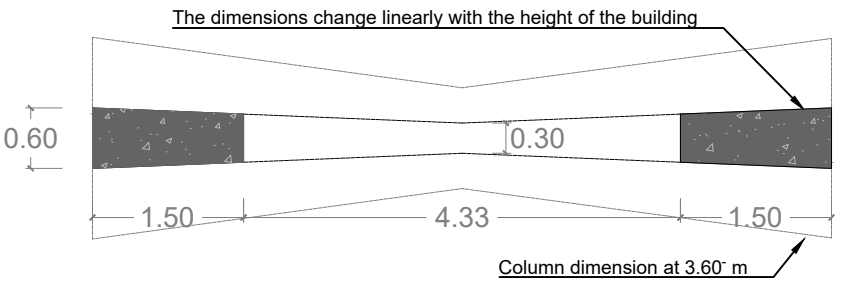

Column C1: section B2-B2 at 3,60⁺m (Scale 1:75)

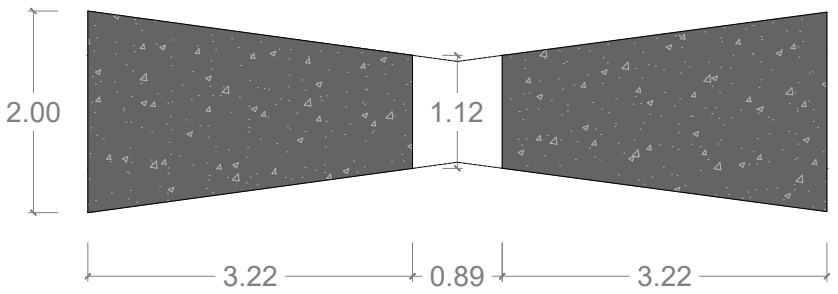

Column C1: section A2-A2 from -7,25 m to 3,60⁻m (Scale 1:75)

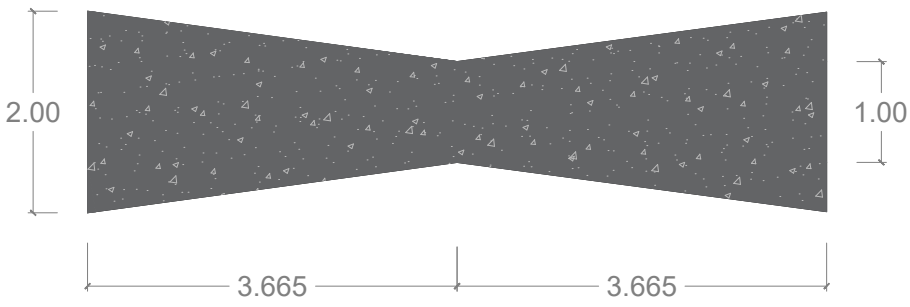

UNIVERSITAT POLITÈCNICA DE VALÈNCIA
Escuela Técnica Superior de Caminos, Canales y Puertos

Advisors: José Miguel Adam Martínez
Marco Ballerini

Student: Francesco Da Rif

Master Thesis: "Structural robustness assessment of the Pirelli Tower in Milan. Consequences of local failures in lateral walls."

Object: Drawing 3, Longitudinal profile and sections of the Columns.

UNIVERSITY OF TRENTO
Master Degree in Civil Engineering, Double Degree Program

Section diaphragms D1 and D3. Q=3,60m

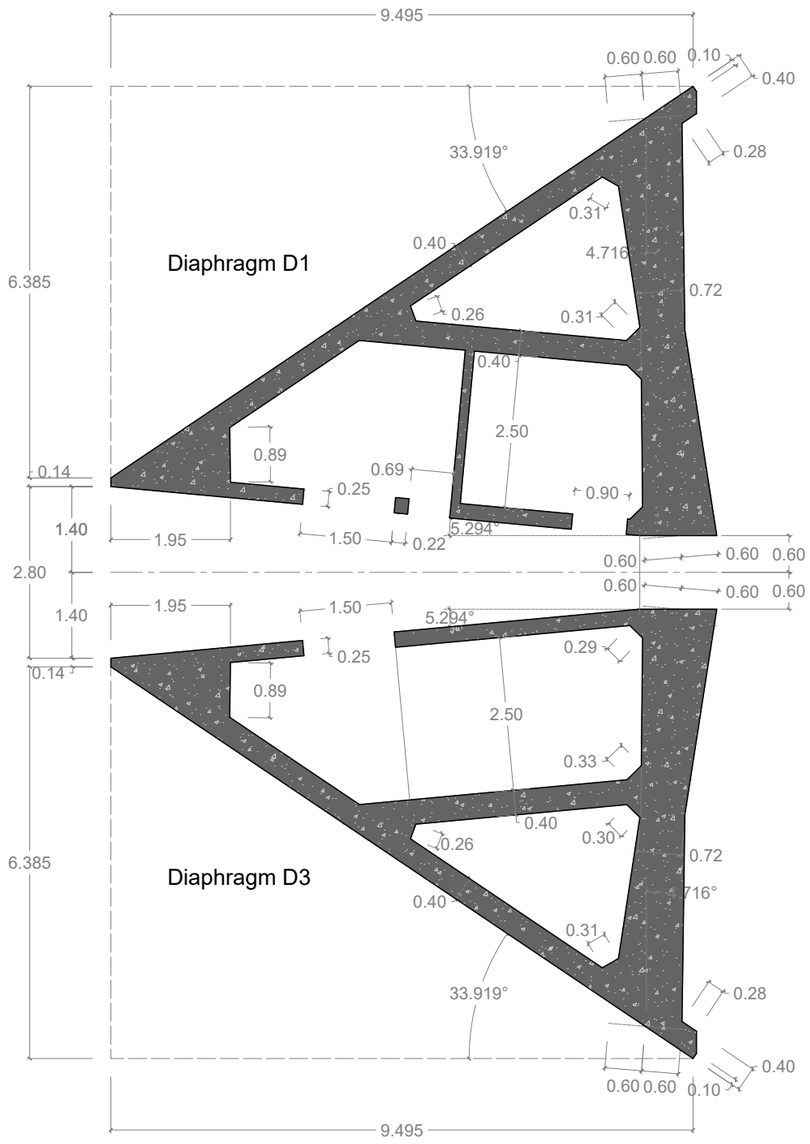

Section diaphragms D1 and D3. Q=61,00m

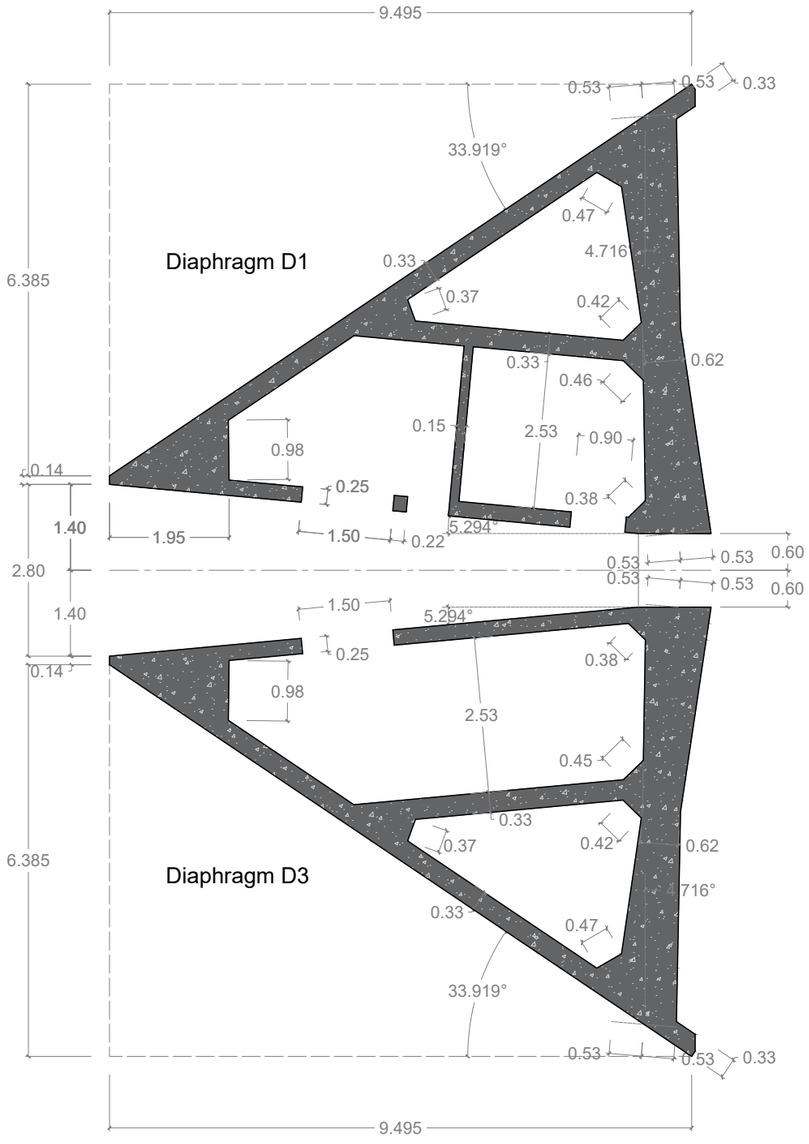

Section diaphragms D1 and D3. Q=124,20m

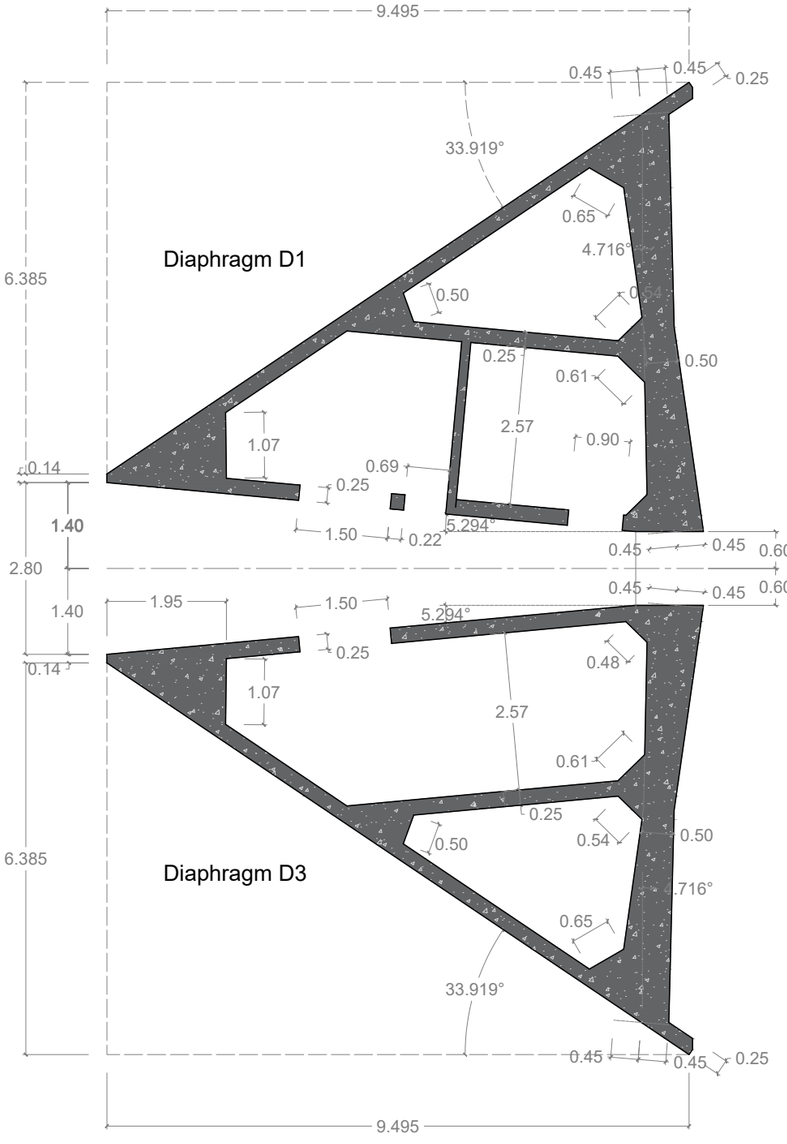

UNIVERSITAT POLITÈCNICA DE VALÈNCIA
Escuela Técnica Superior de Caminos, Canales y Puertos

Advisors: José Miguel Adam Martínez
Marco Ballerini

Student: Francesco Da Rif

Master Thesis: "Structural robustness assessment of the Pirelli Tower in Milan. Consequences of local failures in lateral walls."

Object: Drawing 4, Sections of the Diaphragms D1 and D3.
Scale: 1:100

UNIVERSITY OF TRENTO
Master Degree in Civil Engineering, Double Degree Program

Section diaphragms D2 and D4. Q=3,60m

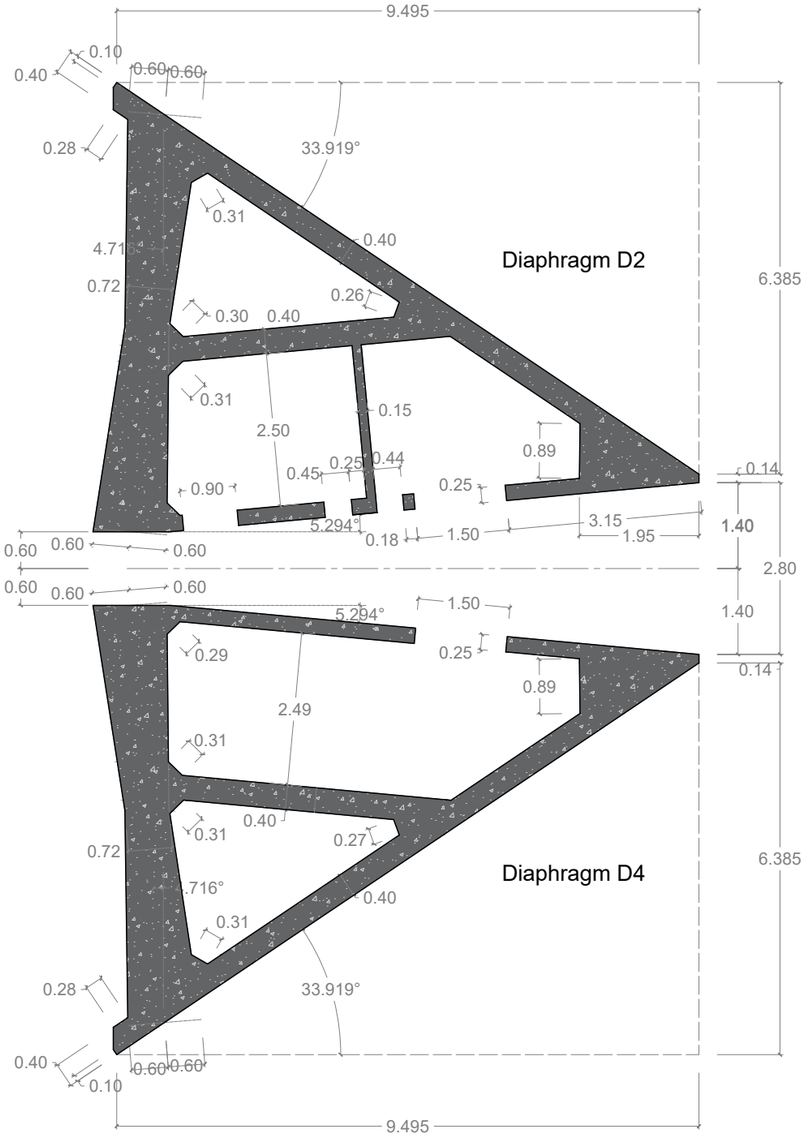

Section diaphragms D2 and D4. Q=61,00m

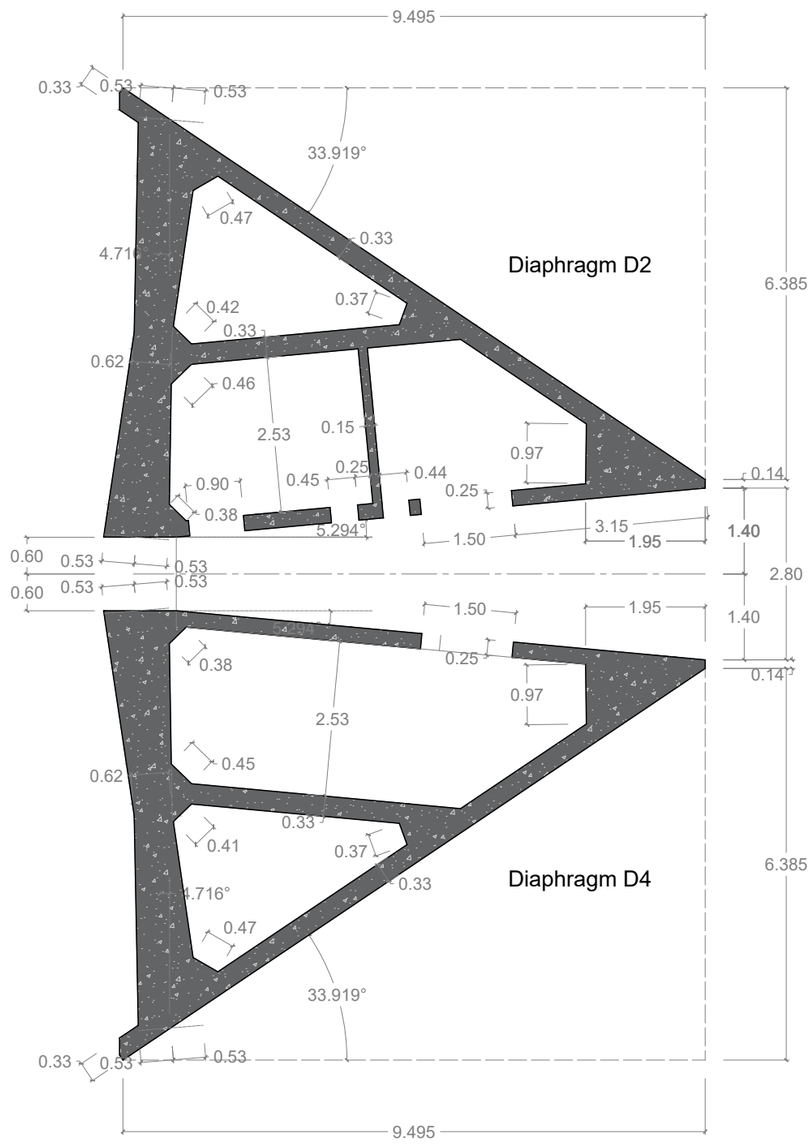

Section diaphragms D2 and D4. Q=124,20m

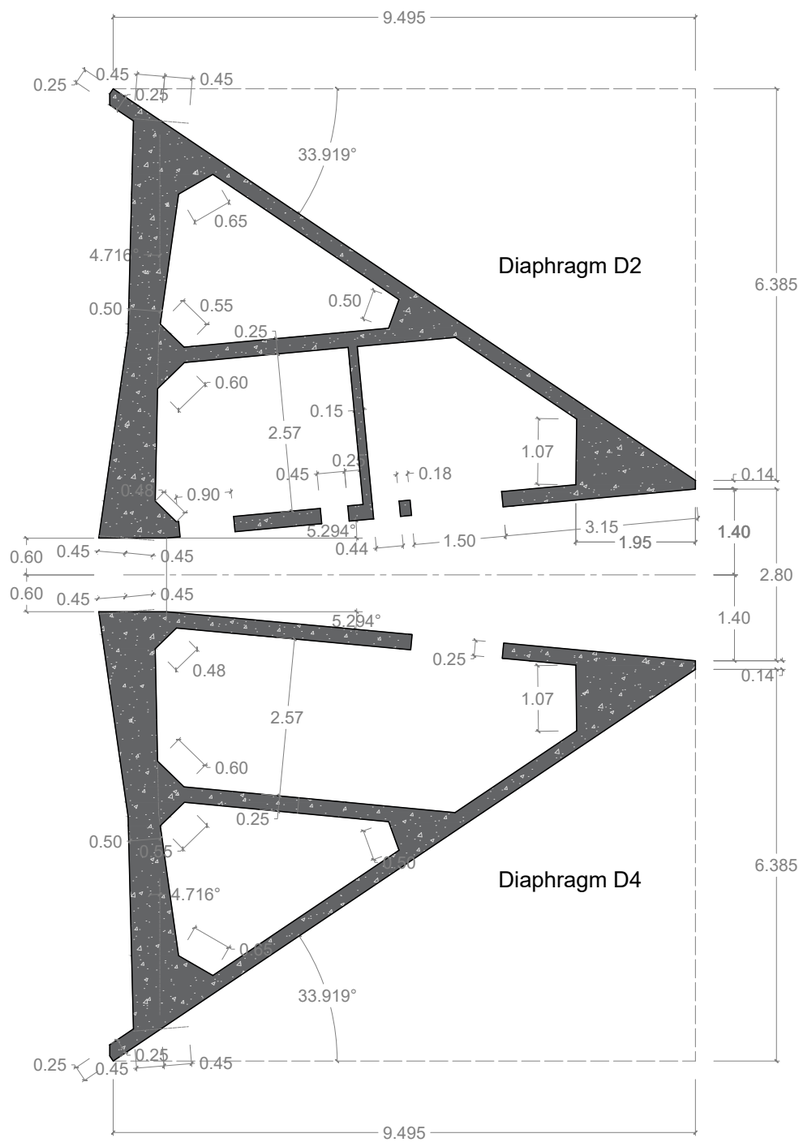

UNIVERSITAT POLITÈCNICA DE VALÈNCIA
Escuela Técnica Superior de Caminos, Canales y Puertos

Advisors: José Miguel Adam Martínez
Marco Ballerini

Student: Francesco Da Rif

Master Thesis: "Structural robustness assessment of the Pirelli Tower in Milan. Consequences of local failures in lateral walls."

Object: Drawing 5, Sections of the Diaphragms D2 and D4.
Scale: 1:100

UNIVERSITY OF TRENTO
Master Degree in Civil Engineering, Double Degree Program

Transversal section 3-3 (scale 1:400)

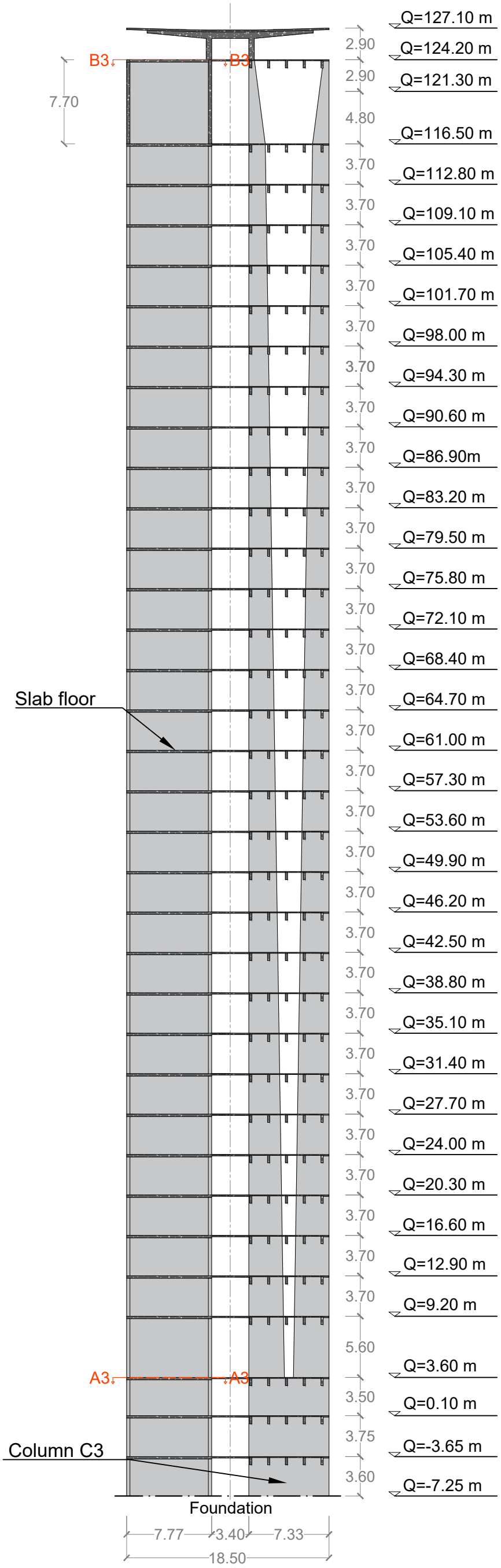

Section B3-B3 between 116,50^{+}m and 124,20m (Scale 1:150)

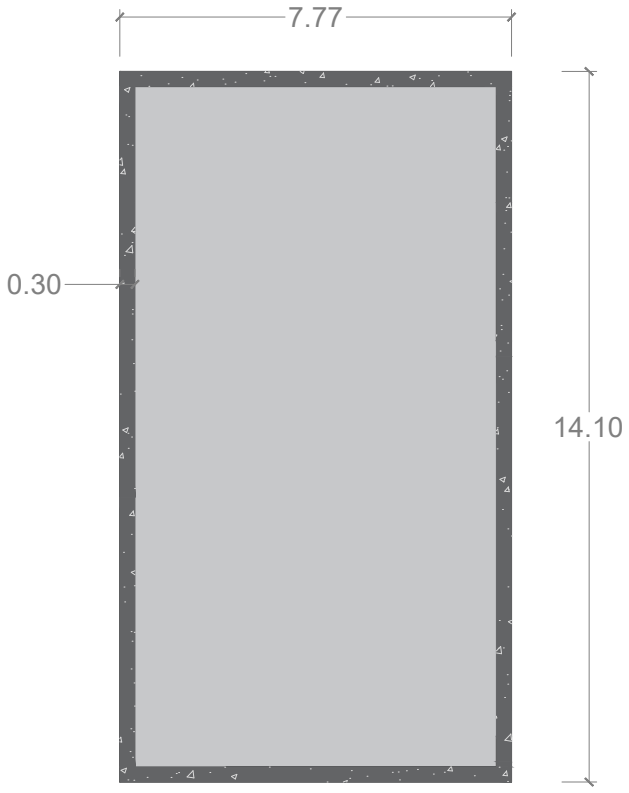

Section A3-A3 between -7,25m and 116,50^{-}m (Scale 1:150)

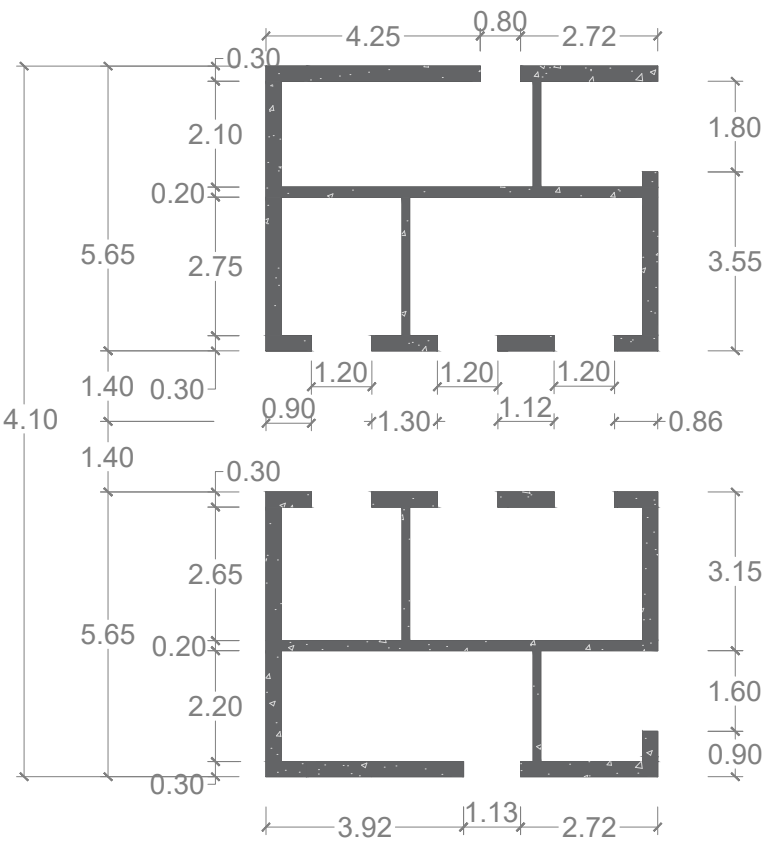

UNIVERSITAT POLITÈCNICA DE VALÈNCIA
Escuela Técnica Superior de Caminos, Canales y Puertos

Advisors: José Miguel Adam Martínez
Marco Ballerini

Student: Francesco Da Rif

Master Thesis: "Structural robustness assessment of the Pirelli Tower in Milan. Consequences of local failures in lateral walls."

Object: Drawing 6, Longitudinal section 3-3 and transversal sections of the rectangular cores.

UNIVERSITY OF TRENTO
Master Degree in Civil Engineering, Double Degree Program

Transversal section 4-4 (scale 1:400)

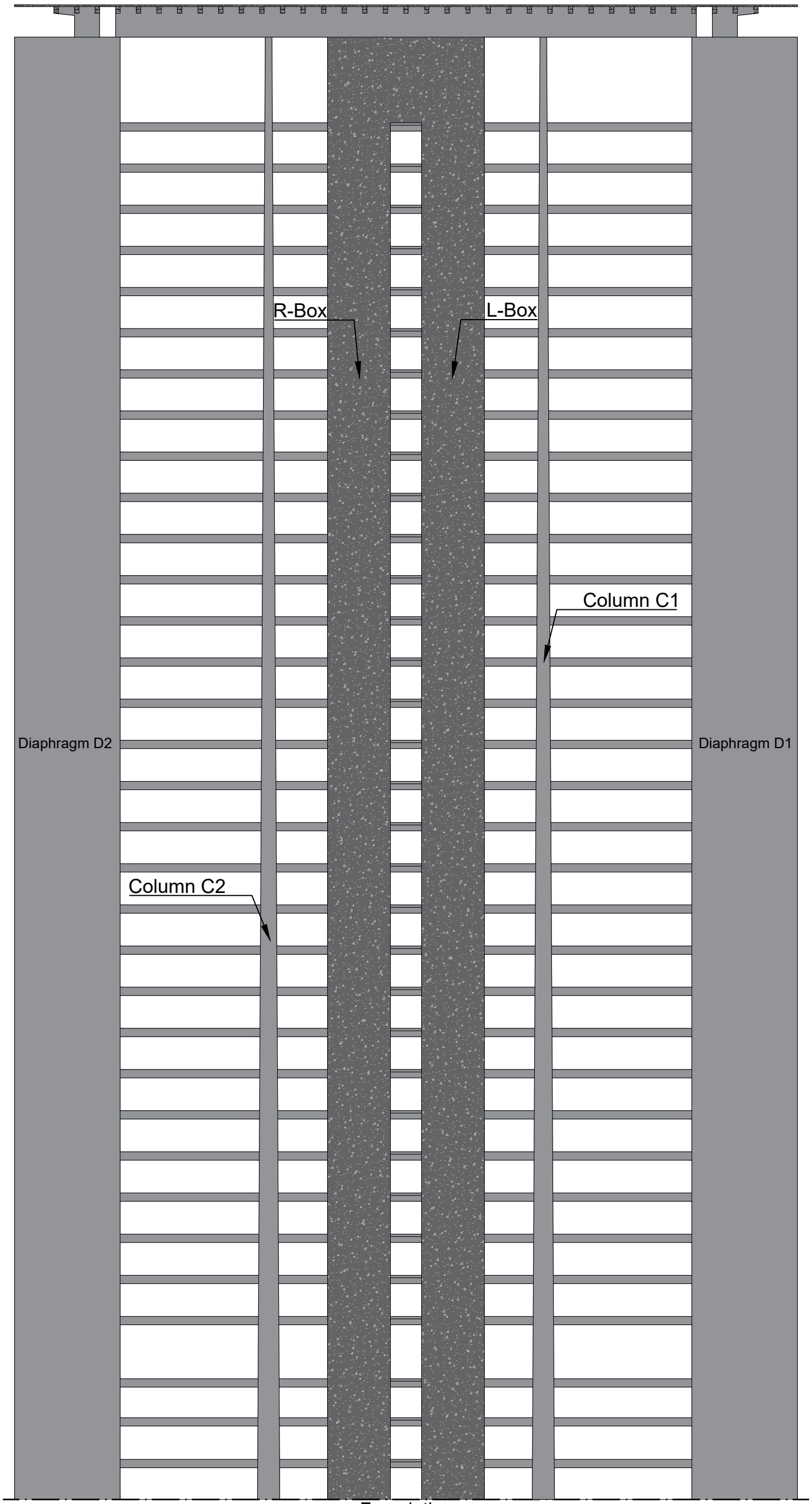

Q=127.10 m	
2.90	Q=124.20 m
2.90	Q=121.30 m
4.80	Q=116.50 m
3.70	Q=112.80 m
3.70	Q=109.10 m
3.70	Q=105.40 m
3.70	Q=101.70 m
3.70	Q=98.00 m
3.70	Q=94.30 m
3.70	Q=90.60 m
3.70	Q=86.90m
3.70	Q=83.20 m
3.70	Q=79.50 m
3.70	Q=75.80 m
3.70	Q=72.10 m
3.70	Q=68.40 m
3.70	Q=64.70 m
3.70	Q=61.00 m
3.70	Q=57.30 m
3.70	Q=53.60 m
3.70	Q=49.90 m
3.70	Q=46.20 m
3.70	Q=42.50 m
3.70	Q=38.80 m
3.70	Q=35.10 m
3.70	Q=31.40 m
3.70	Q=27.70 m
3.70	Q=24.00 m
3.70	Q=20.30 m
3.70	Q=16.60 m
3.70	Q=12.90 m
3.70	Q=9.20 m
5.60	Q=3.60 m
3.50	Q=0.10 m
3.75	Q=-3.65 m
3.60	Q=-7.25 m

UNIVERSITAT POLITÈCNICA DE VALÈNCIA
Escuela Técnica Superior de Caminos, Canales y Puertos

Advisors: José Miguel Adam Martínez
Marco Ballerini

Student: Francesco Da Rif

Master Thesis: "Structural robustness assessment of the Pirelli Tower in Milan. Consequences of local failures in lateral walls."

Object: Drawing 7, Longitudinal section 4-4.

UNIVERSITY OF TRENTO
Master Degree in Civil Engineering, Double Degree Program

Plan view of the covering and sections (scale 1:200)

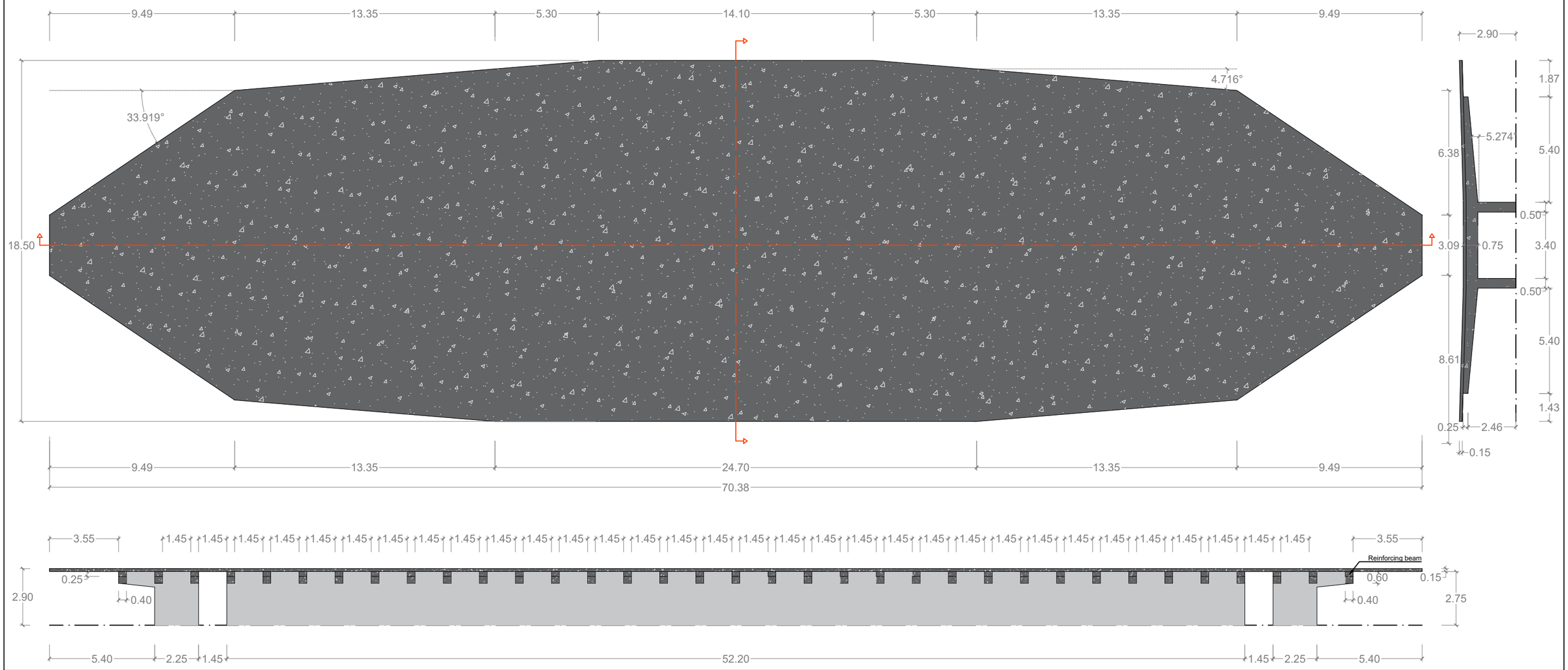

Longitudinal section of a reinforcing beam of the covering (Scale 1:40)

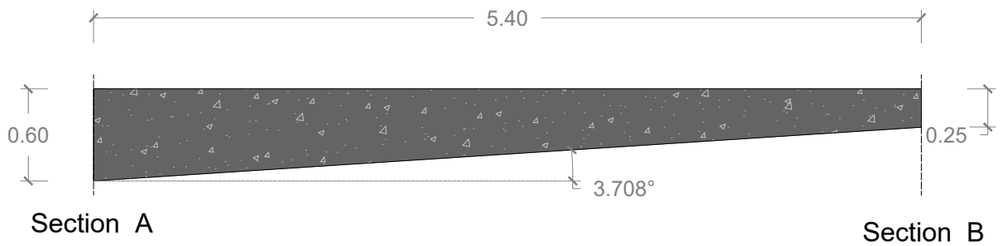

Transversal section A of a reinforcing beam of the covering (Scale 1:15)

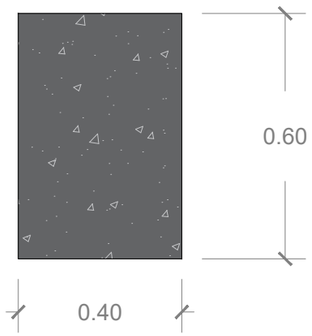

Transversal section B of a reinforcing beam of the covering (Scale 1:15)

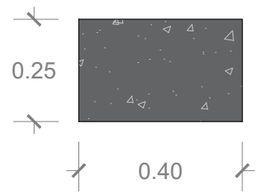

UNIVERSITAT POLITÈCNICA DE VALÈNCIA
Escuela Técnica Superior de Caminos, Canales y Puertos

Advisors: José Miguel Adam Martínez
Marco Ballerini

Student: Francesco Da Rif

Master Thesis: "Structural robustness assessment of the Pirelli Tower in Milan. Consequences of local failures in lateral walls."

Object: Drawing 8, Plan view and sections of the roof slab.

UNIVERSITY OF TRENTO
Master Degree in Civil Engineering, Double Degree Program

Appendix B

Sustainable Development Goals

UNIVERSITAT POLITÈCNICA DE VALÈNCIA

CAMINOS upv ESCUELA TÉCNICA SUPERIOR DE INGENIERÍA DE CAMINOS, CANALES Y PUERTOS
COMPROMETIDA CON LOS OBJETIVOS DE DESARROLLO SOSTENIBLE

Anexo al Trabajo Fin de Grado/Máster

Relación del TFG/TFM "Evaluación de la robustez estructural de la Torre Pirelli de Milán (Italia). Consecuencias de los fallos locales en los muros laterales.**" con los Objetivos de Desarrollo Sostenible de la Agenda 2030.**

Grado de relación del trabajo con los Objetivos de Desarrollo Sostenible (ODS).

Objetivos de Desarrollo Sostenibles	Alto	Medio	Bajo	No Procede
ODS 1. **Fin de la pobreza.**				X
ODS 2. **Hambre cero.**				X
ODS 3. **Salud y bienestar.**				X
ODS 4. **Educación de calidad.**				X
ODS 5. **Igualdad de género.**				X
ODS 6. **Agua limpia y saneamiento.**				X
ODS 7. **Energía asequible y no contaminante.**				X
ODS 8. **Trabajo decente y crecimiento económico.**				X
ODS 9. **Industria, innovación e infraestructuras.**		X		
ODS 10. **Reducción de las desigualdades**.				X
ODS 11. **Ciudades y comunidades sostenibles**.		X		
ODS 12. **Producción y consumo responsables.**				X
ODS 13. **Acción por el clima.**		X		
ODS 14. **Vida submarina.**				X
ODS 15. **Vida de ecosistemas terrestres.**				X
ODS 16. **Paz, justicia e instituciones sólidas.**				X
ODS 17. **Alianzas para lograr objetivos.**				X

Descripción de la alineación del TFG/M con los ODS con un grado de relación más alto.

El trabajo describe algunos análisis estructurales de un importante edificio en Italia para evaluar su robustez estructural, que es un tema en desarrollo en el campo de la Ingeniería Civil, y por lo tanto se relaciona con los objetivos 9 y 11. Además, evitando el colapso de edificios, se reducen las emisiones de CO2 asociadas a la construcción de nuevas estructuras, entonces atañe también el ODS 13.

Bibliography

[1] *Ronan Point*. 2020. URL: https://alchetron.com/Ronan-Point#ronan-point-bd151963-2519-4d0d-8b4a-cddd6305621-resize-750.jpg (visited on 09/05/2020).

[2] *Oklahoma City bombing*. 2020. URL: https://www.britannica.com/event/Oklahoma-City-bombing (visited on 09/05/2020).

[3] Seweryn Kokot and George Solomos. "Progressive collapse risk analysis: literature survey, relevant construction standards and guidelines". In: *Ispra: Joint Research Centre, European Commission* (2012).

[4] Zdeněk P Bažant and Mathieu Verdure. "Mechanics of progressive collapse: Learning from World Trade Center and building demolitions". In: *Journal of Engineering Mechanics* 133.3 (2007), pp. 308–319.

[5] *11 Settembre*. 2020. URL: https://www.tpi.it/foto/foto-inedite-11-settembre/ (visited on 09/05/2020).

[6] Javier Manterola Armisen. "La estructura resistente de los edificios altos". In: *Informes de la Construcción* 37.371 (1985), pp. 5–30.

[7] *Pirelli Tower*. 2020. URL: https://www.bmsprogetti.it/projects/pirelli-tower-refurbishment/ (visited on 09/05/2020).

[8] *High-rise buildings*. 2020. URL: https://www.pinterest.it/ (visited on 09/12/2020).

[9] *The Colon Towers*. 2020. URL: https://www.chamberi30dias.es/reportajes/torres-colon-la-arquitectura-suspendida-que-desafio-al-refranero (visited on 09/11/2020).

[10] José Miguel Adam Martínez. *Estructuras de edificios altos. Notes of the Conceptual Design of Singular Structures course*. 2019.

[11] *Shear lag in tubular frame buildings*. 2020. URL: https://www.sciencedirect.com/topics/engineering/shear-lag-effect (visited on 09/12/2020).

[12] Jose M Adam et al. "Research and practice on progressive collapse and robustness of building structures in the 21st century". In: *Engineering Structures* 173 (2018), pp. 122–149.

[13] Uwe Starossek. "Typology of progressive collapse". In: *Engineering Structures* 29.9 (2007), pp. 2302–2307.

[14] Bruce R Ellingwood and Donald O Dusenberry. “Building design for abnormal loads and progressive collapse”. In: *Computer-Aided Civil and Infrastructure Engineering* 20.3 (2005), pp. 194–205.

[15] Bruce R Ellingwood. “Mitigating risk from abnormal loads and progressive collapse”. In: *Journal of Performance of Constructed Facilities* 20.4 (2006), pp. 315–323.

[16] Uwe Starossek. “Progressive collapse of structures: Nomenclature and procedures”. In: *Structural engineering international* 16.2 (2006), pp. 113–117.

[17] Uwe Starossek and Maren Wolff. “Design of collapse-resistant structures”. In: *JCSS and IABSE Workshop on Robustness of Structures*. Vol. 30. 2005.

[18] Uwe Starossek. “Avoiding disproportionate collapse of tall buildings”. In: *Structural engineering international* 18.3 (2008), pp. 238–246.

[19] Uwe Starossek and Marco Haberland. “Measures of structural robustness—Requirements and applications”. In: *Structures Congress 2008: Crossing Borders*. 2008, pp. 1–10.

[20] Uwe Starossek and Marco Haberland. “Approaches to measures of structural robustness”. In: *Structure and Infrastructure Engineering* 7.7-8 (2011), pp. 625–631.

[21] Niels C Lind. “A measure of vulnerability and damage tolerance”. In: *Reliability Engineering & System Safety* 48.1 (1995), pp. 1–6.

[22] Niels C Lind. “Vulnerability of damage-accumulating systems”. In: *Reliability Engineering & System Safety* 53.2 (1996), pp. 217–219.

[23] Jack W Baker, Matthias Schubert, and Michael H Faber. “On the assessment of robustness”. In: *Structural Safety* 30.3 (2008), pp. 253–267.

[24] Dawid Wisniewski, Joan R Casas, and Michel Ghosn. “Load capacity evaluation of existing railway bridges based on robustness quantification”. In: *Structural Engineering International* 16.2 (2006), pp. 161–166.

[25] MA Maes, KE Fritzsons, and S Glowienka. “Risk-based indicators of structural system robustness”. In: *JCSS and IABSE Workshop on Robustness of Structures*. 2005, pp. 220–225.

[26] John William Smith. “Structural robustness analysis and the fast fracture analogy”. In: *Structural Engineering International* 16.2 (2006), pp. 118–123.

[27] Kfir Menchel. “Progressive collapse: comparison of main standards, formulation and validation of new computational procedures”. In: *Universite Libre de Bruxelles, Faculte des Sciences Appliquees, Ph. D. Thesis* (2009).

[28] Jitendra Agarwal, David Blockley, and Norman Woodman. “Vulnerability of structural systems”. In: *Structural Safety* 25.3 (2003), pp. 263–286.

[29] EN 1990. *Eurocode 0 - EN 1990: Basis of structural design, 2002.*

[30] EN 1991. *Eurocode 0 - EN 1991: Actions on structures, 2004.*

[31] EN 1991-1-7. *Eurocode 1 - EN 1991-1-7: Actions on structures - Part 1-7: General actions - Accidental actions, 2006.*

[32] *Pirelli Tower.* 2020. URL: https://www.webuildvalue.com/en/infrastructure-news/pirellone.html (visited on 09/06/2020).

[33] *Pirelli Tower.* 2020. URL: https://www.bmiaa.com/skyscraper-age-an-exhibition-about-the-history-of-the-pirellone-milans-iconic-tower/ (visited on 09/05/2020).

[34] *SkyscraperCenter.* 2020. URL: https://images.skyscrapercenter.com (visited on 11/05/2020).

[35] *Tripadvisor.* 2020. URL: https://www.tripadvisor.it (visited on 11/05/2020).

[36] *Pirelli Tower.* 2020. URL: https://www.ordinearchitetti.mi.it/ (visited on 11/05/2020).

[37] *ThousandWonders.* 2020. URL: https://www.thousandwonders.net/Pirelli+Tower (visited on 11/05/2020).

[38] *Pirelli Tower.* 2020. URL: https://corvinoemultari.com/restauro-grattacielo-pirelli-interni/ (visited on 11/05/2020).

[39] Pier Luigi Nervi. *Edilizia moderna - L'ossatura, 1960.*

[40] Gabriele Neri. *Capolavori in miniatura.* Mendrisio Academy Press. Silvana Editoriale, 2014.

[41] *Palazzo Pirelli, Regione Lombardia.* 2020. URL: https://www.regione.lombardia.it/wps/portal/istituzionale/HP/DettaglioRedazionale/istituzione/regione/palazzo-pirelli/red-pirelli-REC/palazzo-pirelli (visited on 09/06/2020).

[42] *Pirelli Tower crash, AP archive.* 2020. URL: http://www.aparchive.com/metadata/youtube/72181d77152e5e223b25a0bac80e9776 (visited on 09/06/2020).

[43] Cittadella degli archivi di Milano. *Piazza Duca D'Aosta 5, Grattacielo Pirelli. Atti numero 43919, anno 1968, parte prima.*

[44] Cittadella degli archivi di Milano. *Piazza Duca D'Aosta 5, Grattacielo Pirelli. Atti numero 43919, anno 1968, parte seconda.*

[45] *RUMI LU3 for seismic constructions.* 2020. URL: https://docplayer.it/17398499-Acciaio-ed-evento-sismico-evoluzione-dei-prodotti-in-acciaio-per-le-costruzioni.html (visited on 09/29/2020).

[46] EN 1991-1-7. *Eurocode 2 - EN 1992-1-1: Design of concrete structures - Part 1-1: General rules and rules for buildings, 2005.*

[47] EN 1991. *Eurocode 1 - EN 1991-1-4: General actions - Wind action, 2010.*

[48] EN 1991. *ITALIAN NATIONAL ANNEX UNI EN 1990:2004 - Parameters adopted at national level, 2004.*

[49] Ministero delle Infrastrutture e dei Trasporti. *Nuove norme tecniche per le costruzioni 2018, D.M. Infrastrutture 17 gennaio 2018, 2018.*

[50] GENERAL SERVICE ADMINISTRATION. *General services administration - Alternate path analysis & design guidelines for progressive collapse resistance, 2016.*

[51] *CSIAmerica.* 2020. URL: https://wiki.csiamerica.com/display/kb/Home (visited on 10/27/2020).

Acknowledgements

I would first like to thank my advisors, Professors José Miguel Adam Martínez and Ballerini Marco, whose expertise was precious in completing this Thesis.

I would like to acknowledge the office staff of the "Cittadella degli Archivi di Milano"for their willingness and quickness in allowing the inspection and scans of the originals structural schemes of the Pirelli Tower, despite the difficulties given by the SARS-CoV-2 emergency.

I would also like to thank the organisers of the Double Degree Program in both University of Trento and Polytechnic University of Valencia: Eccli Virna, Simeoni Lucia, Julia Pérez Laserna and Javier Calvo Díaz for their valuable supervision during this academic path of excellence. Furthermore, I additionally want to thank the Deputy Director of Academic Coordination Julián Alcalá González for its help in organising the Thesis defence.

Finally, I would like to thank my dears for their wise counsel and sympathetic ear. You have always been there for me.